

AWARD NUMBER:

W81XWH-13-1-0282

TITLE: The Role of BRCA1 in Suppressing Epithelial-Mesenchymal Transition
in Mammary Gland and Tumor Development

PRINCIPAL INVESTIGATOR: Xin-Hai Pei, M.D., Ph.D

CONTRACTING ORGANIZATION:

University of Miami
Miami, FL 33136

REPORT DATE: November 2016

TYPE OF REPORT: Final

PREPARED FOR: U.S. Army Medical Research and Materiel Command
Fort Detrick, Maryland 21702-5012

DISTRIBUTION STATEMENT: Approved for Public Release;
Distribution Unlimited

The views, opinions and/or findings contained in this report are those of the author(s) and should not be construed as an official Department of the Army position, policy or decision unless so designated by other documentation.

REPORT DOCUMENTATION PAGE

*Form Approved
OMB No. 0704-0188*

Public reporting burden for this collection of information is estimated to average 1 hour per response, including the time for reviewing instructions, searching existing data sources, gathering and maintaining the data needed, and completing and reviewing this collection of information. Send comments regarding this burden estimate or any other aspect of this collection of information, including suggestions for reducing this burden to Department of Defense, Washington Headquarters Services, Directorate for Information Operations and Reports (0704-0188), 1215 Jefferson Davis Highway, Suite 1204, Arlington, VA 22202-4302. Respondents should be aware that notwithstanding any other provision of law, no person shall be subject to any penalty for failing to comply with a collection of information if it does not display a currently valid OMB control number. **PLEASE DO NOT RETURN YOUR FORM TO THE ABOVE ADDRESS.**

1. REPORT DATE November 2016			2. REPORT TYPE Final		3. DATES COVERED 01-SEP-2013 - 31-AUG-2016	
4. TITLE AND SUBTITLE The Role of BRCA1 in Suppressing Epithelial-Mesenchymal Transition in Mammary Gland and Tumor Development			5a. CONTRACT NUMBER			
			5b. GRANT NUMBER W81XWH-13-1-0282			
			5c. PROGRAM ELEMENT NUMBER			
6. AUTHOR(S) Xin-Hai Pei, M.D., Ph.D. E-Mail: xhpei@med.miami.edu			5d. PROJECT NUMBER			
			5e. TASK NUMBER			
			5f. WORK UNIT NUMBER			
7. PERFORMING ORGANIZATION NAME(S) AND ADDRESS(ES) University of Miami Molecular Oncology Program Department of Surgery 1550 NW 10 th Avenue, Miami, FL 33136					8. PERFORMING ORGANIZATION REPORT NUMBER	
9. SPONSORING / MONITORING AGENCY NAME(S) AND ADDRESS(ES) U.S. Army Medical Research and Materiel Command Fort Detrick, Maryland 21702-5012					10. SPONSOR/MONITOR'S ACRONYM(S)	
					11. SPONSOR/MONITOR'S REPORT NUMBER(S)	
12. DISTRIBUTION / AVAILABILITY STATEMENT Approved for Public Release; Distribution Unlimited						
13. SUPPLEMENTARY NOTES						
14. ABSTRACT During the funding period, the PI has found that disrupting <i>Brca1</i> by either germline or epithelium-specific mutation in p18-deficient mice activates epithelial-to-mesenchymal transition (EMT) and induces dedifferentiation of luminal stem cells (LSCs), which associate closely with expansion of basal and cancer stem cells and formation of basal-like tumors. Mechanistically, BRCA1 bound to the <i>TWIST</i> promoter, suppressing its activity and inhibiting EMT in mammary tumor cells. PI has also found that p16 loss transforms Brca1-deficient mammary epithelial cells and induces mammary tumors, though p16 loss alone is not sufficient to induce mammary tumorigenesis. PI has demonstrated that loss of both p16 and Brca1 leads to metastatic, basal-like, mammary tumors with the induction of EMT and an enrichment of tumor initiating cells. Together, our findings show that BRCA1 suppresses TWIST and EMT, inhibits LSC dedifferentiation and represses expansion of basal stem cells and basal-like tumors. In addition, we provide the first genetic evidence directly showing that p16 which is frequently deleted and inactivated in human breast cancers, collaborates with Brca1 controlling mammary tumorigenesis.						
15. SUBJECT TERMS Brca1 suppresses EMT and stem cell dedifferentiation						
16. SECURITY CLASSIFICATION OF: U			17. LIMITATION OF ABSTRACT Unclassified	18. NUMBER OF PAGES 43	19a. NAME OF RESPONSIBLE PERSON USAMRMC	
a. REPORT Unclassified					19b. TELEPHONE NUMBER (include area code)	
b. ABSTRACT Unclassified			c. THIS PAGE Unclassified			

Table of Contents

	<u>Page</u>
1. Introduction.....	4
2. Keywords.....	4
3. Overall Project Summary.....	4
4. Key Research Accomplishments.....	14
5. Conclusion.....	15
6. Publications, Abstracts, and Presentations.....	15
7. Inventions, Patents and Licenses.....	15
8. Reportable Outcomes.....	15
9. Other Achievements.....	16
10. References.....	16
11. Appendices.....	19

1. Introduction

Mammary epithelia are mainly composed of luminal and basal cells whose expansion and maintenance in adult mice are ensured by luminal and basal stem cells, respectively(1, 2). Accordingly breast cancer is divided into two major subtypes—luminal and basal-like tumors—that develop through distinct mechanisms and exhibit different responsiveness to treatment(3). Mutation of *BRCA1* is frequently associated with basal-like breast cancer(4-7). How *Brca1* controls cell lineage commitment, maturation and transformation in the mammary gland and tumor development remain to be defined and are the focus of this application.

p16^{INK4A} (p16) and p18^{INK4C} (p18), two members of the inhibitors of CDK4/6 (INK4) family, inhibit CDK4 and CDK6, whose activation lead to functional inactivation of RB (8). p16 is inactivated in ~30% of and p18 expression is reduced in human breast cancers (9-12). Most BLBCs with functional loss of BRCA1 have dysfunctional INK4-RB and p53 pathways (10, 13-15). BRCA1 deficiency in human and mouse mammary epithelial cells activates both INK4-RB and p53 pathways, inducing premature senescence(16-18), which makes it difficult to determine the role of *Brca1* in tumor initiation and progression. We discovered that mutation of *Brca1* altered luminal cell fate, down-regulated the expression of luminal differentiation genes, up-regulated the expression of basal genes, and activated Twist and other epithelial-mesenchymal transition (EMT)-inducing transcription factors in p16 or p18 deficient luminal and tumor cells. Germline mutation of *Brca1* converts p18 deficient luminal type tumors into basal-like tumors with EMT features. Ectopic expression of WT BRCA1 in *BRCA1* mutant human basal-like cancer cells suppresses Twist and EMT and knockdown of BRCA1 sensitizes luminal cancer cells to induction of Twist and EMT in response to TGFβ.

Based on these findings, we hypothesize that *Brca1* suppresses Twist and EMT to prevent luminal stem and tumor cells from aberrant basal and mesenchymal differentiation. Reduction or loss of *Brca1* activates Twist and EMT, which allow LSCs to gain a multipotent capacity and cancer stem cells (CSC) to enhance self-renewal potential and lead to luminal-to-basal and luminal-to-mesenchymal cell transformation. We propose three specific aims to test this hypothesis: (1) to determine the role of BRCA1 in suppressing EMT and basal differentiation of mammary luminal cells, (2) to determine the function of BRCA1 in suppressing EMT of breast cancer stem cells, and (3) to determine the molecular mechanism of *Brca1* in suppressing TWIST.

2. Keywords

BRCA1, *p18^{ink4c}*, EMT, Luminal stem cell, Basal-like tumor

3. Overall Project summary

(1) Germline mutation of *Brca1* transforms *p18^{-/-}* luminal tumors into basal-like tumors with induction of EMT

In our previous studies, we reported that deletion of p18 in mice stimulates mammary LSC proliferation and leads to spontaneous luminal tumor development(9), and that germline mutation of *Brca1* in p18-deficient mice with Balb/c enriched background blocks the expansion of LSCs and transforms luminal tumors into basal-like tumors(16). Prompted by the highly invasive heterogeneous mammary tumors developed in *p18^{-/-};Brca1^{+/-}* mice with various degrees of whorls and clusters of spindle-shaped cells within these tumors – typical morphological characteristics of mesenchymal cells(16) – we looked at molecular markers associated with EMT. We found that the majority of the luminal tumors from *p18^{-/-}* mice highly expressed E-cadherin (Cdh1), an epithelial marker, whereas basal-like tumors from *p18^{-/-};Brca1^{+/-}* mice expressed very weak and heterogeneous Cdh1. In contrast, most (77%, n=13) of *p18^{-/-};Brca1^{+/-}* tumors that developed after one year of age were stained positive for mesenchymal markers including fibronectin (Fn), vimentin (Vim), and CD29, while only 11% (n=19) of *p18^{-/-}* tumors that developed at a similar age were positive for these markers (Fig. 1A-C, Table 1). This observation suggests that heterozygous germline mutation of *Brca1* activates EMT in mammary tumor progression.

Consistently, *p18^{-/-};Brca1^{+/-}* tumor cells that were positive for Ck5 expressed very low levels of Cdh1 and the majority of Fn positive cells co-expressed Ck5 (Fig. 1B). These data suggest, at the least, that some Ck5+ basal-like tumor cells lost their epithelial characteristics and gained mesenchymal features. In further analysis of these tumors for the expression of CD29 , a basal and mesenchymal marker(19) demonstrated to be

enriched in breast CSCs(20, 21), we found that 69% (n=13) of *p18*^{-/-};*Brca1*^{+/-} tumors expressed various degrees of CD29 positive tumor cells from 2%-60% while only 11% (n=19) of *p18*^{-/-} tumors were positive for CD29 in 2-3% of tumor cells (Fig. 1C, Table 1). These observations support the notion that EMT activation, as previously demonstrated(19, 22), results in cancer cells gaining stem cell properties. Primary *p18*^{-/-};*Brca1*^{+/-} tumor cells formed more and larger colonies in matrigel than *p18*^{-/-} tumor cells (Fig. 1E) and Ck5/Ck8 double positive tumor cells were frequently detected in *p18*^{-/-};*Brca1*^{+/-} tumors but rarely in *p18*^{-/-} tumors, 1.1% (67/6100) vs. 0.04% (2/5120) (Fig. 1F and (9, 16)) which further suggests increased CSCs in *p18*^{-/-};*Brca1*^{+/-} tumors. Together, these results indicate that heterozygous germline mutation of *Brca1* induces EMT, increases CSCs, and transforms p18 null luminal tumors into basal-like tumors.

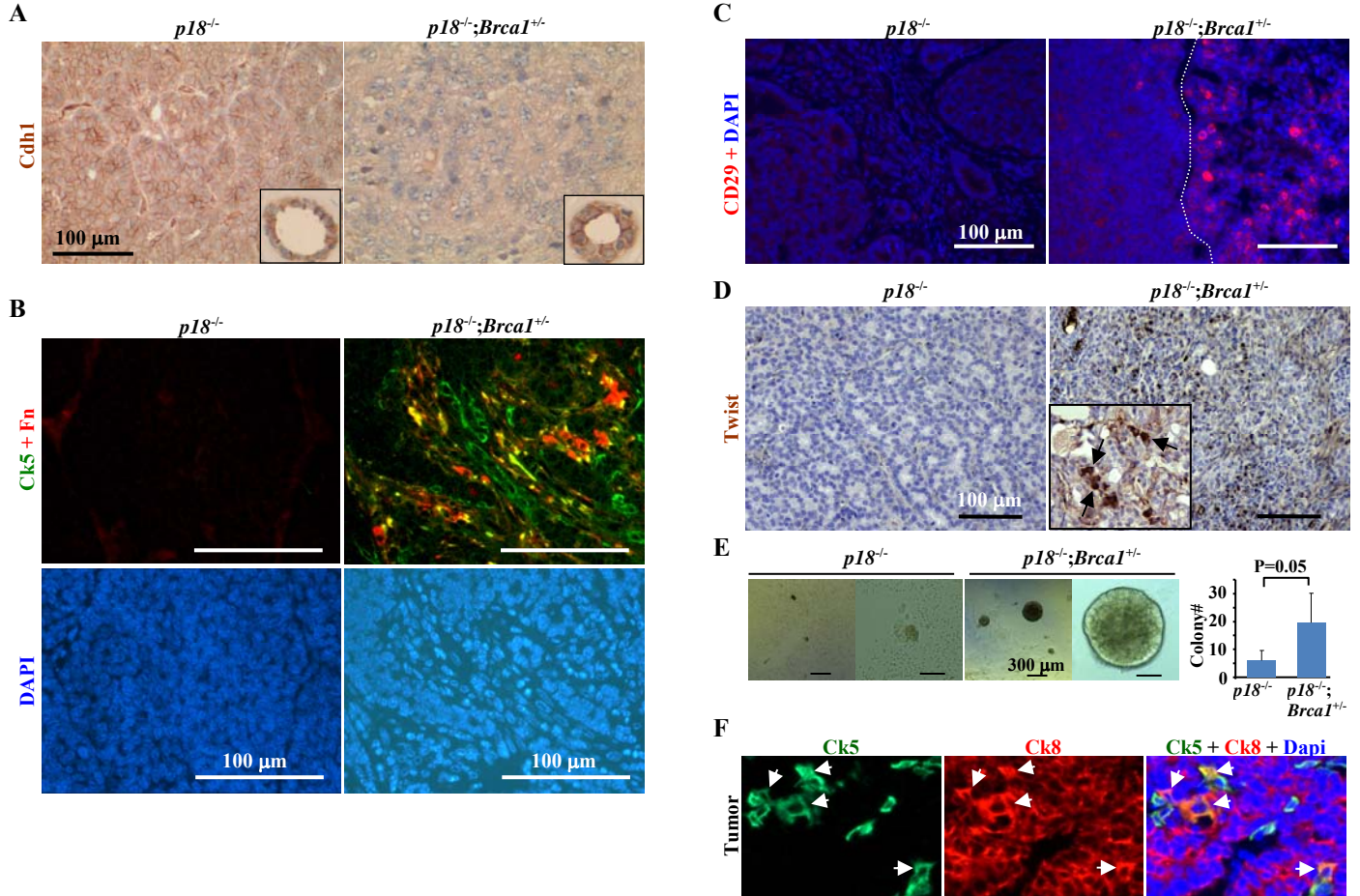


Figure 1. *Brca1* heterozygosity transforms p18-deficient luminal tumors into basal-like tumors with EMT features. (A-D) Representative immunostaining of tumors with Cdh1 (A), Ck5 and Fn1 (B), CD29 (C), and Twist (D). The inset in (A) shows staining of normal glands in the same mouse and in (D) shows staining of lung metastasis. (E) Tumor cells were cultured for two weeks and colonies larger than 300μm were counted. The bar graphs represent the mean ± SD of two tumors per genotype. (F) Representative immunostaining of tumors from *p18*^{-/-};*Brca1*^{+/-} mice with Ck5 and Ck8. Ck5+Ck8+ cells are indicated.

(2) Germline mutation of *Brca1* activates EMT-TFs in mammary and tumor development

We then determined the expression of EMT-TFs and observed that 77% (n=13, >one year of age) of *p18*^{-/-};*Brca1*^{+/-} tumors were stained positive for Twist, Foxc1, Foxc2, Slug, and Snail in greater than 2% of cells per tumor whereas 16% (n=19, >one year of age) of *p18*^{-/-} tumors were positive at similar ages (Fig. 1D, Table 1). Tumors with high expression of EMT-TFs showed high histological grade and strong invasive and metastatic potential as evidenced by EMT-TF positive staining in the invasive front of tumors and metastasized cancers (Fig. 1D). The expression pattern and percentage of positive cells in tumors stained for EMT-TFs and EMT markers were highly correlated with its genotype – *p18*^{-/-} or *p18*^{-/-};*Brca1*^{+/-}, – which not only confirms that germline mutation of *Brca1* promotes EMT in mammary tumors but that this induction of EMT is very likely a result of the aberrant activation of EMT-TFs in *Brca1* mutant tumors. We next isolated mammary epithelial

cells (MECs) from tumor-free virgin mice and found that *Brca1*^{+/−} and *p18*^{−/−};*Brca1*^{+/−} cells expressed significantly less *Cdh1* and more EMT-TFs than WT or *p18*^{−/−} cells (data not shown). These results indicate that EMT-TF activation in *Brca1* mutant MECs occurs prior to tumor initiation.

Table 1. Characterization of spontaneous mammary tumors derived from mutant mice in Balb/c enriched background

Tumor	Wt		<i>p18</i> ^{−/−}		<i>Brca1</i> ^{+/−}		<i>p18</i> ^{−/−} ; <i>Brca1</i> ^{+/−}	
	<12 m	12-27 m	<12 m	12-22 m	<12 m	12-27 m	<12 m	12-22 m
Mammary Tumor	0/5	1/10 ^a (10%)	4/16 (25%)	19/23 ^b (83%)	0/3	1/11 ^c (9%)	6/16 (38%)	13/15 ^d (87%)
Metastasis^e		0/1	0	1/19		0/1	0	4/13
ERα+ tumor % ERα+ cells/tumor		1/1 5%	3/4 2-40%	15/19 2-40%		0/1	1/6 <2%	2/13 <2%
Ck5+ tumor % Ck5+ cells/tumor		0/1	0/4	3/19 ^f 1-5%		1/1 ~2%	4/6 2-20%	11/13 ^g 2-95%
EMT marker+ tumor^h		0/1	0/4	2/19 (11%)		0/1	2/6 (33%)	10/13 (77%)
EMT-TF+ tumorⁱ		0/1	0/4	3/19 (16%)		1/1 (100%)	3/6 (50%)	10/13 (77%)

^a 24-month-old tumor-bearing mouse.

^b Most tumor-bearing mice were 12-16 months old and the oldest was 22 months old. One male developed mammary tumor.

^c 25.5-month-old tumor-bearing mouse.

^d Most tumor-bearing mice were 12-16 months old, and the oldest was 20 months old. One male developed mammary tumor.

^e Mammary tumors metastasized mostly to the lung except one to a blood vessel in a *p18*^{−/−};*Brca1*^{+/−} mouse.

^f One tumor stained positive for Ck5 in ~5% tumor cells and the other two were positive in ~1% tumor cells.

^g Two tumors stained positive for Ck5 in ~95% tumor cells.

^h At least two EMT markers (decreased *Cdh1*, increased Vim, Fn1, Sma or Cd29) were detected in >2% tumor cells.

ⁱ At least two EMT-inducing transcription factors (EMT-TFs), which include Twist, Slug, Snail, *Foxc1* and *Foxc2*, stained positive in >2% tumor cells.

(3) Specific deletion of *Brca1* in mammary epithelia activates EMT and induces aberrant differentiation of LSCs

To directly test the function of *Brca1* in controlling and transforming MECs as well as to determine the implications of loss of *Brca1* on mammary tumorigenesis, we generated *Brca1*^{f/f};MMTV-cre⁺ and *Brca1*^{fl/fl};MMTV-cre⁺ mice with and without *p18* mutation in Balb/c-B6 mixed background, in which MMTV-cre (MC) is active in virgin epithelia but not in stroma(23, 24). Using these mice also enabled us to rule out the impact of *Brca1* mutant stroma on mammary stem cell self-renewal and tumorigenesis.

Brca1^{fl/fl};MC and *p18*^{−/−};*Brca1*^{fl/fl};MC breasts expressed <5% of *Brca1* protein and mRNA relative to the levels in *Brca1*^{+/+};MC and *p18*^{−/−};*Brca1*^{+/+};MC, indicating an efficient and near complete depletion of *Brca1* in the mammary epithelia (Fig. 2A, B). Similarly, *Brca1*^{f/f};MC and *p18*^{−/−};*Brca1*^{f/f};MC breasts expressed <20% of *Brca1* protein and mRNA relative to the levels in MC and *p18*^{−/−};MC (data not shown). Consistent with the data from *Brca*^{+/−} mice(16), the expression of *Gata3*, *Cdh1*, and *Epcam* – genes associated with luminal differentiation – in *Brca1*^{fl/fl};MC and *p18*^{−/−};*Brca1*^{fl/fl};MC breasts was significantly reduced relative to *Brca1*^{+/+};MC and *p18*^{−/−};*Brca1*^{+/+};MC breasts (Fig. 2A, B), suggesting that loss of *Brca1* impairs luminal differentiation. MECs from *p18*^{−/−};*Brca1*^{fl/fl};MC mice showed increased mammosphere-forming ability than those from *p18*^{−/−};*Brca1*^{f/f};MC mice. Most *p18*^{−/−};*Brca1*^{f/f};MC mammospheres were 35-45μm and none larger than 100μm whereas 10-15% of *p18*^{−/−};*Brca1*^{fl/fl};MC mammospheres were larger than 100μm. The average *p18*^{−/−};*Brca1*^{fl/fl};MC mammosphere was significantly larger than that of *p18*^{−/−};*Brca1*^{f/f};MC mammospheres (Fig. 2C). These results suggest that *Brca1* deficiency increased the self-renewal capacity of *p18*^{−/−} mammary stem cells. Accordingly, MECs from *p18*^{−/−};*Brca1*^{fl/fl};MC mice formed more colonies than those from *p18*^{−/−};*Brca1*^{+/+};MC mice and *p18*^{−/−};*Brca1*^{fl/fl};MC mammospheres expressed significantly higher levels of EMT-TFs than those of *p18*^{−/−};*Brca1*^{f/f};MC (Fig. 2D, E). These results confirms that loss of *Brca1* activates EMT-TFs, which is likely responsible for the induction of EMT and increased mammosphere- and colony-forming potential in *p18*^{−/−};*Brca1*^{fl/fl};MC MECs.

We then performed FACS and found that *p18^{-/-};Brca1^{f/+}*;MC MECs had a reduced CD24⁺CD29⁻ LSC-enriched population and increased CD24⁺CD29⁺ BSC-enriched population compared to *p18^{-/-};Brca1^{f/+}*;MC MECs at 22 weeks of age (Fig. 2F). Similar, but less significant, trends were also observed in *p18^{-/-};Brca1^{f/+}*;MC mice relative to *p18^{-/-}*;MC mice at 16 weeks of age (data not shown). These results suggest that Brca1 deficiency results in the expansion of BSCs and blockage of LSCs, the latter of which is consistent with our findings derived from heterozygous germline *Brca1* mutant mice(16).

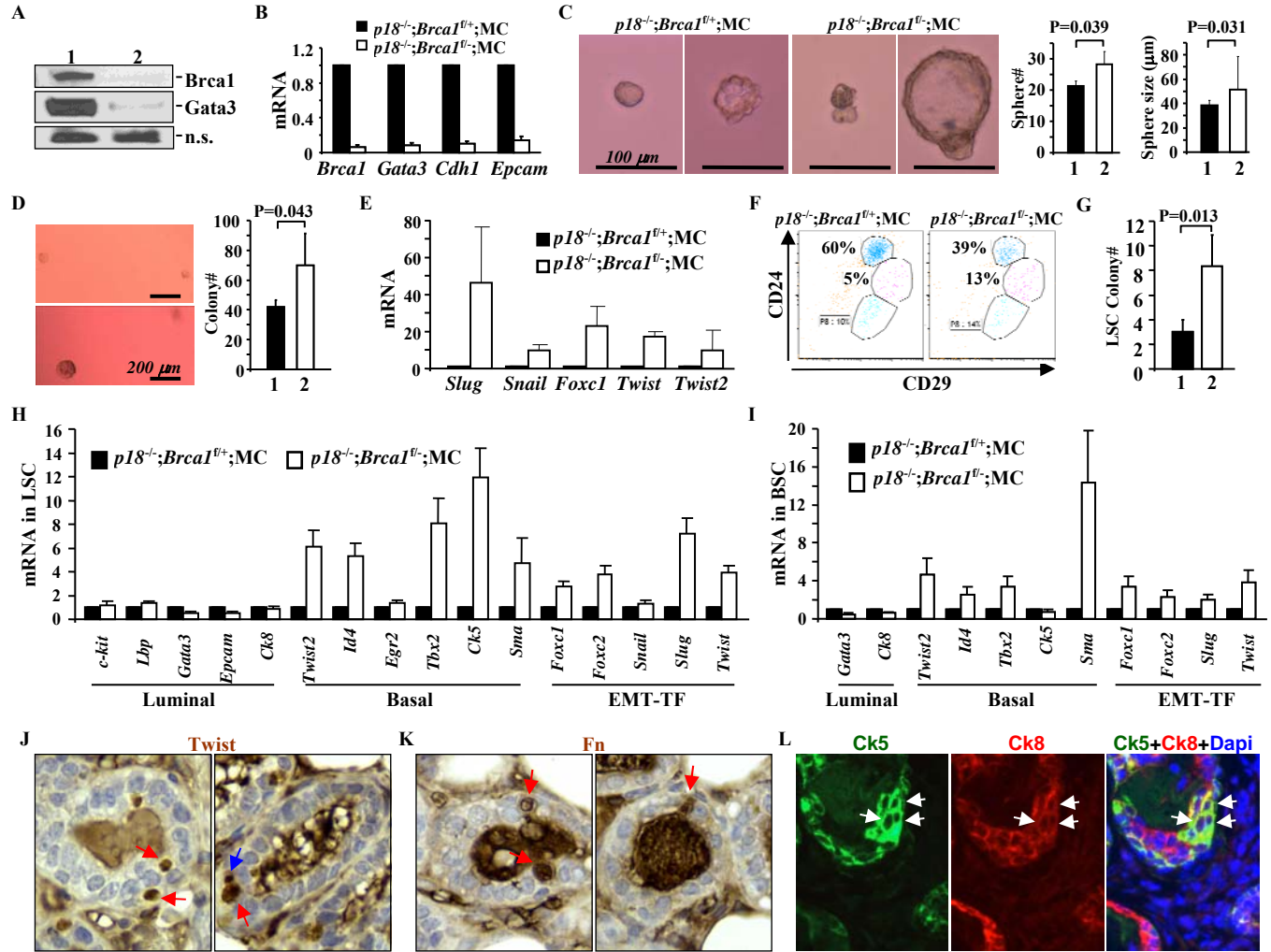


Figure 2. Deletion of Brca1 in mammary epithelia inhibits luminal differentiation and activates EMT-TFs in mammary stem cells. (A, B) Mammary tissues from *p18^{-/-};Brca1^{f/+}*;MC (Lane 1) and *p18^{-/-};Brca1^{f/-}*;MC (Lane 2) mice were analyzed by western blot (A), and Q-RT-PCR (B). n.s., non-specific band. Q-RT-PCR data are expressed as the mean \pm SD from triplicates of each of three separate mice. (C, D) Mammary cells were analyzed by mammosphere (C) and colony formation assay (D). The number of spheres larger than 30 μ m, the sizes of spheres, and the number of colonies larger than 30 \square m were quantified. 1, *p18^{-/-};Brca1^{f/+}*;MC; 2, *p18^{-/-};Brca1^{f/-}*;MC. The bar graphs represent the mean \pm SD of two animals per genotype. (E) RNA from mammospheres was analyzed. Data are expressed as mean \pm SD from triplicates of each of two separate mice. (F) Mammary cells were analyzed by flow cytometry. (G) FACS-sorted LSCs from (F) were analyzed by colony formation assay. The bar graphs represent the mean \pm SD of two animals per genotype. 1, *p18^{-/-};Brca1^{f/+}*;MC; 2, *p18^{-/-};Brca1^{f/-}*;MC. (H, I) RNA from LSCs (H) and BSCs (I) was analyzed. Data are expressed as the mean \pm SD from triplicates of each of two separate mice. (J, K, L) Tumor-free mammary glands from *p18^{-/-};Brca1^{f/-}*;MC mice were stained with antibodies against Twist (J), Fn (K), Ck5 and Ck8 (L). Twist or Fn positive ULLC (red arrows) and SLC (blue arrows), as well as Ck5+Ck8+ epithelial cells (white arrows) are indicated.

FACS-sorted cells of the BSC-enriched population expressed higher basal genes (*Twist2*, *Id4*, and *Tbx2*) and lower luminal genes (*c-kit*, *Epcam*, and *Gata3*) than those of the LSC-enriched population, confirming that these cell populations are, as reported(25), the basal and luminal cell enriched populations, respectively (data not shown). LSCs derived from *p18^{-/-};Brca1^{f/-}*;MC mice formed more colonies in matrigel and expressed lower

luminal and epithelial genes and significantly higher basal genes and EMT-TFs when compared with *p18;Brca1^{f/+}*;MC LSCs (Fig. 2G, H). Consistently, LSCs from *p18^{-/-};Brca1^{f/+}*;MC mice also expressed lower luminal genes and higher basal genes and EMT-TFs than those from *p18^{-/-}*;MC mice (data not shown). These results indicate that haploid or near complete loss of *Brca1* in mammary epithelium not only inhibits the expression of luminal genes but also stimulates the expression of basal genes and EMT-TFs in *p18^{-/-}* LSCs. Interestingly, expression of basal genes and EMT-TFs was also significantly increased in the BSCs from *p18^{-/-};Brca1^{f/-}*;MC mice relative to those from *p18;Brca1^{f/+}*;MC mice (Fig. 2I). Together, these results suggest that *Brca1* deficiency results in the expansion of BSCs that is likely, at least partially, resulting from the dedifferentiation of LSCs.

We have previously analyzed five histologically distinct epithelial cell populations and defined the small light cell (SLC) and undifferentiated large light cell (ULLC) populations as enriched for stem and luminal stem/progenitor cells, respectively(9). To determine the impact of EMT on stem/progenitor cell populations *in situ*, we examined tumor-free mammary glands and found that Twist or Fn positive MECs were frequently detected in *p18^{-/-};Brca1^{f/-}*;MC or *p18^{-/-};Brca1^{f/f}*;MC mice but not in *p18^{-/-}*;MC mice and that most, if not all, Twist or Fn positive cells were either SLC or ULLC, ULLC in particular (Fig. 2J, K). Furthermore, Ck5 and Ck8 double positive epithelial cells were also frequently detected in *p18^{-/-};Brca1^{f/-}*;MC but not in *p18^{-/-}*;MC mammary (Fig. 2L, and data not shown). These results further suggest that loss of *Brca1* in MECs activates Twist, induces EMT, and leads to dedifferentiation of LSCs.

(4) Specific deletion of *Brca1* in mammary epithelia recapitulates basal-like tumorigenesis and EMT activation

To determine the tumorigenic impact of specific loss of *Brca1* in mammary epithelia, we first examined *Brca1^{f/-}*;MC and *p18^{-/-};Brca1^{f/-}*;MC mice and found that no hyperplasia nor tumors developed in 5 female *Brca1^{f/-}*;MC mice at 10-12 months of age. Of the 8 *p18^{-/-};Brca1^{f/-}*;MC mice examined at similar ages, all developed mammary hyperplasia though no mammary tumors were detected. A majority (7/8) of *p18^{-/-};Brca1^{f/-}*;MC mice died at early ages from carcinomas in the pancreas, skin, pituitary or lung (data not shown), very likely due to active MMTV-Cre expression and near complete deletion of *Brca1* in these tissues(26), which prevented us from observing the relatively late onset mammary tumorigenesis in these mice. These results, however, confirm the previous findings that loss of *Brca1* alone is insufficient to promote tumorigenesis and that *Brca1* cooperates with *p18* to control tumorigenesis.

We then examined *p18^{-/-};Brca1^{f/+}*;MC and *p18^{-/-};Brca1^{f/f}*;MC mice and found that 1 of 4 *p18^{-/-};Brca1^{f/+}*;MC mice and 4 of 5 *p18^{-/-};Brca1^{f/f}*;MC mice developed mammary tumors in 12-16 months (Fig. 3). In accordance with the tumors developed in *p18^{-/-};Brca1^{+/-}* mice, mammary tumors in *p18^{-/-};Brca1^{f/+}*;MC and *p18^{-/-};Brca1^{f/f}*;MC mice were also highly heterogenous, poorly differentiated, and more aggressive than those developed in *p18^{-/-}* mice (Fig. 3, Fig. 1, and data not shown). About 25-30% *p18^{-/-};Brca1^{f/+}*;MC tumor cells were spindle-shaped and were positive for Twist and Fn (Fig. 3A, B), and more than 40% of the tumor cells were positive for Ck5 and negative for Cdh1 or Ck8 (Fig. 3C, D), indications of a basal-like tumor undergoing EMT. The *p18^{-/-};Brca1^{f/+}*;MC mammary tumors also expressed 1/3 of *Brca1* and 1/5 of *Gata3* relative to the tumor-free mammary tissues of the same mouse (Fig. 3E), confirming deficient *Brca1* and downregulation of *Gata3* in the tumor.

More than 25% of tumor cells were spindle-shaped in all four *p18^{-/-};Brca1^{f/f}*;MC mammary tumors and two displayed more than 90% spindle-shaped cells (Fig. 3F). These tumors were also positive for Twist and Fn (Fig. 3G), indications of typical metaplastic breast carcinomas undergoing EMT. A *p18^{-/-};Brca1^{f/f}*;MC tumor expressed less than 10% *Brca1* and *Gata3* when compared to tumor-free mammary of the same mouse (Fig. 3I). FACS showed that the LSC-enriched population in *p18^{-/-};Brca1^{f/f}*;MC mammary tumors was significantly reduced in comparison to the tumor-free mammary tissues of the same mouse (6% versus 56%) and when compared to *p18^{-/-}* mammary tumor cells (6% versus 57%). Contrastingly, the BSC-enriched population, also enriched with breast CSCs, was significantly expanded in *p18^{-/-};Brca1^{f/f}*;MC mammary tumors relative to the tumor-free mammary tissues of the same mouse (19% versus 11%) and when compared to *p18^{-/-}* mammary tumor cells (19% versus 4%) (Fig. 3H). These results further support that *p18^{-/-};Brca1^{f/f}*;MC mammary tumors

are basal-like tumors undergoing EMT that are enriched with CSCs, which is in line with the data derived from human patients showing that metaplastic breast carcinomas are basal-like breast cancers with EMT-like molecular make-up and are closely correlated with BRCA1 dysfunction(27).

Taken together, these results suggest that insufficient Brca1 in mammary epithelial cells represses Gata3, activates Twist and EMT, and results in basal-like tumorigenesis with an increase in the CSC population. Since *p18^{-/-};Brca1^{fl/fl}*;MC and *p18^{-/-};Brca1^{fl/fl}*;MC mice are in B6 and Balb/c mixed backgrounds, unlike *p18^{-/-};Brca1^{+/+}* mice in pure Balb/c background, these data also suggest that the role of Brca1 controlling basal-like tumorigenesis and EMT is independent of genetic background.

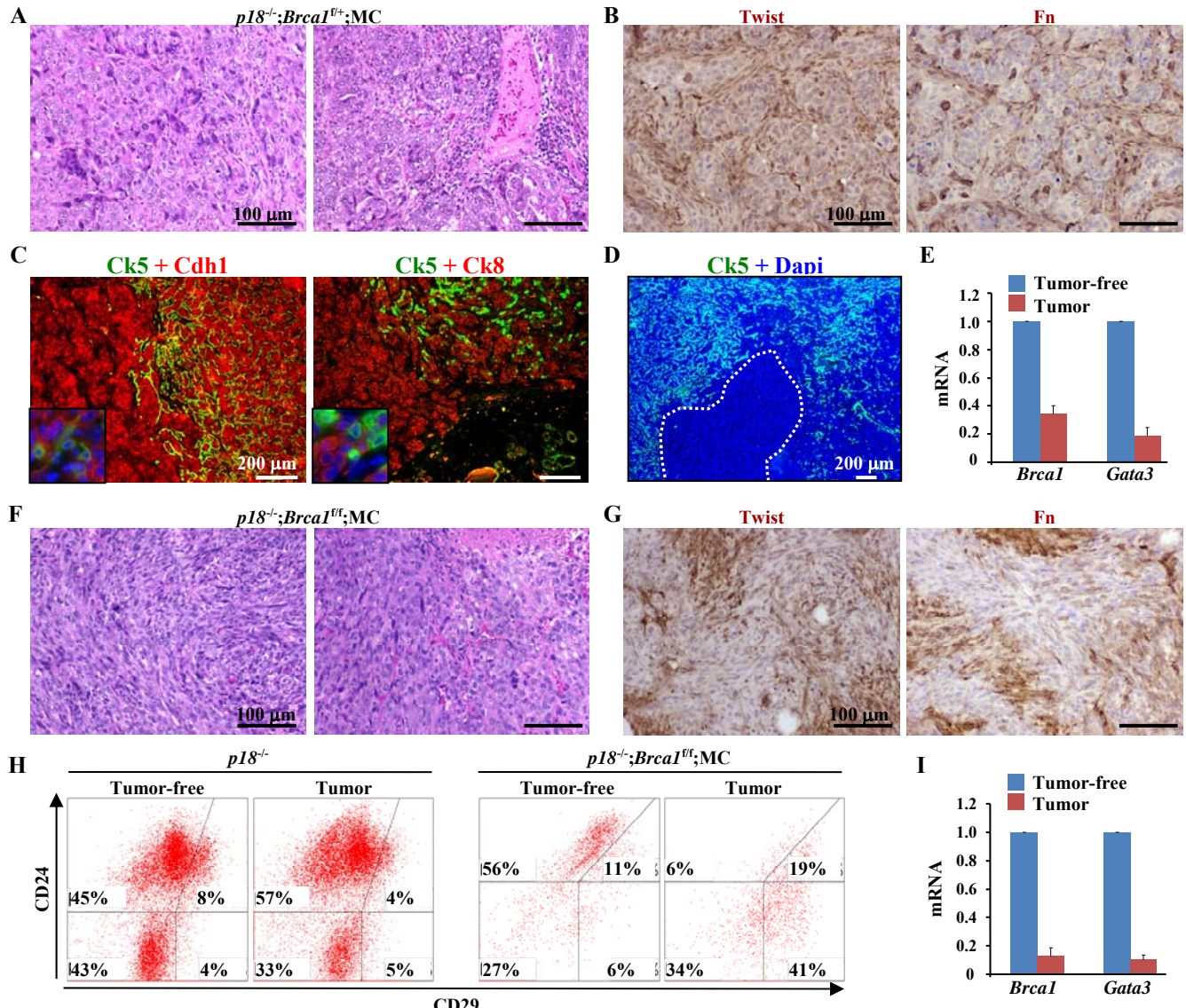


Figure 3. Deletion of Brca1 in mammary epithelia recapitulates basal-like tumor formation and EMT activation. Mammary tumors derived from *p18^{-/-};Brca1^{0+/-}*;MC (A-E) or *p18^{-/-};Brca1^{fl/fl}*;MC (F-I) mice were stained with H.E (A, F), Twist or Fn (B, G), Ck5 and Cdh1 or Ck8 (C), Ck5 (D), or analyzed by Q-RT-PCR (E, I) and FACS (H). Tumor-free mammary cells or tissues from the same mouse were used as controls. Q-RT-PCR data are expressed as the mean ± SD from triplicates.

We transplanted primary tumor cells derived from *p18^{-/-}* and *p18^{-/-};Brca1^{fl/fl}*;MC mice into mammary fat pad (MFP) of NSG mice. We found that *p18^{-/-};Brca1^{fl/fl}*;MC tumor cells regenerated basal-like breast tumors in recipient mice whereas *p18^{-/-}* cells did not yield tumors in the same time period with the same cell numbers (Fig. 3B, C). These results suggest that loss of Brca1 in *p18* deficient mice enhances CSC properties.

Genotype	# of tumor cells transplanted	Tumor incidence*
<i>p18^{-/-}</i>	3×10^6	0/4
<i>p18^{-/-};Brca1^{fl/fl};MC</i>	3×10^6	3/3
	0.5×10^6	2/2
	0.1×10^6	4/4

Table 2. Loss of Brca1 promotes CSC properties. Primary tumor cells were transplanted into MFP of NSG mice. 4 weeks post-transplantation, tumors developed in recipient mice were counted and analyzed. All regenerated tumors are basal-like tumors and 0.8-1.3 cm³ in size

(5) BRCA1 suppresses TWIST transcription and EMT

We screened a panel of human breast cancer cell lines and found that MCF7 and T47D cells expressed higher CDH1 and GATA3 and lower VIM and EMT-TFs than SUM149 and HCC1937 cells (data not shown), confirming that MCF7 and T47D cells are luminal/epithelial-like and SUM149 and HCC1937 cells are basal/mesenchymal-like cancer cells in our culture system(28). Transfection of WT *BRCA1* into HCC1937 (*BRCA1* mutant, transcriptionally null) cells resulted in increase of *CDH1* and decrease of *VIM* and *FN*, indicating that BRCA1 suppresses EMT. Importantly, ectopic expression of BRCA1 significantly repressed *TWIST* by more than 50% compared to control, moderately repressed *FOXC2*, but hardly repressed other EMT-TFs (Fig. 4A). A similar inhibitory effect on *TWIST* and *FOXC2* expression was also detected in 293T cells transfected with BRCA1 (data not shown). Since the ability of BRCA1 in regulating transcription controls normal differentiation and suppresses tumor development(29, 30), we determined whether BRCA1 is recruited to the *TWIST* promoter. A previous study demonstrated that GATA3 recruits BRCA1 to its binding sites in the *FOXC1/2* promoters to repress their transcription(31). We performed bioinformatic analysis of the *TWIST* gene promoter and found that there exists, at the least, six putative GATA3 binding sites on the *TWIST* promoter (Fig. 4B), which are conserved in both human and mouse (data not shown). We then performed a ChIP assay and found that one of five amplicons that contained two GATA3 sites was specifically enriched in the immunoprecipitation of BRCA1 in HCC1937 cells transfected with WT *BRCA1* compared to control (P5 in Fig. 4C). In sum, these results suggest that BRCA1 specifically binds to the *TWIST* promoter and negatively regulates its transcription.

To confirm the role of Brca1 in the suppression of Twist and tumor development *in situ*, primary mammary tumors derived from *p18^{-/-};Brca1^{+/+}* mice were immunostained with antibodies against Brca1 and Twist. We found that tumor cells positive for Brca1 expressed very low or no Twist whereas Brca1 mutant tumor cells expressed high levels of Twist, most of which were spindle-shaped basal-like cells (Fig. 4D), demonstrating that Brca1 inhibits Twist and EMT in mammary tumor development and progression.

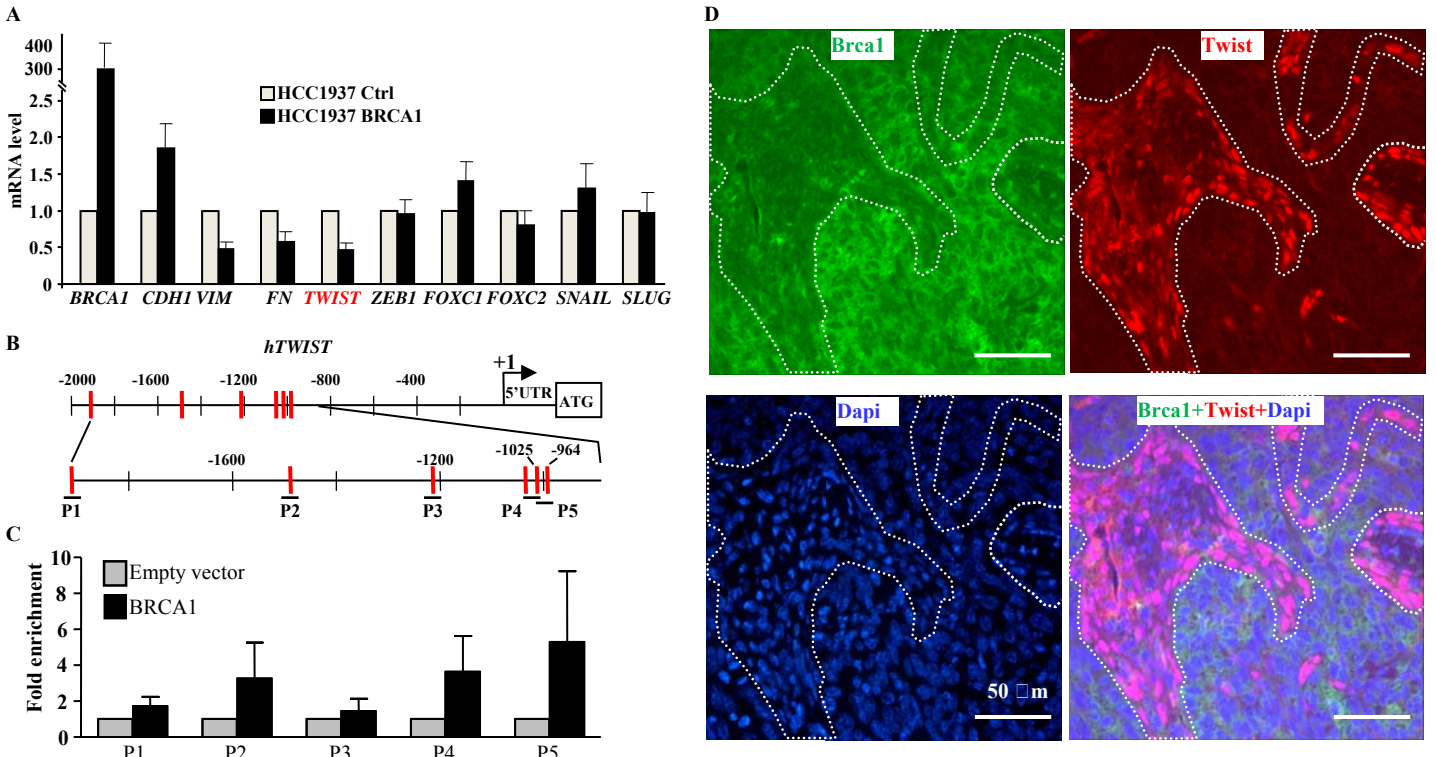


Figure 4. BRCA1 suppresses TWIST and EMT in mammary tumor cells. (A) HCC1937 cells were transfected with pcDNA3-empty (Ctrl) or pcDNA3-BRCA1 (BRCA1) and RNA was analyzed. Data are expressed as the mean \pm SD from triplicates of two independent experiments. (B) Diagram showing the locations of putative GATA3 sites in the human *TWIST* gene. (C) ChIP analysis of BRCA1 binding to putative GATA3 sites on the *TWIST* promoter in HCC1937 cells transfected with *BRCA1*. Data are expressed as the mean \pm SD from triplicates of two independent experiments. (D) Mammary tumors from *p18^{-/-};Brca1^{+/+}* mice were stained with antibodies against Brca1 (green) and Twist (red).

(6) Knockdown of BRCA1 activates TWIST and EMT with enhanced tumor formation potential

We knocked down BRCA1 in two human luminal cancer cell lines, MCF7 and T47D, using BRCA1 shRNA targeting 3 different sequences (Fig. 5A, and data not shown), and transplanted these cells into the mammary fat pads of NSG mice. We found that mammary tumors from T47D-Sh-BRCA1 cells were palpable in eight weeks whereas tumors formed from T47D-Sh-Ctrl. cells were undetectable at this stage (data not shown). Eighteen weeks after transplantation, T47D-Sh-BRCA1 tumors were significantly bigger than T47D-Sh-Ctrl. tumors (Fig. 5B, C). Consistently, mammary tumors from MCF7-Sh-BRCA1 cells were palpable significantly sooner and were larger compared to tumors from MCF7-Sh-Ctrl. cells (data not shown). These results indicate that knockdown (KD) of BRCA1 in luminal cancer cells enhances their tumor formation potential. Histo- and pathological analysis revealed that, unlike homogeneous and well differentiated T47D-Sh-Ctrl. mammary tumors, T47D-Sh-BRCA1 tumors were highly heterogeneous with an abundance of large and poorly differentiated cells (Fig. 5D), suggesting that KD of BRCA1 induced the dedifferentiation of luminal tumor cells. IHC analysis indicated that most cells in T47D-Sh-BRCA1 tumors expressed very faint or no CDH1 and ER \square but high levels of TWIST, VIM, and FN in comparison to T47D-Sh-Ctrl. tumors (Fig. 5E-G, data not shown), indicating that T47D-Sh-BRCA1 tumor cells had undergone EMT. These results collectively suggest that KD of BRCA1 in breast luminal tumor cells activates TWIST and EMT which is associated with increased tumor formation potential, further supporting the data derived from *p18;Brca1* double mutant mice.

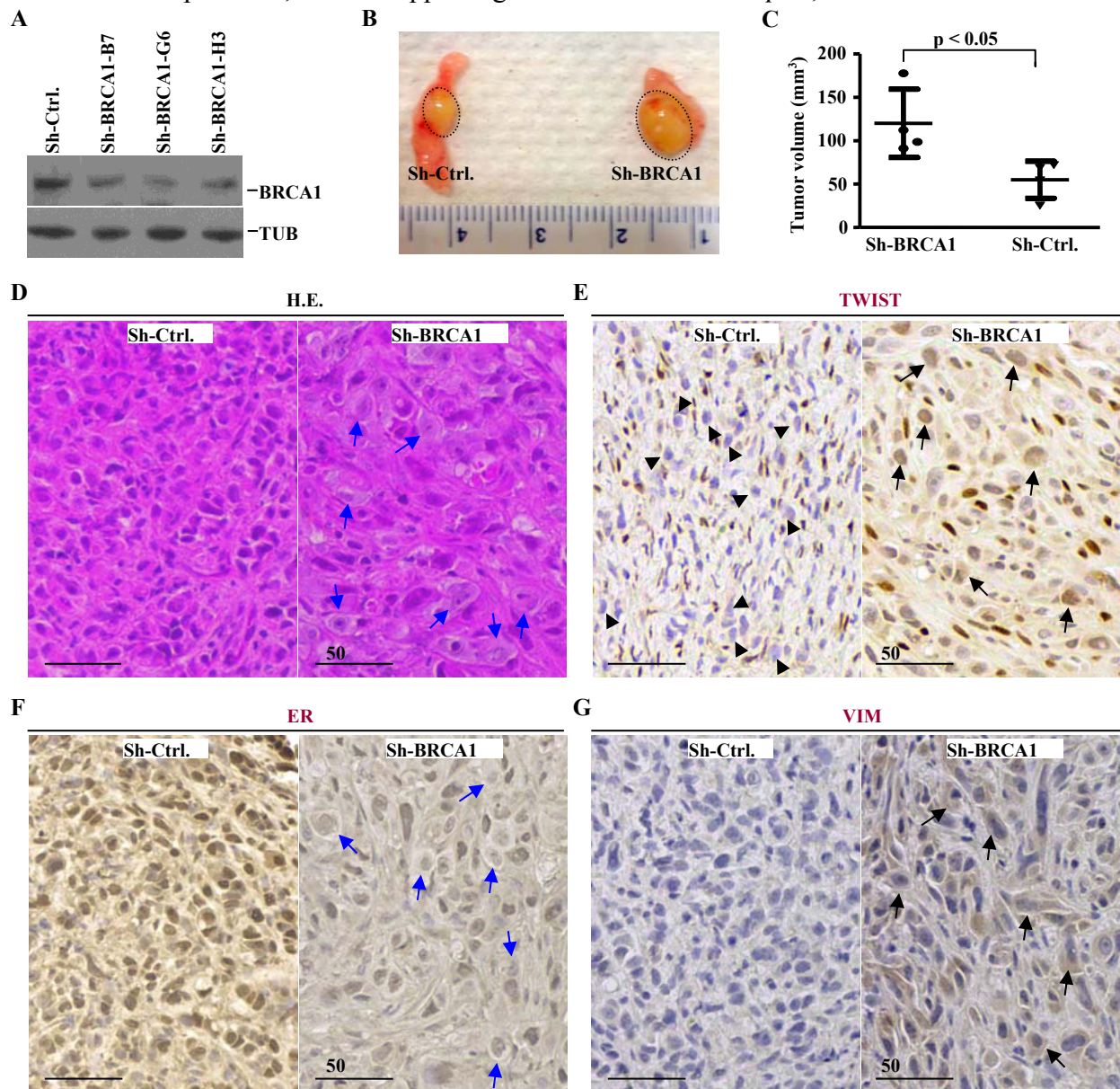


Figure 5. Knockdown of BRCA1 in luminal cancer cells increases tumor formation potential and TWIST expression

(A) T47D cells were infected with either pGIPZ-empty (sh-Ctrl.) or pGIPZ-shBRCA1 targeting different sequences of human *BRCA1* (sh-BRCA1-B7, sh-BRCA1-G6, and sh-BRCA1-H3). Cells stably expressing sh-Ctrl or shBRCA1 were analyzed by Western blot. (B, C) T47D cells stably expressing sh-Ctrl or shBRCA1-G6 (sh-BRCA1) were transplanted into the mammary fat pads of female NSG. Representative gross appearance of tumors formed is shown (B) and tumor volumes were plotted (C). Values represent the average tumor volumes \pm SD of 4 tumors. (D - G) Mammary tumors formed by transplantation of T47D cells stably expressing sh-Ctrl or sh-BRCA1 were stained with H.E (D), TWIST (E), ER α (F), and VIM (G). Note the highly heterogeneous Sh-BRCA1 tumor cells that are positive for TWIST and VIM (black arrows) and negative for TWIST (black arrowheads) and for VIM in Sh-Ctrl. tumors. Large and less-differentiated cells in Sh-BRCA1 tumors are indicated by blue arrows.

(7) *BRCA1* and *TWIST* expression are inversely related in human claudin-low type breast cancers

Gene expression profiling analyses have categorized human breast tumors into six intrinsic subtypes: basal-like (BL), claudin-low (CL), Her2+ (H2), luminal A (LA), luminal B (LB), and normal breast-like (NBL), each of which has unique biological and prognostic features(32). Of these subtypes of breast cancer, the CL subtype is characterized by the low to absent expression of luminal differentiation markers and high enrichment for EMT markers and cancer stem cell-like features. Clinically, the majority of CL tumors are poor prognosis triple negative (ER-, PR-, and HER2-) invasive carcinomas with high frequencies of metaplastic and medullary differentiation(32-34). To determine whether our mouse genetic analysis models human breast cancers, we queried the expression of *BRCA1* and EMT-TFs in the UNC337 breast cancer patient sample sets(32). We found that expression of *BRCA1* and EMT-TFs were highly correlated with breast tumor intrinsic subtypes (Figure 6A). Specifically, the mRNA level of *BRCA1* was low while that of EMT-TFs – *TWIST*, *SNAIL*, and *SLUG* in particular – was high in the CL subtype. Pearson correlation analysis revealed an inverse correlation between *BRCA1* with *TWIST* mRNA levels, but not with *SNAIL*, *SLUG*, and *FOXC1* (Fig. 6B). We performed similar analyses on the MetaBric dataset with 2,000 breast tumors(35) and detected similar results – *BRCA1* and *TWIST* mRNA levels were inversely correlated in all breast cancers and in the CL subtype in particular (data not shown).

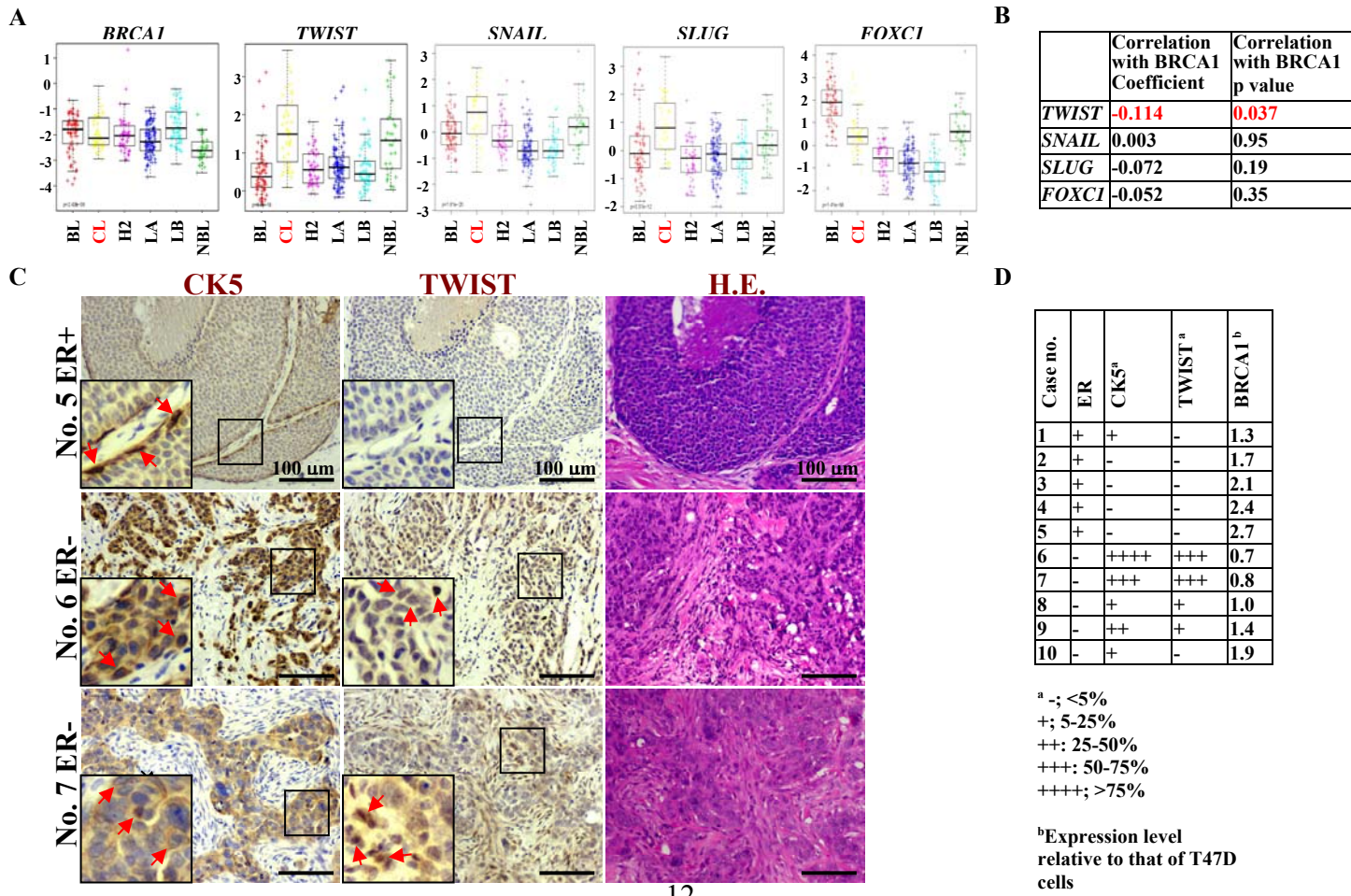


Figure 6. BRCA1 and TWIST levels are inversely related to the CL subtype of human breast cancer. (A) Analysis of gene expression in UNC337 breast cancer patients according to tumor subtype. (B) Correlation analysis of the expression of *BRCA1* and EMT-TFs for UNC337 breast cancer patients. (C) Serial sections from ER positive and negative invasive human breast cancers were stained with H.E., CK5, and TWIST. The boxed areas were enlarged in the insets. Representative cytoplasmic staining of CK5+ cells and nuclear staining of TWIST+ cells are indicated by arrows. (D) Summary of expression of CK5 and TWIST by IHC and *BRCA1* by Q-RT-PCR. The expression levels of CK5 and TWIST were scored by the percentage of positive tumor cells in total tumor cells. The expression of *BRCA1* was determined by Q-RT-PCR. The levels of *BRCA1* mRNA were expressed as the mean values from triplicates of the two sets of the primers.

We screened 43 invasive breast cancers then selected 5 ER positive and 5 ER negative samples. RNA was prepared from microdissected FFPE sections of tumors. The expression levels of *BRCA1* in ER negative tumors were significantly lower than in ER positive tumors (1.16 ± 0.49 versus 2.04 ± 0.56 ; $P=0.015$), reflecting the downregulation of *BRCA1* mRNA in ER negative tumors (Fig. 6D). IHC indicated that TWIST positive tumor cells were only detected in ER negative, CK5 positive tumors, not in ER positive tumors. The expression of TWIST was closely associated with that of CK5 and was inversely correlated with the mRNA level of *BRCA1* (Fig. 6C, D). Furthermore, all TWIST positive tumors were highly heterogeneous, poorly differentiated, and showed typical morphological EMT features, evidenced by the various degrees of whorls and clusters of spindle-shaped cells within these tumors. Together, these clinical findings, consistent with our results in mice, further confirm that BRCA1 suppresses TWIST and EMT in breast basal-like cancer development and progression.

(8) Depletion of both p16 and Brca1 leads to basal-like mammary tumors with EMT features

To determine whether p16 loss induces tumorigenesis for Brca1 deficient MECs, we generated *Brca1^{MGKO}*, *Brca1^{ff}*;MMTV-Cre and *Brca1^{f/-}*;MMTV-Cre mice in p16 deficient background. We found that 63% of the *p16^{f/-};Brca1^{MGKO}* mice (n=8) and 44% of *p16^{+/+};Brca1^{MGKO}* mice (n=9) developed mammary tumors at 11-20 months and 16-23 months, respectively (Table 2), whereas no *p16^{f/-}*, *p16^{+/+}* or *Brca1^{MGKO}* mice did so at similar ages (Table 2). Median mammary tumor-free survival time in *p16^{mt};Brca1^{MGKO}* mice (including *p16^{f/-};Brca1^{MGKO}* and *p16^{+/+};Brca1^{MGKO}* mice) was 18 months (Fig. 7A). These results indicate that haploid or complete loss of p16 transforms Brca1-deficient mammary epithelial cells and induces mammary tumors.

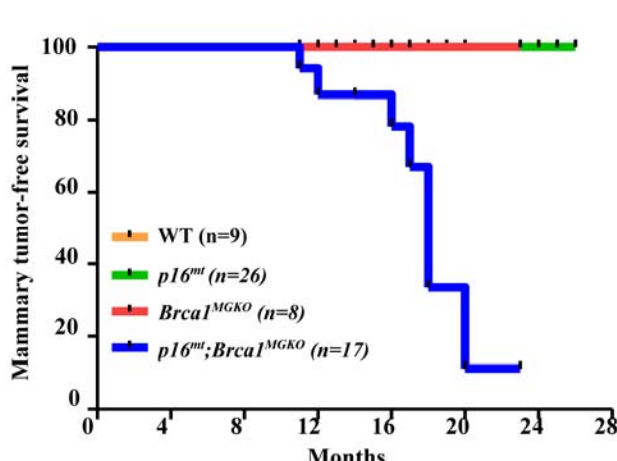
Mammary tumors developed in *p16^{mt};Brca1^{MGKO}* mice were very aggressive and displayed typical morphological characteristics of highly malignant features (increased necrosis, spindle cells, nuclear-cytoplasm ratio, and mitotic indices) (Fig. 7B,D). 18% of the *p16^{mt};Brca1^{MGKO}* mice (n=17) developed two distinct mammary tumors in two separate mammary glands, demonstrating the ability of these mice to develop both intra- and inter-tumoral heterogeneity (Fig. 7B). Furthermore, 56% of the *p16^{mt};Brca1^{MGKO}* mammary tumors (n=9) metastasized to the lung in 17-20 months (Table 2, Fig. 7D). All mammary tumors developed in *p16^{mt};Brca1^{MGKO}* mice were positively stained with basal markers, Ck5 and Ck14 in 2-75% of total tumor cells (Fig. 7C,D). Further analysis revealed that most of these tumor cells expressed significantly reduced levels of Cdh1 protein when compared with levels in luminal cells of the mammary glands. All mammary tumors derived from *p16^{mt};Brca1^{MGKO}* mice were stained positively for Vim and Twist (Table 2). These data indicate that depletion of Brca1 in p16 null mice also results in basal-like mammary tumors with activation of EMT.

Table 2. Spontaneous tumor development in WT and mutant female mice

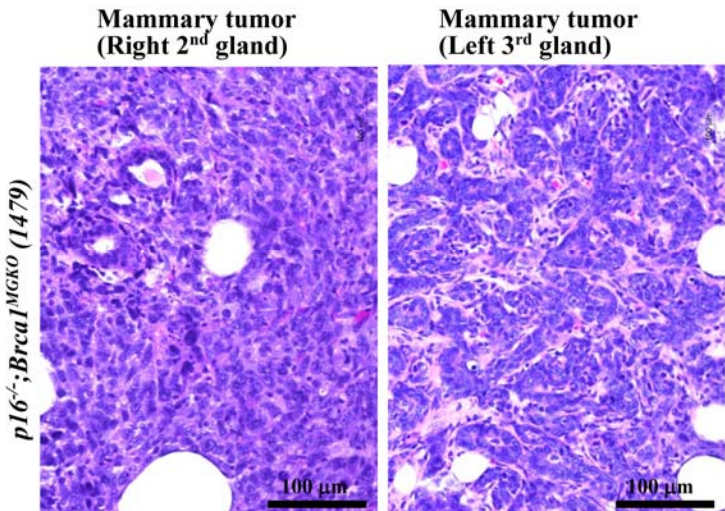
Tumor	Wt	<i>p16^{+/+}</i>	<i>p16^{f/-}</i>	<i>Brca1^{MGKO}</i>	<i>p16^{+/+};Brca1^{MGKO}</i>	<i>p16^{f/-};Brca1^{MGKO}</i>
	11-24 m	11-24 m	11-24 m	11-24 m	11-24 m	11-24 m
Mammary Tumor	0/9	0/6	0/20	0/8	4/9 (44%)	5/8 (63%)
Metastasis					3/4	2/5
CK14+ tumor					4/4	5/5
EMT+ tumor ^a					4/4	5/5
Other tumors	1/9		9/20	1/8	3/9	5/8

^a At least two EMT markers (decreased Cdh1, increased Vim or Twist) were detected in >2% tumor cells.

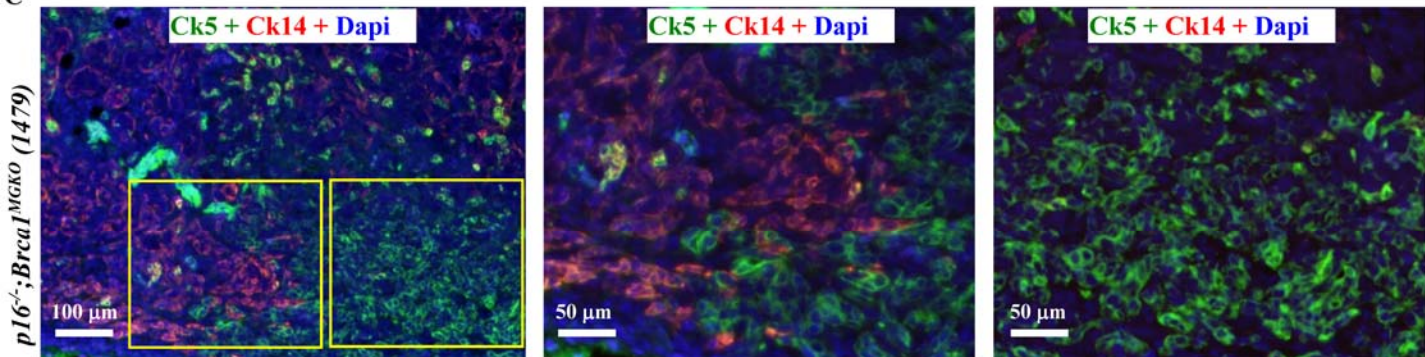
A



B



C



D

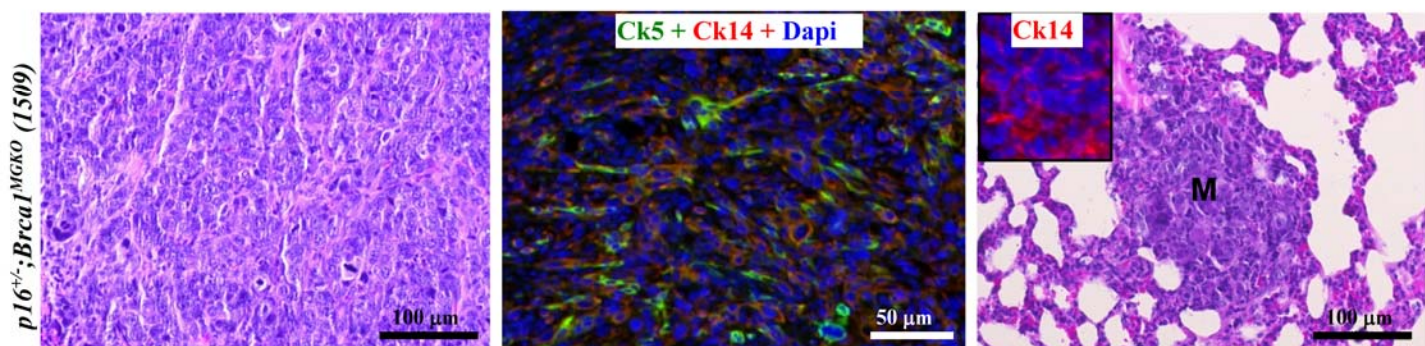


Figure 7. Characterization of primary tumors and distant metastases in p16;Brca1 double mutant mice. (A) Mammary tumor-free survival curve. *p16^{mmt};Brca1^{MGKO}* includes: *p16^{+/−};Brca1^{MGKO}* and *p16^{−/−};Brca1^{MGKO}* mice. *p16^{mmt}* includes: *p16^{+/−}* and *p16^{−/−}* mice. Log-rank (Mantel-cox) test: p<0.0001 (B) H.E. staining of tumors in a *p16^{−/−}; Brca1^{MGKO}* mouse (1479) at 11 months of age. Note this mouse developed two different mammary tumors. (C) Immunofluorescence staining of mammary tumors in mouse 1479 with Ck14 and Ck5. The boxed areas in the left panel are enlarged in the middle and right panels. Note the majority of tumor cells are positive for either Ck5 or Ck14. (D) Immunofluorescence and H.E. staining of mammary tumor in a *p16^{−/−}; Brca1^{MGKO}* mouse (1509) at 18 months of age. Note this tumor was comprised predominately of Ck5 and Ck14+ cells (middle panel) and developed a distant metastasis (M) to the lung (right panel), which also comprised of Ck14+ cells (inset in the right panel).

4. Key Research Accomplishments

(1) Discovery that disrupting *Brca1* by either germline or epithelium-specific mutation in p18-deficient mice activates EMT and induces dedifferentiation of luminal stem cells, which associate closely with expansion of basal and cancer stem cells and formation of basal-like tumors [published in ref. (36)].

- (2) Discovery that BRCA1 binds to the *TWIST* promoter, suppressing its activity and inhibiting EMT in mammary tumor cells [published in ref. (36)].
- (3) Discovery that, in human luminal cancer cells, BRCA1 silencing is sufficient to activate TWIST and EMT and increase tumor formation. In parallel, *TWIST* expression and EMT features correlate inversely with *BRCA1* expression in human breast cancers [published in ref. (36)].
- (4) Discovery that deletion of *Brcal* in p16-deficient mammary epithelia also activates EMT and induces basal-like mammary tumors [published in ref. (37)]

5. Conclusion

Our findings showed that BRCA1 suppressed TWIST and EMT, inhibited LSC dedifferentiation and repressed expansion of basal stem cells and basal-like tumors. Thus, our work offers the first genetic evidence that *Brcal* directly suppresses EMT and LSC de-differentiation during breast tumorigenesis

6. Publications, Abstracts, and Presentations

(1) Publication:

- A. Bai F, Chan HL, Scott A, Smith MD, Fan C, Herschkowitz JI, Perou CM, Livingstone AS, Robbins DJ, Capobianco AJ, **Pei XH***. (2014) BRCA1 suppresses epithelial-to-mesenchymal transition and stem cell dedifferentiation during mammary and tumor development. *Cancer Research*. 74(21):6161-6172. PMID: 25239453. ***Corresponding Author.**
- B. Scott A, Bai F, Chan HL, Liu S, Ma J, Slingerland JM, Robbins DJ, Capobianco AJ, **Pei XH***. (2016) *p16^{INK4a}* suppresses BRCA1-deficient mammary tumorigenesis. *Oncotarget*. In press. ***Corresponding Author.**

(2) Meeting Presentation:

- A. Pei XH. *p16^{INK4a}* induces mammary stem cell aging and protects BRCA1 deficient mammary epithelial cells from tumorigenesis. Advances in breast cancer research. October 17-20, 2015. Bellevue, Washington.
- B. Pei XH. Genetic analysis of the role of *Brcal* in suppression of basal-like breast cancer. 2014 San Antonio Breast Cancer Symposium. December 9-13, 2014. San Antonio, TX.
- C. Bai F, Chan HL, Scott A, Perou CM, and Pei XH. BRCA1 suppresses epithelial-to-mesenchymal transition in basal-like tumorigenesis. An AACR special conference-Advances in breast cancer research. October 3-6, 2013. San Diego, CA.

7. Inventions, Patents, and Licenses

Nothing to report

8. Reportable Outcomes

We found that disrupting *Brcal* in p16- or p18-deficient mice activates EMT and induces dedifferentiation of LSCs, which associate closely with expansion of basal and cancer stem cells and formation of basal-like tumors. Mechanistically, BRCA1 bound to the *TWIST* promoter, suppressing its activity and inhibiting EMT in mammary tumor cells. In human luminal cancer cells, BRCA1 silencing was sufficient to activate TWIST and EMT and increase tumor formation. In parallel, *TWIST* expression and EMT features correlated inversely with *BRCA1* expression in human breast cancers. Together, our findings showed that BRCA1 suppressed TWIST and EMT, inhibited LSC dedifferentiation and repressed expansion of basal stem cells and basal-like tumors. Thus, our work offers the first genetic evidence that *Brcal* directly suppresses EMT and LSC de-differentiation during breast tumorigenesis.

9. Other Achievements

(1) Generation of p16;Brca1 and p18;Brca1 double mutant mouse strains that develop basal-like breast cancers with high penetrance.

(2) Development of human breast cancer cell lines, of T47D-sh-Ctrol. and T47D-sh-BRCA1, which develop luminal and basal-like tumors, respectively, in mice.

10. References

1. Van Keymeulen A, Rocha AS, Ousset M, Beck B, Bouvencourt G, Rock J, Sharma N, Dekoninck S, Blanpain C. Distinct stem cells contribute to mammary gland development and maintenance. *Nature*. 2011;479(7372):189-93. Epub 2011/10/11. doi: nature10573 [pii]10.1038/nature10573. PubMed PMID: 21983963.
2. van Amerongen R, Bowman AN, Nusse R. Developmental Stage and Time Dictate the Fate of Wnt/beta-Catenin-Responsive Stem Cells in the Mammary Gland. *Cell Stem Cell*. 2012;11(3):387-400. Epub 2012/08/07. doi: S1934-5909(12)00342-6 [pii]10.1016/j.stem.2012.05.023. PubMed PMID: 22863533.
3. Althuis MD, Fergenbaum JH, Garcia-Closas M, Brinton LA, Madigan MP, Sherman ME. Etiology of hormone receptor-defined breast cancer: a systematic review of the literature. *Cancer Epidemiol Biomarkers Prev*. 2004;13(10):1558-68. Epub 2004/10/07. doi: 13/10/1558 [pii]. PubMed PMID: 15466970.
4. Arnes JB, Brunet JS, Stefansson I, Begin LR, Wong N, Chappuis PO, Akslen LA, Foulkes WD. Placental cadherin and the basal epithelial phenotype of BRCA1-related breast cancer. *Clin Cancer Res*. 2005;11(11):4003-11. Epub 2005/06/03. doi: 11/11/4003 [pii]10.1158/1078-0432.CCR-04-2064. PubMed PMID: 15930334.
5. Foulkes WD, Brunet JS, Stefansson IM, Straume O, Chappuis PO, Begin LR, Hamel N, Goffin JR, Wong N, Trudel M, Kapusta L, Porter P, Akslen LA. The prognostic implication of the basal-like (cyclin E high/p27 low/p53+/glomeruloid-microvascular-proliferation+) phenotype of BRCA1-related breast cancer. *Cancer Res*. 2004;64(3):830-5. Epub 2004/02/12. PubMed PMID: 14871808.
6. Lakhani SR, Reis-Filho JS, Fulford L, Penault-Llorca F, van der Vijver M, Parry S, Bishop T, Benitez J, Rivas C, Bignon YJ, Chang-Claude J, Hamann U, Cornelisse CJ, Devilee P, Beckmann MW, Nestle-Kramling C, Daly PA, Haites N, Varley J, Lalloo F, Evans G, Maugard C, Meijers-Heijboer H, Klijn JG, Olah E, Gusterson BA, Pilotti S, Radice P, Scherneck S, Sobol H, Jacquemier J, Wagner T, Peto J, Stratton MR, McGuffog L, Easton DF. Prediction of BRCA1 status in patients with breast cancer using estrogen receptor and basal phenotype. *Clin Cancer Res*. 2005;11(14):5175-80. Epub 2005/07/22. doi: 11/14/5175 [pii]10.1158/1078-0432.CCR-04-2424. PubMed PMID: 16033833.
7. Ribeiro-Silva A, Ramalho LN, Garcia SB, Brandao DF, Chahud F, Zucoloto S. p63 correlates with both BRCA1 and cytokeratin 5 in invasive breast carcinomas: further evidence for the pathogenesis of the basal phenotype of breast cancer. *Histopathology*. 2005;47(5):458-66. Epub 2005/10/26. doi: HIS2249 [pii]10.1111/j.1365-2559.2005.02249.x. PubMed PMID: 16241993.
8. Pei XH, Xiong Y. Biochemical and cellular mechanisms of mammalian CDK inhibitors: a few unresolved issues. *Oncogene*. 2005;24(17):2787-95. Epub 2005/04/20. doi: 1208611 [pii]10.1038/sj.onc.1208611. PubMed PMID: 15838515.
9. Pei XH, Bai F, Smith MD, Usary J, Fan C, Pai SY, Ho IC, Perou CM, Xiong Y. CDK inhibitor p18(INK4c) is a downstream target of GATA3 and restrains mammary luminal progenitor cell proliferation and tumorigenesis. *Cancer Cell*. 2009;15(5):389-401. Epub 2009/05/05. doi: S1535-6108(09)00079-8 [pii]10.1016/j.ccr.2009.03.004. PubMed PMID: 19411068; PubMed Central PMCID: PMC2699569.
10. Koboldt DC, Fulton RS, McLellan MD, Schmidt H, Kalicki-Veizer J, McMichael JF, Fulton LL, Dooling DJ, Ding L, Mardis ER, Wilson RK, Ally A, Balasundaram M, Butterfield YS, Carlsen R, Carter C, Chu A, Chuah E, Chun HJ, Coope RJ, Dhalla N, Guin R, Hirst C, Hirst M, Holt RA, Lee D, Li HI, Mayo M, Moore RA, Mungall AJ, Pleasance E, Gordon Robertson A, Schein JE, Shafiee A, Sipahimalani P, Slobodan JR, Stoll D, Tam A, Thiessen N, Varhol RJ, Wye N, Zeng T, Zhao Y, Birol I, Jones SJ, Marra MA, Cherniack AD,

Saksena G, Onofrio RC, Pho NH, Carter SL, Schumacher SE, Tabak B, Hernandez B, Gentry J, Nguyen H, Crenshaw A, Ardlie K, Beroukhim R, Winckler W, Getz G, Gabriel SB, Meyerson M, Chin L, Park PJ, Kucherlapati R, Hoadley KA, Todd Auman J, Fan C, Turman YJ, Shi Y, Li L, Topal MD, He X, Chao HH, Prat A, Silva GO, Iglesia MD, Zhao W, Usary J, Berg JS, Adams M, Brooker J, Wu J, Gulabani A, Bodenheimer T, Hoyle AP, Simons JV, Soloway MG, Mose LE, Jefferys SR, Balu S, Parker JS, Neil Hayes D, Perou CM, Malik S, Mahurkar S, Shen H, Weisenberger DJ, Triche Jr T, Lai PH, Bootwalla MS, Maglente DT, Berman BP, Van Den Berg DJ, Baylin SB, Laird PW, Creighton CJ, Donehower LA, Noble M, Voet D, Gehlenborg N, Dicara D, Zhang J, Zhang H, Wu CJ, Yingchun Liu S, Lawrence MS, Zou L, Sivachenko A, Lin P, Stojanov P, Jing R, Cho J, Sinha R, Park RW, Nazaire MD, Robinson J, Thorvaldsdottir H, Mesirov J, Reynolds S, Kreisberg RB, Bernard B, Bressler R, Erkkila T, Lin J, Thorsson V, Zhang W, Shmulevich I, Ciriello G, Weinhold N, Schultz N, Gao J, Cerami E, Gross B, Jacobsen A, Arman Aksoy B, Antipin Y, Reva B, Shen R, Taylor BS, Ladanyi M, Sander C, Anur P, Spellman PT, Lu Y, Liu W, Verhaak RR, Mills GB, Akbani R, Zhang N, Broom BM, Casasent TD, Wakefield C, Unruh AK, Baggerly K, Coombes K, Weinstein JN, Haussler D, Benz CC, Stuart JM, Benz SC, Zhu J, Szeto CC, Scott GK, Yau C, Paull EO, Carlin D, Wong C, Sokolov A, Thusberg J, Mooney S, Ng S, Goldstein TC, Ellrott K, Grifford M, Wilks C, Ma S, Craft B, Yan C, Hu Y, Meerzaman D, Gastier-Foster JM, Bowen J, Ramirez NC, Black AD, Xpath Error Unknown Variable Tname RE, White P, Zmuda EJ, Frick J, Lichtenberg TM, Brookens R, George MM, Gerken MA, Harper HA, Leraas KM, Wise LJ, Tabler TR, McAllister C, Barr T, Hart-Kothari M, Tarvin K, Saller C, Sandusky G, Mitchell C, Iacocca MV, Brown J, Rabeno B, Czerwinski C, Petrelli N, Dolzhansky O, Abramov M, Voronina O, Potapova O, Marks JR, Suchorska WM, Murawa D, Kyeler W, Ibbs M, Korski K, Spychal A, Murawa P, Brzezinski JJ, Perz H, Lazniak R, Teresiak M, Tatka H, Leporowska E, Bogusz-Czerniewicz M, Malicki J, Mackiewicz A, Wiznerowicz M, Van Le X, Kohl B, Viet Tien N, Thorp R, Van Bang N, Sussman H, Duc Phu B, Hajek R, Phi Hung N, Viet The Phuong T, Quyet Thang H, Zaki Khan K, Penny R, Mallory D, Curley E, Shelton C, Yena P, Ingle JN, Couch FJ, Lingle WL, King TA, Maria Gonzalez-Angulo A, Dyer MD, Liu S, Meng X, Patangan M, Waldman F, Stoppler H, Kimryn Rathmell W, Thorne L, Huang M, Boice L, Hill A, Morrison C, Gaudioso C, Bshara W, Daily K, Egea SC, Pegram MD, Gomez-Fernandez C, Dhir R, Bhargava R, Brufsky A, Shriver CD, Hooke JA, Leigh Campbell J, Mural RJ, Hu H, Somiari S, Larson C, Deyarmin B, Kvecher L, Kovatich AJ, Ellis MJ, Stricker T, White K, Olopade O, Luo C, Chen Y, Bose R, Chang LW, Beck AH, Pihl T, Jensen M, Sfeir R, Kahn A, Kothiyal P, Wang Z, Snyder E, Pontius J, Ayala B, Backus M, Walton J, Baboud J, Berton D, Nicholls M, Srinivasan D, Raman R, Girshik S, Kigonya P, Alonso S, Sanbhadt R, Barletta S, Pot D, Sheth M, Demchok JA, Mills Shaw KR, Yang L, Eley G, Ferguson ML, Tarnuzzer RW, Dillon LA, Buetow K, Fielding P, Ozemberger BA, Guyer MS, Sofia HJ, Palchik JD. Comprehensive molecular portraits of human breast tumours. Nature. 2012. Epub 2012/09/25. doi: nature11412 [pii]10.1038/nature11412. PubMed PMID: 23000897.

11. Kamb A, Gruis NA, Weaver-Feldhaus J, Liu Q, Harshman K, Tavitian SV, Stockert E, Day RS, Johnson BE, Skolnick MH. A cell cycle regulator potentially involved in genesis of many tumor types. Science. 1994;264:436-40.
12. Herman JG, Merlo A, Mao L, Lapidus RG, Issa J-PJ, Davidson NE, Sidransky D, Baylin SB. Inactivation of the *CDKN2/p16/MTS1* gene is frequently associated with aberrant DNA methylation in all common human cancers. Cancer Res. 1995;55:4525-30.
13. Jonsson G, Staaf J, Vallon-Christersson J, Ringner M, Gruvberger-Saal SK, Saal LH, Holm K, Hegardt C, Arason A, Fagerholm R, Persson C, Grabau D, Johnsson E, Lovgren K, Magnusson L, Heikkila P, Agnarsson BA, Johannsson OT, Malmstrom P, Ferno M, Olsson H, Loman N, Nevanlinna H, Barkardottir RB, Borg A. The retinoblastoma gene undergoes rearrangements in BRCA1-deficient basal-like breast cancer. Cancer Res. 2012;72(16):4028-36. Epub 2012/06/19. doi: 0008-5472.CAN-12-0097 [pii]10.1158/0008-5472.CAN-12-0097. PubMed PMID: 22706203.
14. Stefansson OA, Jonasson JG, Olafsdottir K, Hilmarsdottir H, Olafsdottir G, Esteller M, Johannsson OT, Eyfjord JE. CpG island hypermethylation of BRCA1 and loss of pRb as co-occurring events in basal/triple-negative breast cancer. Epigenetics. 2011;6(5):638-49. Epub 2011/05/20. doi: 15667 [pii] 0.4161/epi.6.5.15667. PubMed PMID: 21593597; PubMed Central PMCID: PMC3121973.

15. Herschkowitz JI, He X, Fan C, Perou CM. The functional loss of the retinoblastoma tumour suppressor is a common event in basal-like and luminal B breast carcinomas. *Breast Cancer Res.* 2008;10(5):R75. Epub 2008/09/11. doi: bcr2142 [pii]10.1186/bcr2142. PubMed PMID: 18782450; PubMed Central PMCID: PMC2614508.
16. Bai F, Smith MD, Chan HL, Pei XH. Germline mutation of Brca1 alters the fate of mammary luminal cells and causes luminal-to-basal mammary tumor transformation. *Oncogene*. 2013;32(22):2715-25. Epub 2012/07/11. doi: onc2012293 [pii]10.1038/onc.2012.293. PubMed PMID: 22777348.
17. Bai F, Chan HL, Scott A, Smith MD, Fan C, Herschkowitz JI, Perou CM, Livingstone AS, Robbins DJ, Capobianco AJ, Pei XH. BRCA1 Suppresses Epithelial-to-Mesenchymal Transition and Stem Cell Dedifferentiation during Mammary and Tumor Development. *Cancer Res.* 2014;74(21):6161-72. Epub 2014/09/23. doi: 0008-5472.CAN-14-1119 [pii]10.1158/0008-5472.CAN-14-1119. PubMed PMID: 25239453.
18. Sedic M, Skibinski A, Brown N, Gallardo M, Mulligan P, Martinez P, Keller PJ, Glover E, Richardson AL, Cowan J, Toland AE, Ravichandran K, Riethman H, Naber SP, Naar AM, Blasco MA, Hinds PW, Kuperwasser C. Haploinsufficiency for BRCA1 leads to cell-type-specific genomic instability and premature senescence. *Nature communications*. 2015;6:7505. doi: 10.1038/ncomms8505. PubMed PMID: 26106036; PubMed Central PMCID: PMC4491827.
19. Kalluri R, Weinberg RA. The basics of epithelial-mesenchymal transition. *J Clin Invest.* 2009;119(6):1420-8. Epub 2009/06/03. doi: 39104 [pii]10.1172/JCI39104. PubMed PMID: 19487818; PubMed Central PMCID: PMC2689101.
20. Shafee N, Smith CR, Wei S, Kim Y, Mills GB, Hortobagyi GN, Stanbridge EJ, Lee EY. Cancer stem cells contribute to cisplatin resistance in Brca1/p53-mediated mouse mammary tumors. *Cancer Res.* 2008;68(9):3243-50. Epub 2008/05/03. doi: 68/9/3243 [pii]10.1158/0008-5472.CAN-07-5480. PubMed PMID: 18451150; PubMed Central PMCID: PMC2929908.
21. Shackleton M, Vaillant F, Simpson KJ, Stingl J, Smyth GK, Asselin-Labat ML, Wu L, Lindeman GJ, Visvader JE. Generation of a functional mammary gland from a single stem cell. *Nature*. 2006;439(7072):84-8. PubMed PMID: 16397499.
22. Wright MH, Robles AI, Herschkowitz JI, Hollingshead MG, Anver MR, Perou CM, Varticovski L. Molecular analysis reveals heterogeneity of mouse mammary tumors conditionally mutant for Brca1. *Mol Cancer*. 2008;7:29. Epub 2008/04/09. doi: 1476-4598-7-29 [pii]10.1186/1476-4598-7-29. PubMed PMID: 18394172; PubMed Central PMCID: PMC2329667.
23. Buono KD, Robinson GW, Martin C, Shi S, Stanley P, Tanigaki K, Honjo T, Hennighausen L. The canonical Notch/RBP-J signaling pathway controls the balance of cell lineages in mammary epithelium during pregnancy. *Dev Biol*. 2006;293(2):565-80. Epub 2006/04/04. doi: S0012-1606(06)00128-X [pii]10.1016/j.ydbio.2006.02.043. PubMed PMID: 16581056.
24. Wagner KU, Wall RJ, St-Onge L, Gruss P, Wynshaw-Boris A, Garrett L, Li M, Furth PA, Hennighausen L. Cre-mediated gene deletion in the mammary gland. *Nucleic Acids Res*. 1997;25(21):4323-30. Epub 1997/10/23. doi: gka680 [pii]. PubMed PMID: 9336464; PubMed Central PMCID: PMC147032.
25. Lim E, Wu D, Pal B, Bouras T, Asselin-Labat ML, Vaillant F, Yagita H, Lindeman GJ, Smyth GK, Visvader JE. Transcriptome analyses of mouse and human mammary cell subpopulations reveal multiple conserved genes and pathways. *Breast Cancer Res*. 2010;12(2):R21. Epub 2010/03/30. doi: bcr2560 [pii]10.1186/bcr2560. PubMed PMID: 20346151; PubMed Central PMCID: PMC2879567.
26. Wagner KU, McAllister K, Ward T, Davis B, Wiseman R, Hennighausen L. Spatial and temporal expression of the Cre gene under the control of the MMTV-LTR in different lines of transgenic mice. *Transgenic Res*. 2001;10(6):545-53. Epub 2002/01/31. PubMed PMID: 11817542.
27. Weigelt B, Kreike B, Reis-Filho JS. Metaplastic breast carcinomas are basal-like breast cancers: a genomic profiling analysis. *Breast Cancer Res Treat*. 2009;117(2):273-80. Epub 2008/09/26. doi: 10.1007/s10549-008-0197-9. PubMed PMID: 18815879.
28. Keller PJ, Lin AF, Arendt LM, Klebba I, Jones AD, Rudnick JA, DiMeo TA, Gilmore H, Jefferson DM, Graham RA, Naber SP, Schnitt S, Kuperwasser C. Mapping the cellular and molecular heterogeneity of normal

- and malignant breast tissues and cultured cell lines. *Breast Cancer Res.* 2010;12(5):R87. Epub 2010/10/23. doi: bcr2755 [pii]10.1186/bcr2755. PubMed PMID: 20964822; PubMed Central PMCID: PMC3096980.
29. Shakya R, Reid LJ, Reczek CR, Cole F, Egli D, Lin CS, deRooij DG, Hirsch S, Ravi K, Hicks JB, Szabolcs M, Jasin M, Baer R, Ludwig T. BRCA1 tumor suppression depends on BRCT phosphoprotein binding, but not its E3 ligase activity. *Science.* 2011;334(6055):525-8. Epub 2011/10/29. doi: 334/6055/525 [pii] 10.1126/science.1209909. PubMed PMID: 22034435.
30. Buckley NE, Mullan PB. BRCA1 - Conductor of the Breast Stem Cell Orchestra: The Role of BRCA1 in Mammary Gland Development and Identification of Cell of Origin of BRCA1 Mutant Breast Cancer. *Stem Cell Rev.* 2012. Epub 2012/03/20. doi: 10.1007/s12015-012-9354-y. PubMed PMID: 22426855.
31. Tkocz D, Crawford NT, Buckley NE, Berry FB, Kennedy RD, Gorski JJ, Harkin DP, Mullan PB. BRCA1 and GATA3 corepress FOXC1 to inhibit the pathogenesis of basal-like breast cancers. *Oncogene.* 2011. Epub 2011/11/29. doi: onc2011531 [pii]10.1038/onc.2011.531. PubMed PMID: 22120723.
32. Prat A, Parker JS, Karginova O, Fan C, Livasy C, Herschkowitz JI, He X, Perou CM. Phenotypic and molecular characterization of the claudin-low intrinsic subtype of breast cancer. *Breast Cancer Res.* 2010;12(5):R68. Epub 2010/09/04. doi: bcr2635 [pii]10.1186/bcr2635. PubMed PMID: 20813035; PubMed Central PMCID: PMC3096954.
33. Herschkowitz JI, Zhao W, Zhang M, Usary J, Murrow G, Edwards D, Knezevic J, Greene SB, Darr D, Troester MA, Hilsenbeck SG, Medina D, Perou CM, Rosen JM. Comparative oncogenomics identifies breast tumors enriched in functional tumor-initiating cells. *Proc Natl Acad Sci U S A.* 2012;109(8):2778-83. Epub 2011/06/03. doi: 1018862108 [pii]10.1073/pnas.1018862108. PubMed PMID: 21633010; PubMed Central PMCID: PMC3286979.
34. Taube JH, Herschkowitz JI, Komurov K, Zhou AY, Gupta S, Yang J, Hartwell K, Onder TT, Gupta PB, Evans KW, Hollier BG, Ram PT, Lander ES, Rosen JM, Weinberg RA, Mani SA. Core epithelial-to-mesenchymal transition interactome gene-expression signature is associated with claudin-low and metaplastic breast cancer subtypes. *Proc Natl Acad Sci U S A.* 2010;107(35):15449-54. Epub 2010/08/18. doi: 1004900107 [pii]10.1073/pnas.1004900107. PubMed PMID: 20713713; PubMed Central PMCID: PMC2932589.
35. Curtis C, Shah SP, Chin SF, Turashvili G, Rueda OM, Dunning MJ, Speed D, Lynch AG, Samarajiwa S, Yuan Y, Graf S, Ha G, Haffari G, Bashashati A, Russell R, McKinney S, Langerod A, Green A, Provenzano E, Wishart G, Pinder S, Watson P, Markowetz F, Murphy L, Ellis I, Purushotham A, Borresen-Dale AL, Brenton JD, Tavare S, Caldas C, Aparicio S. The genomic and transcriptomic architecture of 2,000 breast tumours reveals novel subgroups. *Nature.* 2012;486(7403):346-52. Epub 2012/04/24. doi: nature10983 [pii] 10.1038/nature10983. PubMed PMID: 22522925; PubMed Central PMCID: PMC3440846.
36. Bai F, Chan HL, Scott A, Smith MD, Fan C, Herschkowitz JI, Perou CM, Livingstone AS, Robbins DJ, Capobianco AJ, Pei XH. BRCA1 suppresses epithelial-to-mesenchymal transition and stem cell dedifferentiation during mammary and tumor development. *Cancer Res.* 2014. Epub 2014/09/23. doi: 0008-5472.CAN-14-1119 [pii]10.1158/0008-5472.CAN-14-1119. PubMed PMID: 25239453.
37. Scott A, Bai F, Chan HL, Liu S, Ma J, Slingerland JM, Robbins DJ, Capobianco AJ, Pei XH*. (2016) *p16^{INK4a}* suppresses BRCA1-deficient mammary tumorigenesis. *Oncotarget.* In press.

11. Appendices

References 36 and 37 were direct results of this award and are attached.

BRCA1 Suppresses Epithelial-to-Mesenchymal Transition and Stem Cell Dedifferentiation during Mammary and Tumor Development

Feng Bai^{1,2}, Ho Lam Chan^{1,2}, Alexandria Scott^{1,2}, Matthew D. Smith⁴, Cheng Fan⁴, Jason I. Herschkowitz⁴, Charles M. Perou^{4,5}, Alan S. Livingstone², David J. Robbins^{1,2,3}, Anthony J. Capobianco^{1,2,3}, and Xin-Hai Pei^{1,2,3}

Abstract

BRCA1 mutation carriers are predisposed to developing basal-like breast cancers with high metastasis and poor prognosis. Yet, how *BRCA1* suppresses formation of basal-like breast cancers is still obscure. Deletion of *p18^{Ink4c}* (*p18*), an inhibitor of CDK4 and CDK6, functionally inactivates the RB pathway, stimulates mammary luminal stem cell (LSC) proliferation, and leads to spontaneous luminal tumor development. Alternately, germline mutation of *Brcal* shifts the fate of luminal cells to cause luminal-to-basal mammary tumor transformation. Here, we report that disrupting *Brcal* by either germline or epithelium-specific mutation in *p18*-deficient mice activates epithelial-to-mesenchymal transition (EMT) and induces dedifferentiation of LSCs, which associate closely with expansion of basal and cancer stem cells and formation of basal-like tumors. Mechanistically, *BRCA1* bound to the *TWIST* promoter, suppressing its activity and inhibiting EMT in mammary tumor cells. In human luminal cancer cells, *BRCA1* silencing was sufficient to activate *TWIST* and EMT and increase tumor formation. In parallel, *TWIST* expression and EMT features correlated inversely with *BRCA1* expression in human breast cancers. Together, our findings showed that *BRCA1* suppressed *TWIST* and EMT, inhibited LSC dedifferentiation, and repressed expansion of basal stem cells and basal-like tumors. Thus, our work offers the first genetic evidence that *Brcal* directly suppresses EMT and LSC dedifferentiation during breast tumorigenesis. *Cancer Res*; 74(21); 6161–72. ©2014 AACR.

Introduction

Mammary luminal and basal epithelial cells originate from multipotent progenitors in the embryo (1–2), and expansion and maintenance of these cells in adults are ensured by unipotent luminal stem cells (LSC) and basal stem cells (BSC), respectively (1, 3). Cancer stem cells (CSC) are a subpopulation of cancer cells that shares characteristics with stem cells such as self-renewal ability and multipotency. CSCs could generate daughter cells, thus contributing to tumor growth, and are associated with radioresistance and chemoresistance, metas-

tasis, and poor prognosis (4). Germline mutations in the tumor suppressor *BRCA1* contribute to about half of familial breast cancer cases and increase the risk of developing basal-like breast tumors with high metastasis and poor prognosis. Basal-like tumors developed in *BRCA1* mutation carriers were thought to originate from either mammary stem cells or basal progenitors (5, 6). Recently, we and others discovered that aberrant LSCs, not BSCs/progenitors, are likely the origin of basal-like tumors developed in patients harboring *BRCA1* mutations as well as in germline *Brcal*^{+/-}-mutant mice (7–10). Furthermore, breast cancer stem cells are enriched in human *BRCA1*-mutant breast cancers (11, 12). However, whether *BRCA1* functions in LSCs to maintain their unipotency, and whether and how *BRCA1* controls breast cancer stem cells and basal-like tumors *in vivo*, remain elusive.

Epithelial-to-mesenchymal transition (EMT) plays an important role in intratumoral heterogeneity, breast basal-like tumor development, and generation of breast epithelial and cancer cells with stem cell-like characteristics, directly linking EMT with the gain of stem cell properties (13, 14). A set of transcription factors, including *TWIST1/2*, *SNAIL*, *SLUG*, *ZEB1/2*, and *FOXC1/2*, was identified as EMT-inducing transcription factors (EMT-TF). Among these, *TWIST1* (*TWIST*) is a master regulator of EMT and plays an essential role in tumor metastasis (15).

p18 is a member of the INK4 family of cell-cycle inhibitors that inhibits CDK4/6 and, when activated by D-type cyclins,

¹Molecular Oncology Program, ²Department of Surgery and ³Sylvester Cancer Center, Miller School of Medicine, University of Miami, Miami, Florida. ⁴Lineberger Cancer Center, University of North Carolina at Chapel Hill, Chapel Hill, North Carolina. ⁵Department of Genetics, University of North Carolina at Chapel Hill, Chapel Hill, North Carolina.

Note: Supplemental data for this article are available at Cancer Research Online (<http://cancerres.aacrjournals.org/>).

F. Bai and H.L. Chan contributed equally to this article.

Current address for J.I. Herschkowitz: Department of Biomedical Sciences, University at Albany, Rensselaer, New York.

Corresponding Author: Xin-Hai Pei, University of Miami, Department of Surgery and Sylvester Cancer Center, 1600 NW 10th Avenue, Miami, FL 33136. Phone: 305-243-4419; Fax: 305-243-4476; E-mail: xhpei@med.miami.edu

doi: 10.1158/0008-5472.CAN-14-1119

©2014 American Association for Cancer Research.

phosphorylates and functionally inactivates RB, p107, and p130. *p18* expression is significantly lower in human breast cancers than normal breast (refs. 16, 17; F. Bai, unpublished data). *RB* has been identified as a major target for genomic disruption in basal-like breast cancers of *BRCA1* mutation carriers (18), and loss of both *RB* and *BRCA1* is, indeed, a feature of basal-like human breast cancers (17, 19). Deletion of *Rb* alone in mouse mammary epithelia does not induce tumors (20), and deletion of both *Rb* and *p107* results in luminal type tumors (19), suggesting a role of the *Rb* pathway in controlling luminal tumorigenesis. Interestingly, deletion of *p18*, which functionally inactivates the *Rb* pathway, stimulates mammary LSC proliferation and results in luminal type tumors (16) as well as rescues the premature senescence caused by *Brcal* deficiency. Thus, *p18;Brcal* double-mutant mice provide a unique mouse model with a genetically intact *p53* pathway and functionally inactivated *Rb* pathway (10) to study the role of *Brcal* in breast tumor suppression.

In this report, we used *Brcal* germline and conditional mutant mice as well as human breast cancer cells and samples to determine the function and mechanism of *Brcal* in suppressing EMT and basal-like tumors.

Materials and Methods

Mice, histopathology, and IHC

The generation of *p18* and *Brcal* germline mutant mice has been described previously (10, 16). *Brcal*^{fl/fl} and Tg(MMTV-Cre) 4Mam mice were obtained from the NCI Mouse Repository and JAX lab, respectively (21, 22). All animal procedures were approved by the Institutional Animal Care and Use Committee at the University of North Carolina and University of Miami. Histopathology and IHC were performed as described previously (10, 16). Primary antibodies used are as follows: Ck5 (Covance), Ck8 (American Research Products), Ck14, SMA (Thermo Scientific), ER α , CD29, *Brcal*, Gata3, Foxc1, Foxc2 (Santa Cruz), E-cadherin (BD Biosciences), fibronectin, vimentin, Twist, Snail (Abcam), and Slug (Novus Biologicals).

Mammary cell preparation, FACS analysis, cell sorting, mammosphere assay, colony-formation assay, cell lines, transfection, and lentiviral infection

Mammary glands were dissected from female mice at the indicated ages, and the tissue was processed as previously described (10, 16, 23, 24). MCF-7, T47D (ATCC), SUM149 (Dr. Sendurai Mani, University of Texas, Houston, TX), and HCC1937 (Dr. Jennifer Hu, University of Miami, Miami, FL) cells were tested and authenticated (10, 25, 26). For ectopic expression of *BRCA1*, HCC1937 cells were transfected with pcDNA3-empty or pcDNA3-*BRCA1* with FuGene. For *BRCA1* knockdown (KD), pGIPZ-empty (Sh-Ctrl) and pGIPZ-sh*BRCA1* (Sh-*BRCA1*) lentiviral vectors were purchased from Open Biosystems.

Xenograft models of breast cancer

T47D and MCF-7 Sh-Ctrl and Sh-*BRCA1* cells were suspended in a 50% solution of Matrigel (BD), and then inoculated into the left and right inguinal mammary fat pads of 6-week-old

female NSG mice (Jackson Laboratory), respectively. Eighteen weeks after transplantation, animals were euthanized and mammary tumors were dissected for analyses. No estrogen was administered to animals during the course of the study.

Western blot, qRT-PCR, and chromatin immunoprecipitation assay

Western blot, QRT-PCR, and chromatin immunoprecipitation (ChIP) assay were carried out as previously described (10, 16, 27). Primary antibodies used for Western blot are as follows: *Brcal*, Gata3 (Santa Cruz), E-cadherin, fibronectin, tubulin- α (DM1A; NeoMarkers), and actin (ACTN05; NeoMarkers). Anti-*BRCA1* antibody (D-9; Santa Cruz) or control mouse IgG was used to precipitate chromatin associated with *BRCA1*. qPCR was performed to determine the relative abundance of target DNA. Specific primers for the analysis of *BRCA1* binding to *TWIST* are available upon request.

Human tumor samples

Formalin-fixed paraffin-embedded (FFPE) human breast cancer samples lacking patient-identifying information were obtained from the Tissue Bank Core Facility at the University of Miami. All samples obtained were nontreated invasive breast cancers with known estrogen receptor (ER) status. Regions from tumor samples were microdissected, and only samples with a consistent tumor cell content >75% of tissues were used for RNA extraction. The expression of *BRCA1* was determined by qRT-PCR.

Patients and gene-expression datasets

The UNC337 human breast cancer dataset (28) with 337 breast cancer samples and the MetaBric dataset (29) with 2,000 samples were analyzed. We compared gene expression versus six breast cancer subtypes using two-way ANOVA.

Results

Germline mutation of *Brcal* transforms *p18*^{-/-} luminal tumors into basal-like tumors with induction of EMT

In our previous studies, we reported that deletion of *p18* in mice stimulates mammary LSC proliferation and leads to spontaneous luminal tumor development (16), and that germline mutation of *Brcal* in *p18*-deficient mice blocks the expansion of LSCs and transforms luminal tumors into basal-like tumors (10). Prompted by the highly invasive heterogeneous mammary tumors developed in *p18*^{-/-}; *Brcal*^{+/-} mice with various degrees of whorls and clusters of spindle-shaped cells within these tumors—typical morphologic characteristics of mesenchymal cells (10)—we looked at molecular markers associated with EMT. We found that the majority of the luminal tumors from *p18*^{-/-} mice highly expressed E-cadherin (*Cdh1*), an epithelial marker, whereas basal-like tumors from *p18*^{-/-}; *Brcal*^{+/-} mice expressed very weak and heterogeneous *Cdh1*. In contrast, most (77%, $n = 13$) of *p18*^{-/-}; *Brcal*^{+/-} tumors that developed after one year of age were stained positive for mesenchymal markers, including fibronectin (*Fn*), vimentin (*Vim*), and *CD29*, whereas only 11% ($n = 19$) of *p18*^{-/-}

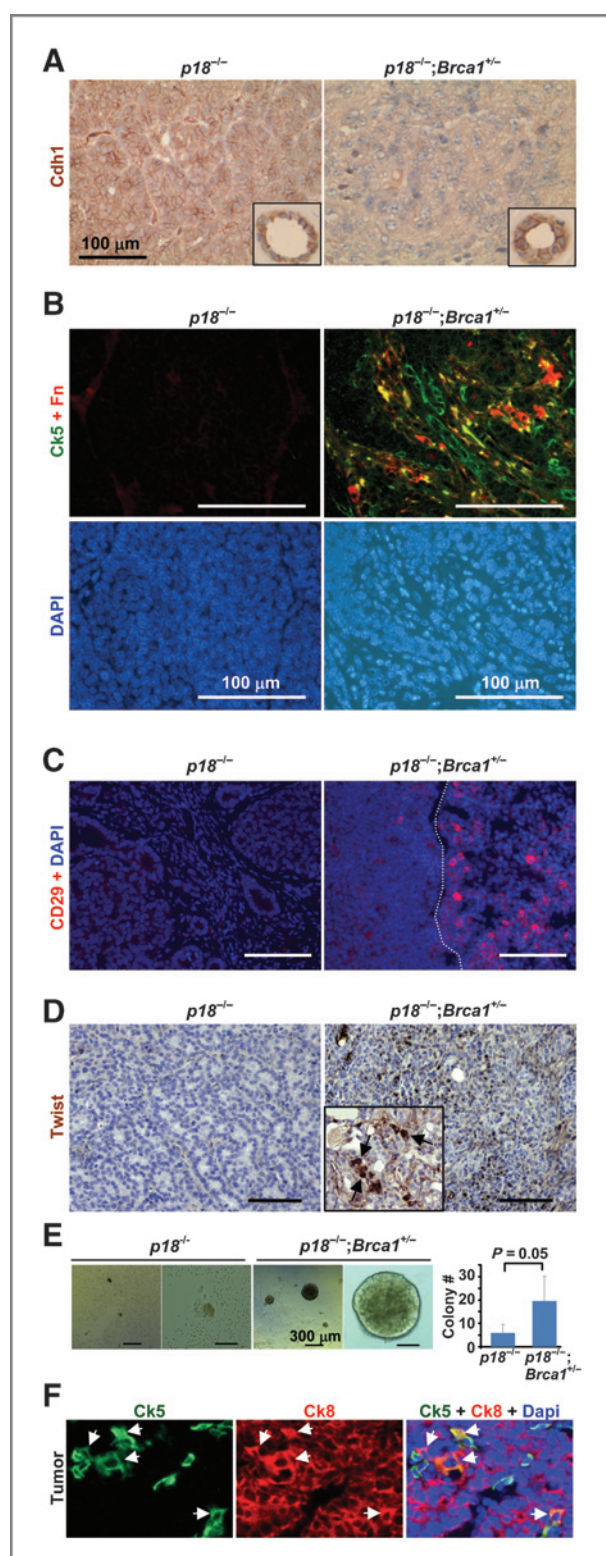


Figure 1. *Brca1* heterozygosity transforms *p18*-deficient luminal tumors into basal-like tumors with EMT features. A–D, representative immunostaining of tumors with *Cdh1* (A), *Ck5* and *Fn1* (B), *CD29* (C), and *Twist* (D). The inset in A shows staining of normal glands in the same mouse and in D shows staining of lung metastasis. E, tumor cells were

tumors that developed at a similar age were positive for these markers (Fig. 1A–C; Supplementary Fig. S1A–S1D; Table 1). This observation suggests that heterozygous germline mutation of *Brca1* activates EMT in mammary tumor progression.

Consistently, *p18^{-/-};Brca1^{+/+}* tumor cells that were positive for *Ck5* expressed very low levels of *Cdh1* (Supplementary Fig. S1A) and the majority of *Fn1*-positive cells coexpressed *Ck5* (Fig. 1B; Supplementary Fig. S1C). These data suggest, at the least, that some *Ck5⁺* basal-like tumor cells lost their epithelial characteristics and gained mesenchymal features. In further analysis of these tumors for the expression of *CD29*, a basal and mesenchymal marker (14) demonstrated to be enriched in breast CSCs (23, 30), we found that 69% ($n = 13$) of *p18^{-/-};Brca1^{+/+}* tumors expressed various degrees of *CD29*-positive tumor cells from 2% to 60%, whereas only 11% ($n = 19$) of *p18^{-/-}* tumors were positive for *CD29* in 2% to 3% of tumor cells (Fig. 1C and Table 1). These observations support the notion that EMT activation, as previously demonstrated (13, 14), results in cancer cells gaining stem cell properties. Primary *p18^{-/-};Brca1^{+/+}* tumor cells formed more and larger colonies in Matrigel than *p18^{-/-}* tumor cells (Fig. 1E), and *Ck5/Ck8* double-positive tumor cells were frequently detected in *p18^{-/-};Brca1^{+/+}* tumors, but rarely in *p18^{-/-}* tumors, 1.1% (67/6,100) versus 0.04% (2/5,120; Fig. 1F; Supplementary Fig. S1E and refs. 10, 16), which further suggests increased CSCs in *p18^{-/-};Brca1^{+/+}* tumors. Together, these results indicate that heterozygous germline mutation of *Brca1* induces EMT, increases CSCs, and transforms *p18* null luminal tumors into basal-like tumors.

Germline mutation of *Brca1* activates EMT-TFs in mammary and tumor development

We then determined the expression of EMT-TFs and observed that 77% ($n = 13$, >1 year of age) of *p18^{-/-};Brca1^{+/+}* tumors were stained positive for *Twist*, *Foxc1*, *Foxc2*, *Slug*, and *Snail* in greater than 2% of cells per tumor, whereas 16% ($n = 19$, >1 year of age) of *p18^{-/-}* tumors were positive at similar ages (Fig. 1D; Supplementary Fig. S2A–S2C; and Table 1). Tumors with high expression of EMT-TFs showed high histologic grade and strong invasive and metastatic potential as evidenced by EMT-TF-positive staining in the invasive front of tumors and metastasized cancers (Fig. 1D). The expression pattern and percentage of positive cells in tumors stained for EMT-TFs and EMT markers were highly correlated with its genotype—*p18^{-/-}* or *p18^{-/-};Brca1^{+/+}*—which not only confirms that germline mutation of *Brca1* promotes EMT in mammary tumors but that this induction of EMT is very likely a result of the aberrant activation of EMT-TFs in *Brca1*-mutant tumors. We next isolated mammary epithelial cells (MEC) from tumor-free virgin mice and found that *Brca1^{+/+}* and *p18^{-/-};Brca1^{+/+}* cells expressed significantly less *Cdh1* and more EMT-TFs than wild-type (WT) or *p18^{-/-}* cells (Supplementary

cultured for 2 weeks, and colonies larger than 30 μm were counted. Bar graph, mean \pm SD of two tumors per genotype. F, representative immunostaining of tumors from *p18^{-/-};Brca1^{+/+}* mice with *Ck5* and *Ck8*. *Ck5⁺ Ck8⁺* cells are indicated.

Table 1. Characterization of spontaneous mammary tumors derived from mutant mice

Tumor	WT		<i>p18</i> ^{-/-}		<i>Brca1</i> ^{+/-}		<i>p18</i> ^{-/-} ; <i>Brca1</i> ^{+/-}	
	<12 mo	12–27 mo	<12 mo	12–22 mo	<12 mo	12–27 mo	<12 mo	12–22 mo
Mammary tumor	0/5	1/10 ^a (10%)	4/16 (25%)	19/23 ^b (83%)	0/3	1/11 ^c (9%)	6/16 (38%)	13/15 ^d (87%)
Metastasis ^e	0/1	0	1/19	0/1	0/1	0/1	0	4/13
ERα ⁺ tumor	1/1	3/4	15/19			1/6	2/13	
% ERα ⁺ cells/tumor	5%	2%–40%	2%–40%			<2%	<2%	
Ck5 ⁺ tumor	0/1	0/4	3/19 ^f		1/1	4/6	11/13 ^g	
% Ck5 ⁺ cells/tumor			1%–5%		~2%	2%–20%	2%–95%	
EMT marker ⁺ tumor ^h	0/1	0/4	2/19 (11%)		0/1	2/6	10/13	
EMT-TF ⁺ tumor ⁱ	0/1	0/4	3/19 (16%)		1/1 (100%)	3/6 (50%)	10/13 (77%)	

^a24-month-old tumor-bearing mouse.^bMost tumor-bearing mice were 12 to 16 months old, and the oldest was 22 months old. One male developed mammary tumor.^c25.5-month-old tumor-bearing mouse.^dMost tumor-bearing mice were 12 to 16 months old, and the oldest was 20 months old. One male developed mammary tumor.^eMammary tumors metastasized mostly to the lung except one to a blood vessel in a *p18*^{-/-};*Brca1*^{+/-} mouse.^fOne tumor stained positive for Ck5 in approximately 5% tumor cells and the other two were positive in approximately 1% tumor cells.^gTwo tumors stained positive for Ck5 in approximately 95% tumor cells.^hAt least two EMT markers (decreased Cdh1, increased Vim, Fn1, Sma, or Cd29) were detected in >2% tumor cells.ⁱAt least two EMT-TFs, which include Twist, Slug, Snail, Foxc1, and Foxc2, stained positive in >2% tumor cells.

Fig. S2D). These results indicate that EMT-TF activation in *Brca1*-mutant MECs occurs before tumor initiation.

Specific deletion of *Brca1* in mammary epithelia activates EMT and induces aberrant differentiation of LSCs

To directly test the function of *Brca1* in controlling and transforming MECs as well as to determine the implications of loss of *Brca1* on mammary tumorigenesis, we generated *Brca1*^{f/f};MMTV-cre⁺ and *Brca1*^{f/f};MMTV-cre⁺ mice with and without *p18* mutation, in which MMTV-cre (MC) is active in virgin epithelia but not in stroma (22, 31). Using these mice also enabled us to rule out the impact of *Brca1*-mutant stroma on mammary stem cell self-renewal and tumorigenesis.

Brca1^{f/f};MC and *p18*^{-/-};*Brca1*^{f/f};MC breasts expressed <5% of *Brca1* protein and mRNA relative to the levels in *Brca1*^{f/f};MC and *p18*^{-/-};*Brca1*^{f/f};MC, indicating an efficient and near complete depletion of *Brca1* in the mammary epithelia (Fig. 2A and B; Supplementary Fig. S3). Similarly, *Brca1*^{f/f};MC and *p18*^{-/-};*Brca1*^{f/f};MC breasts expressed <20% of *Brca1* protein and mRNA relative to the levels in MC and *p18*^{-/-};MC (data not shown). Consistent with the data from *Brca1*^{+/-} mice (10), the expression of *Gata3*, *Cdh1*, and *Epcam*—genes associated with luminal differentiation—in *Brca1*^{f/f};MC and *p18*^{-/-};*Brca1*^{f/f};MC breasts was significantly reduced relative to *Brca1*^{f/f};MC and *p18*^{-/-};*Brca1*^{f/f};MC breasts (Fig. 2A and B; Supplementary Fig. S3), suggesting that loss of *Brca1* impairs luminal differentiation. MECs from *p18*^{-/-};*Brca1*^{f/f};MC mice showed increased mammosphere-forming ability than those

from *p18*^{-/-};*Brca1*^{f/f};MC mice. Most *p18*^{-/-};*Brca1*^{f/f};MC mammospheres were 35 to 45 μm and none larger than 100 μm, whereas 10% to 15% of *p18*^{-/-};*Brca1*^{f/f};MC mammospheres were larger than 100 μm. The average *p18*^{-/-};*Brca1*^{f/f};MC mammosphere was significantly larger than that of *p18*^{-/-};*Br*^{f/f};MC mammospheres (Fig. 2C). These results suggest that *Brca1* deficiency increased the self-renewal capacity of *p18*^{-/-} mammary stem cells. Accordingly, MECs from *p18*^{-/-};*Brca1*^{f/f};MC mice formed more colonies than those from *p18*^{-/-};*Brca1*^{f/f};MC mice and *p18*^{-/-};*Brca1*^{f/f};MC mammospheres expressed significantly higher levels of EMT-TFs than those of *p18*^{-/-};*Brca1*^{f/f};MC (Fig. 2D and E). These results confirm that loss of *Brca1* activates EMT-TFs, which is likely responsible for the induction of EMT and increased mammosphere- and colony-forming potential in *p18*^{-/-};*Brca1*^{f/f};MC MECs.

We then performed FACS and found that *p18*^{-/-};*Brca1*^{f/f};MC MECs had a reduced CD24⁺CD29⁻ LSC-enriched population and increased CD24⁺CD29⁺ BSC-enriched population compared with *p18*^{-/-};*Brca1*^{f/f};MC MECs at 22 weeks of age (Fig. 2F). Similar, but less significant, trends were also observed in *p18*^{-/-};*Brca1*^{f/f};MC mice relative to *p18*^{-/-};MC mice at 16 weeks of age (Supplementary Fig. S4A and S4B). These results suggest that *Brca1* deficiency results in the expansion of BSCs and blockage of LSCs, the latter of which is consistent with our findings derived from heterozygous germline *Brca1*-mutant mice (10).

FACS-sorted cells of the BSC-enriched population expressed higher basal genes (*Twist2*, *Id4*, and *Tbx2*) and lower luminal

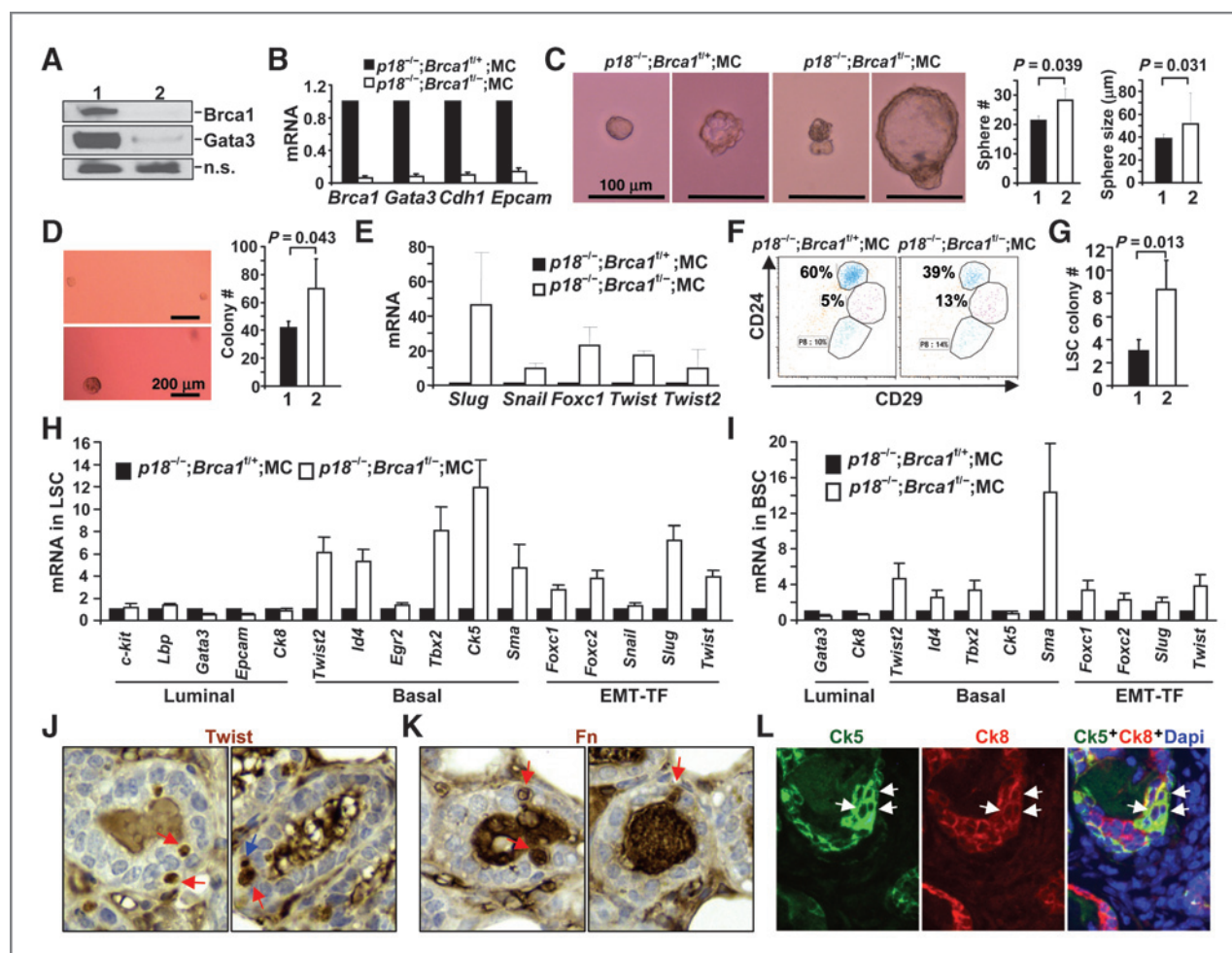


Figure 2. Deletion of Brca1 in mammary epithelia inhibits luminal differentiation and activates EMT-TFs in mammary stem cells. **A** and **B**, mammary tissues from *p18^{-/-};Brca1^{t/+}*;MC (lane 1) and *p18^{-/-};Brca1^{t/-}*;MC (lane 2) mice were analyzed by Western blot (**A**) and qRT-PCR (**B**). n.s., non-specific band. qRT-PCR data are expressed as the mean \pm SD from triplicates of each of three separate mice. **C** and **D**, mammary cells were analyzed by mammosphere (**C**) and colony-formation assay (**D**). The number of spheres larger than 30 μ m, the sizes of spheres, and the number of colonies larger than 30 μ m were quantified. 1, *p18^{-/-};Brca1^{t/+}*;MC; 2, *p18^{-/-};Brca1^{t/-}*;MC. The bar graphs represent the mean \pm SD of two animals per genotype. **E**, RNA from mammospheres was analyzed. Data are expressed as mean \pm SD from triplicates of each of two separate mice. **F**, mammary cells were analyzed by flow cytometry. **G**, FACS-sorted LSCs from **F** were analyzed by colony-formation assay. The bar graphs represent the mean \pm SD of two animals per genotype. 1, *p18^{-/-};Brca1^{t/+}*;MC; 2, *p18^{-/-};Brca1^{t/-}*;MC. **H** and **I**, RNA from LSCs (**H**) and BSCs (**I**) was analyzed. Data are expressed as the mean \pm SD from triplicates of each of two separate mice. **J–L**, tumor-free mammary glands from *p18^{-/-};Brca1^{t/-}*;MC mice were stained with antibodies against Twist (**J**), Fn (**K**), Ck5 and Ck8 (**L**). Twist or Fn-positive ULLC (red arrows) and SLC (blue arrows), as well as Ck5⁺ Ck8⁺ epithelial cells (white arrows), are indicated.

genes (*c-kit*, *Epcam*, and *Gata3*) than those of the LSC-enriched population, confirming that these cell populations are, as reported (32), the basal and luminal cell-enriched populations, respectively (Supplementary Fig. S4D). LSCs derived from *p18^{-/-};Brca1^{t/-}*;MC mice formed more colonies in Matrikel and expressed lower luminal and epithelial genes and significantly higher basal genes and EMT-TFs when compared with *p18^{-/-};Brca1^{t/+}*;MC LSCs (Fig. 2G and H). Consistently, LSCs from *p18^{-/-};Brca1^{t/-}*;MC mice also expressed lower luminal genes and higher basal genes and EMT-TFs than those from *p18^{-/-}*;MC mice (Supplementary Fig. S4C). These results indicate that haploid or near complete loss of *Brca1* in mammary epithelium not only inhibits the expression of luminal genes but also stimulates the expression of basal genes and EMT-TFs in

p18^{-/-} LSCs. Interestingly, expression of basal genes and EMT-TFs was also significantly increased in the BSCs from *p18^{-/-};Brca1^{t/-}*;MC mice relative to those from *p18^{-/-};Brca1^{t/+}*;MC mice (Fig. 2I). Together, these results suggest that *Brca1* deficiency leads to the expansion of BSCs, which is likely, at least partially, a result of the dedifferentiation of LSCs.

We have previously analyzed five histologically distinct epithelial cell populations and defined the small light cell (SLC) and undifferentiated large light cell (ULLC) populations as enriched for stem and luminal stem/progenitor cells, respectively (16). To determine the impact of EMT on stem/progenitor cell populations *in situ*, we examined tumor-free mammary glands and found that Twist or Fn-positive MECs were frequently detected in *p18^{-/-};Brca1^{t/-}*;MC or *p18^{-/-};Brca1^{f/f}*;MC

mice but not in *p18*^{-/-};MC mice and that most, if not all, Twist or Fn-positive cells were either SLC or ULLC, ULLC in particular (Fig. 2J and K). Furthermore, Ck5 and Ck8 double-positive epithelial cells were also frequently detected in *p18*^{-/-};*Brcal*^{f/f};MC but not in *p18*^{-/-};MC mammary (Fig. 2L; Supplementary Fig. S5; data not shown). These results further suggest that loss of Brcal in MECs activates Twist, induces EMT, and leads to dedifferentiation of LSCs.

Specific deletion of Brcal in mammary epithelia recapitulates basal-like tumorigenesis and EMT activation

To determine the tumorigenic impact of specific loss of Brcal in mammary epithelia, we first examined *Brcal*^{f/f};MC and *p18*^{-/-};*Brcal*^{f/f};MC mice and found that no hyperplasia nor tumors developed in 5 female *Brcal*^{f/f};MC mice at 10 to 12 months of age. Of the 8 *p18*^{-/-};*Brcal*^{f/f};MC mice examined at similar ages, all developed mammary hyperplasia, though no mammary tumors, were detected. A majority (7/8) of *p18*^{-/-};*Brcal*^{f/f};MC mice died at early ages from carcinomas in the pancreas, skin, pituitary, or lung (data not shown), very likely due to active MMTV-Cre expression and near complete deletion of Brcal in these tissues (33), which prevented us from observing the relatively late-onset mammary tumorigenesis in these mice. These results, however, confirm the previous findings that loss of Brcal alone is insufficient to promote tumorigenesis and that Brcal cooperates with p18 to control tumorigenesis.

We then examined *p18*^{-/-};*Brcal*^{f/+};MC and *p18*^{-/-};*Brcal*^{f/f};MC mice and found that 1 of 4 *p18*^{-/-};*Brcal*^{f/+};MC mice and 4 of 5 *p18*^{-/-};*Brcal*^{f/f};MC mice developed mammary tumors in 12 to 16 months (Fig. 3). In accordance with the tumors developed in *p18*^{-/-};*Brcal*^{+/-} mice, mammary tumors in *p18*^{-/-};*Brcal*^{f/+};MC and *p18*^{-/-};*Brcal*^{f/f};MC mice were also highly heterogeneous, poorly differentiated, and more aggressive than those developed in *p18*^{-/-} mice (Figs. 1, 3; Supplementary Fig. S1 and S2). About 25% to 30% *p18*^{-/-};*Brcal*^{f/+};MC tumor cells were spindle-shaped and were positive for Twist and Fn (Fig. 3A and B), and more than 40% of the tumor cells were positive for Ck5 and negative for Cdh1 or Ck8 (Fig. 3C and D), indications of a basal-like tumor undergoing EMT. The *p18*^{-/-};*Brcal*^{f/+};MC mammary tumors also expressed 1/3 of *Brcal* and 1/5 of *Gata3* relative to the tumor-free mammary tissues of the same mouse (Fig. 3E), confirming deficient Brcal and downregulation of Gata3 in the tumor.

More than 25% of tumor cells were spindle-shaped in all four *p18*^{-/-};*Brcal*^{f/f};MC mammary tumors, and two displayed more than 90% spindle-shaped cells (Fig. 3F). These tumors were also positive for Twist and Fn (Fig. 3G), indications of typical metaplastic breast carcinomas undergoing EMT. A *p18*^{-/-};*Brcal*^{f/f};MC tumor expressed less than 10% *Brcal* and *Gata3* when compared with tumor-free mammary of the same mouse (Fig. 3I). FACS showed that the LSC-enriched population in *p18*^{-/-};*Brcal*^{f/f};MC mammary tumors was significantly reduced in comparison with the tumor-free mammary tissues of the same mouse (6% vs. 56%) and when compared with *p18*^{-/-} mammary tumor cells (6% vs. 57%). Contrastingly, the BSC-enriched population, also enriched with breast CSCs, was

significantly expanded in *p18*^{-/-};*Brcal*^{f/f};MC mammary tumors relative to the tumor-free mammary tissues of the same mouse (19% vs. 11%) and when compared with *p18*^{-/-} mammary tumor cells (19% vs. 4%; Fig. 3H). These results further support that *p18*^{-/-};*Brcal*^{f/f};MC mammary tumors are basal-like tumors undergoing EMT that are enriched with CSCs, which is in line with the data derived from human patients showing that metaplastic breast carcinomas are basal-like breast cancers with EMT-like molecular make-up and are closely correlated with BRCA1 dysfunction (34).

Taken together, these results suggest that insufficient Brcal in mammary epithelial cells represses Gata3, activates Twist and EMT, and results in basal-like tumorigenesis with an increase in the CSC population. Because *p18*^{-/-};*Brcal*^{f/+};MC and *p18*^{-/-};*Brcal*^{f/f};MC mice are in B6 and Balb/c mixed backgrounds, unlike *p18*^{-/-};*Brcal*^{+/-} mice in pure Balb/c background, these data also suggest that the role of Brcal controlling basal-like tumorigenesis and EMT is independent of genetic background.

BRCA1 suppresses TWIST transcription and EMT

We screened a panel of human breast cancer cell lines and found that MCF7 and T47D cells expressed higher CDH1 and GATA3 and lower VIM and EMT-TFs than SUM149 and HCC1937 cells (Supplementary Fig. S6), confirming that MCF7 and T47D cells are luminal/epithelial-like and SUM149 and HCC1937 cells are basal/mesenchymal-like cancer cells in our culture system (35). Transfection of WT *BRCA1* into HCC1937 (*BRCA1* mutant, transcriptionally null) cells resulted in increase of *CDH1* and decrease of *VIM* and *FN*, indicating that BRCA1 suppresses EMT. Importantly, ectopic expression of BRCA1 significantly repressed *TWIST* by more than 50% compared with control, moderately repressed *FOXC2*, but hardly repressed other EMT-TFs (Fig. 4A). A similar inhibitory effect on *TWIST* and *FOXC2* expression was also detected in 293T cells transfected with BRCA1 (Supplementary Fig. S7). Because the ability of BRCA1 in regulating transcription controls normal differentiation and suppresses tumor development (36, 37), we determined whether BRCA1 is recruited to the *TWIST* promoter. A previous study demonstrated that GATA3 recruits BRCA1 to its binding sites in the *FOXC1/2* promoters to repress their transcription (27). We performed bioinformatic analysis of the *TWIST* gene promoter and found that there exists, at the least, six putative GATA3 binding sites on the *TWIST* promoter (Fig. 4B), which are conserved in both human and mouse (data not shown). We then performed a ChIP assay and found that one of five amplicons that contained two GATA3 sites was specifically enriched in the immunoprecipitation of BRCA1 in HCC1937 cells transfected with WT *BRCA1* compared with control (P5 in Fig. 4C). In sum, these results suggest that BRCA1 specifically binds to the *TWIST* promoter and negatively regulates its transcription.

To confirm the role of Brcal in the suppression of Twist and tumor development *in situ*, primary mammary tumors derived from *p18*^{-/-};*Brcal*^{+/-} mice were immunostained with antibodies against Brcal and Twist. We found that tumor cells positive for Brcal expressed very low or no Twist, whereas Brcal-mutant tumor cells expressed high levels of Twist, most

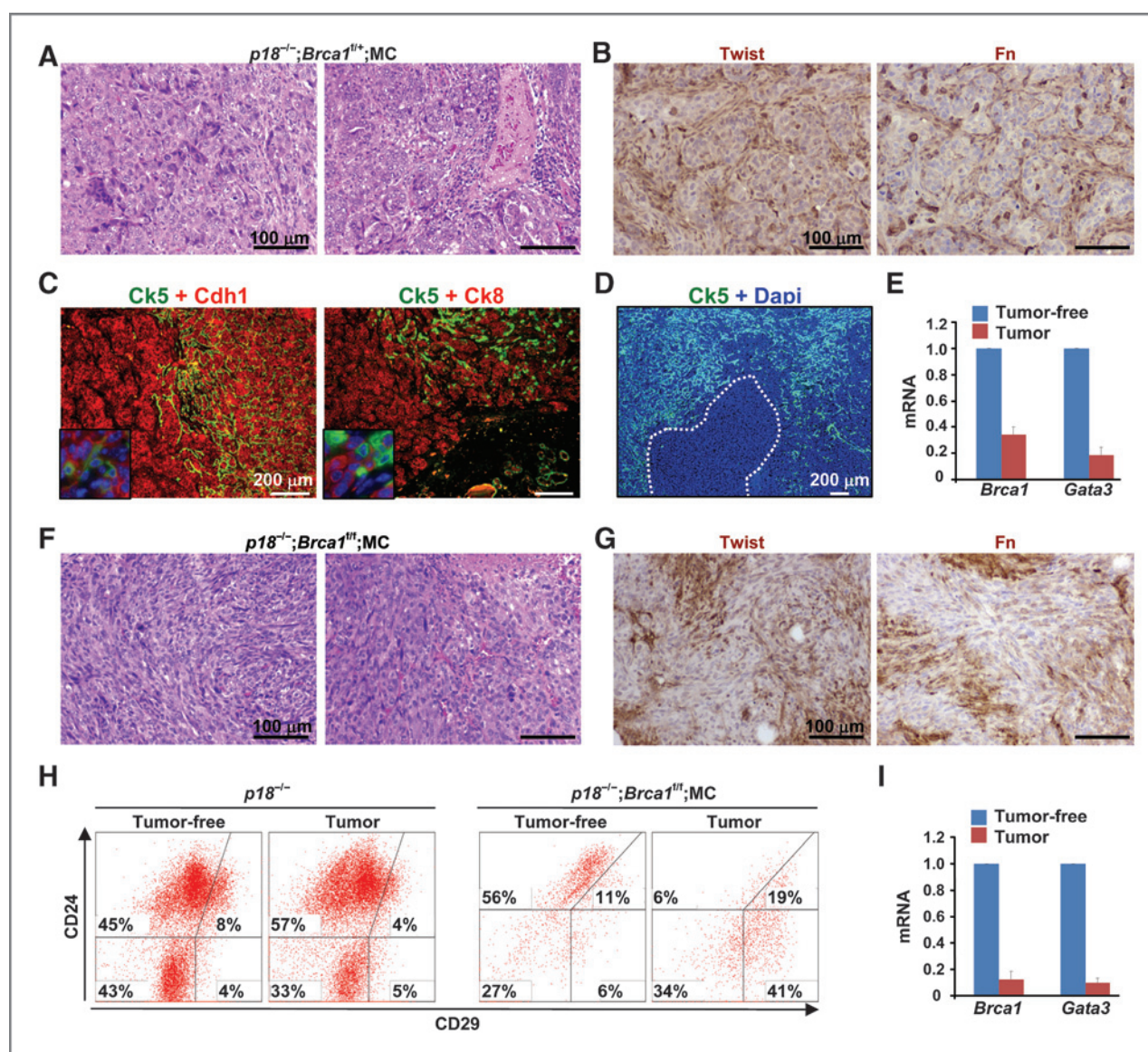


Figure 3. Deletion of Brca1 in mammary epithelia recapitulates basal-like tumor formation and EMT activation. Mammary tumors derived from *p18^{-/-};Brca1^{t/t};MC* (A–E) or *p18^{-/-};Brca1^{t/t};MC* (F–I) mice were stained with hematoxylin and eosin (A and F), Twist or Fn (B, G), Ck5 and Cdh1 or Ck8 (C), Ck5 (D), or analyzed by qRT-PCR (E, I) and FACS (H). Tumor-free mammary cells or tissues from the same mouse were used as controls. qRT-PCR data are expressed as the mean \pm SD from triplicates.

of which were spindle-shaped basal-like cells (Fig. 4D), demonstrating that Brca1 inhibits Twist and EMT in mammary tumor development and progression.

Knockdown of BRCA1 inactivates TWIST and EMT with enhanced tumor formation potential

We knocked down BRCA1 in two human luminal cancer cell lines, MCF7 and T47D, using BRCA1 shRNA targeting 3 different sequences (Fig. 5A, data not shown), and transplanted these cells into the mammary fat pads of NSG mice. We found that mammary tumors from T47D-Sh-BRCA1 cells were palpable in 8 weeks, whereas tumors formed from T47D-Sh-Ctrl. cells were undetectable at this stage (data not shown). Eighteen

weeks after transplantation, T47D-Sh-BRCA1 tumors were significantly bigger than T47D-Sh-Ctrl. tumors (Fig. 5B and C). Consistently, mammary tumors from MCF7-Sh-BRCA1 cells were palpable significantly sooner and were larger compared with tumors from MCF7-Sh-Ctrl. cells (data not shown). These results indicate that KD of BRCA1 in luminal cancer cells enhances their tumor formation potential. Histo- and pathologic analysis revealed that, unlike homogeneous and well-differentiated T47D-Sh-Ctrl. mammary tumors, T47D-Sh-BRCA1 tumors were highly heterogeneous with an abundance of large and poorly differentiated cells (Fig. 5D), suggesting that KD of BRCA1 induced the dedifferentiation of luminal tumor cells. IHC analysis indicated that most cells in T47D-Sh-BRCA1

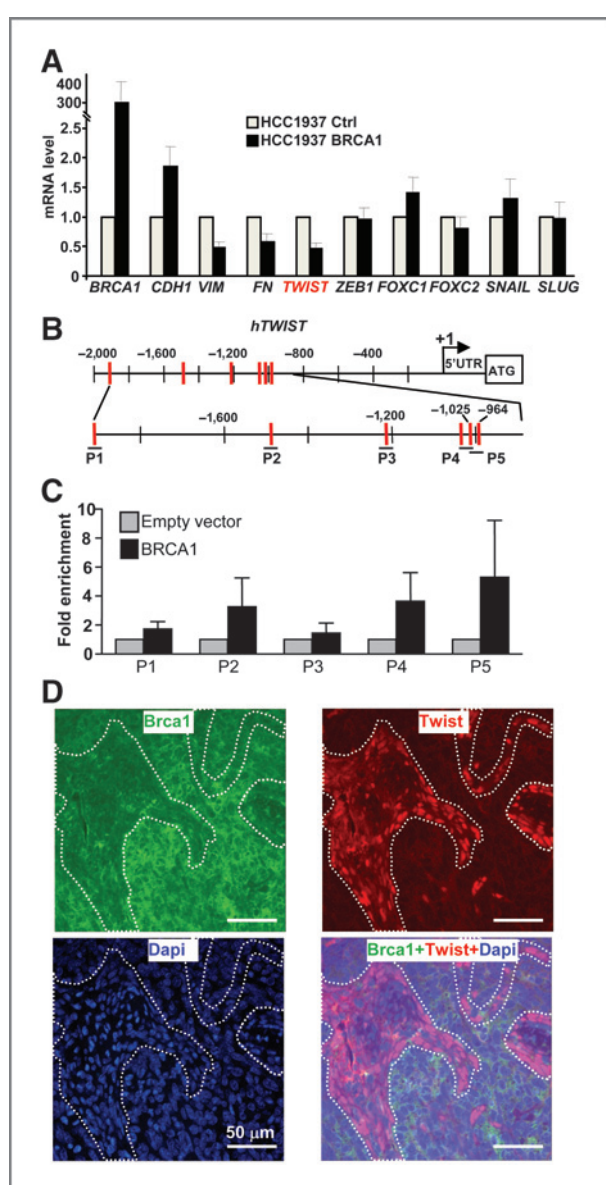


Figure 4. BRCA1 suppresses TWIST and EMT in mammary tumor cells. **A**, HCC1937 cells were transfected with pcDNA3-empty (Ctrl) or pcDNA3-BRCA1 (BRCA1), and RNA was analyzed. Data are expressed as the mean \pm SD from triplicates of two independent experiments. **B**, diagram showing the locations of putative GATA3 sites in the human *TWIST* gene. **C**, ChIP analysis of BRCA1 binding to putative GATA3 sites on the *TWIST* promoter in HCC1937 cells transfected with BRCA1. Data are expressed as the mean \pm SD from triplicates of two independent experiments. **D**, mammary tumors from *p18*^{-/-};*Brca1*^{+/+} mice were stained with antibodies against Brca1 (green) and Twist (red).

tumors expressed very faint or no CDH1 and ER α , but high levels of TWIST, VIM, and FN in comparison with T47D-Sh-Ctrl tumors (Fig. 5E–G; Supplementary Fig. S8), indicating that T47D-Sh-BRCA1 tumor cells had undergone EMT. These results collectively suggest that KD of BRCA1 in breast luminal tumor cells activates TWIST and EMT, which is associated with increased tumor formation potential, further supporting the data derived from *p18;Brca1* double-mutant mice.

***BRCA1* and *TWIST* expression levels are inversely related in human claudin-low type breast cancers**

Gene-expression profiling analyses have categorized human breast tumors into six intrinsic subtypes: basal-like (BL), claudin-low (CL), Her2 $^+$ (H2), luminal A (LA), luminal B (LB), and normal breast-like (NBL), each of which has unique biologic and prognostic features (28). Of these subtypes of breast cancer, the CL subtype is characterized by the low to absent expression of luminal differentiation markers and high enrichment for EMT markers and cancer stem cell-like features. Clinically, the majority of CL tumors are poor prognosis triple-negative (ER $^-$, PR $^-$, and HER2 $^-$) invasive carcinomas with high frequencies of metaplastic and medullary differentiation (28, 38, 39). To determine whether our mouse genetic analysis models human breast cancers, we queried the expression of *BRCA1* and EMT-TFs in the UNC337 breast cancer patient sample sets (28). We found that expressions of *BRCA1* and EMT-TFs were highly correlated with breast tumor-intrinsic subtypes (Fig. 6A). Specifically, the mRNA level of *BRCA1* was low, whereas that of EMT-TFs—*TWIST*, *SNAIL*, and *SLUG* in particular—was high in the CL subtype. Pearson correlation analysis revealed an inverse correlation between *BRCA1* with *TWIST* mRNA levels, but not with *SNAIL*, *SLUG*, and *FOXC1* (Fig. 6B). We performed similar analyses on the MetaBric dataset with 2,000 breast tumors (29) and detected similar results—*BRCA1* and *TWIST* mRNA levels were inversely correlated in all breast cancers and in the CL subtype in particular (Supplementary Fig. S9).

We screened 43 invasive breast cancers then selected five ER-positive and five ER-negative samples. RNA was prepared from microdissected FFPE sections of tumors. The expression levels of *BRCA1* in ER-negative tumors were significantly lower than in ER-positive tumors (1.16 ± 0.49 vs. 2.04 ± 0.56 ; $P = 0.015$), reflecting the downregulation of *BRCA1* mRNA in ER-negative tumors (Fig. 6D). IHC indicated that TWIST-positive tumor cells were only detected in ER-negative, CK5-positive tumors, not in ER-positive tumors. The expression of TWIST was closely associated with that of CK5 and was inversely correlated with the mRNA level of *BRCA1* (Fig. 6C and D). Furthermore, all TWIST-positive tumors were highly heterogeneous, poorly differentiated, and showed typical morphologic EMT features, evidenced by the various degrees of whorls and clusters of spindle-shaped cells within these tumors. Together, these clinical findings, consistent with our results in mice, further confirm that BRCA1 suppresses TWIST and EMT in breast basal-like cancer development and progression.

Discussion

In this article, we confirm our previous finding that heterozygous mutation of *Brca1* in *p18*-deficient mice transforms luminal tumors into basal-like tumors (10) and report here that it activates EMT-TFs and induces EMT. Consistently, specific deletion of *Brca1* in mammary epithelia led to enhanced self-renewal potential of stem cells, blockage of LSC expansion, impaired luminal gene expression, increased basal gene

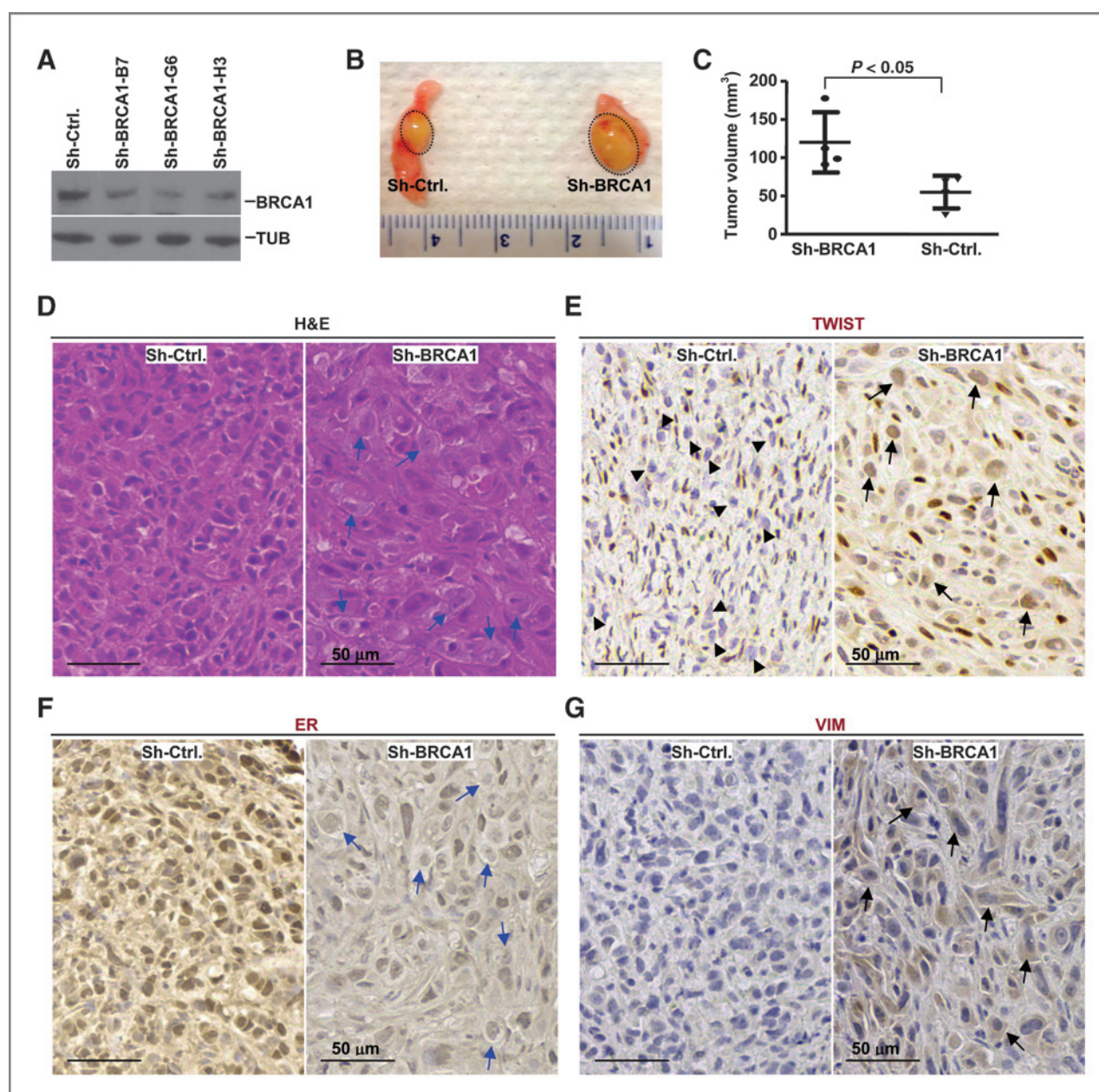


Figure 5. Knockdown of BRCA1 in luminal cancer cells increases tumor formation potential and TWIST expression. **A**, T47D cells were infected with either pGIPZ-empty (sh-Ctrl.) or pGIPZ-shBRCA1 targeting different sequences of human BRCA1 (sh-BRCA1-B7, sh-BRCA1-G6, and sh-BRCA1-H3). Cells stably expressing sh-Ctrl or shBRCA1 were analyzed by Western blot. **B** and **C**, T47D cells stably expressing sh-Ctrl or shBRCA1-G6 (sh-BRCA1) were transplanted into the mammary fat pads of female NSG. Representative gross appearance of tumors formed is shown (**B**) and tumor volumes were plotted (**C**). Values represent the average tumor volumes ± SD of four tumors. **D–G**, mammary tumors formed by transplantation of T47D cells stably expressing sh-Ctrl or sh-BRCA1 were stained with hematoxylin and eosin (**D**), TWIST (**E**), ER α (**F**), and VIM (**G**). Note the highly heterogeneous Sh-BRCA1 tumor cells that are positive for TWIST and VIM (black arrows) and negative for TWIST (black arrowheads) and for VIM in Sh-Ctrl. tumors. Large and less-differentiated cells in Sh-BRCA1 tumors are indicated by blue arrows.

expression, expansion of BSCs and CSCs, and induction of EMT and basal-like tumors. These results suggest that either germ-line mutation of *Brca1* or mammary epithelia-specific deletion of *Brca1* is responsible for the activation of EMT-TFs, induction of EMT, dedifferentiation of LSCs, expansion of BSCs and CSCs as well as the development of basal-like tumors. This study

provides the first genetic evidence suggesting that *Brca1* suppresses EMT and dedifferentiation of LSCs in mammary and tumor development. We also show that KD of BRCA1 in human luminal breast cancer cells activates EMT and increases tumor formation potential, further supporting the data derived from *p18;Brca1* double-mutant mice.

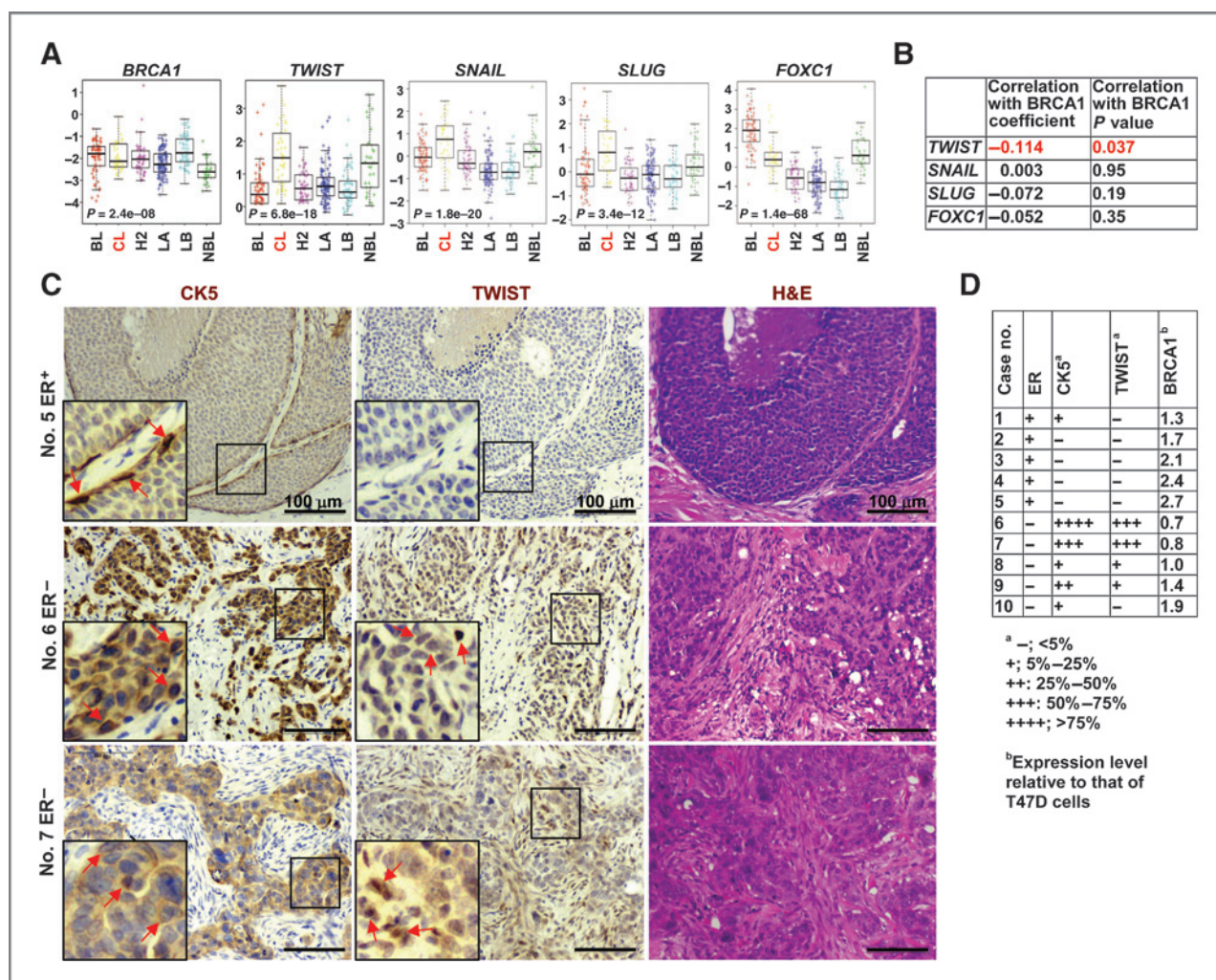


Figure 6. BRCA1 and TWIST levels are inversely related to the CL subtype of human breast cancer. **A**, analysis of gene expression in UNC337 breast cancer patients according to tumor subtype. **B**, correlation analysis of the expression of BRCA1 and EMT-TFs for UNC337 breast cancer patients. **C**, serial sections from ER-positive and -negative invasive human breast cancers were stained with hematoxylin and eosin (H&E), CK5, and TWIST. The boxed areas were enlarged in the insets. Representative cytoplasmic staining of CK5⁺ cells and nuclear staining of TWIST⁺ cells are indicated by arrows. **D**, summary of expression of CK5 and TWIST by IHC and BRCA1 by qRT-PCR. The expression levels of CK5 and TWIST were scored by the percentage of positive tumor cells in total tumor cells. The expression of BRCA1 was determined by qRT-PCR. The levels of BRCA1 mRNA were expressed as the mean values from triplicates of the two sets of the primers.

Because of growth defects induced by *Brcal* deficiency (40–42), mice carrying *Brcal* mutation in mammary epithelia rarely develop tumors, making it difficult to identify the cells of origin of *Brcal*-mutant basal-like tumors. Most, if not all, genetic studies have used comutation of one of the genes in the *p53* pathway to overcome the growth defects induced by mutation of *Brcal* in mice (8–9, 40–43). Specific deletion of *Brcal* in mammary epithelia by MMTV-Cre or Wap-Cre resulted in basal-like tumor development in *p53*-deficient mice (40, 43), supporting the notion that the cells of origin of basal-like tumors could be luminal cells. *p53^{f/f};Brcal^{f/f};K14-Cre* mice targeting deletion in the basal cell lineage developed basal-like tumors, suggesting that *BRCA1*-mutant breast cancer may also arise from basal stem/progenitor cells (44). Direct comparison of *p53^{+/−};Brcal^{f/f};K14-Cre* and *p53^{+/−};Brcal^{f/f};Blg-Cre*

mice targeting luminal stem/progenitor cells revealed that *p53^{+/−};Brcal^{f/f};Blg-Cre* tumors phenocopy human *BRCA1*-mutant basal-like breast cancers, whereas *p53^{+/−};Brcal^{f/f};K14-Cre* tumors do not resemble human *BRCA1* breast cancers, further supporting the notion that *Brcal*-mutant basal-like tumors originate from luminal stem/progenitor cells (9). However, mutation of *p53* in these studies may induce EMT and mammary tumors falling into multiple molecular subtypes, including the basal-like and claudin-low subtypes (45–48), masking the contribution of *Brcal* mutation alone in basal-like tumorigenesis. Hence, it is imperative that the role of *Brcal* in controlling mammary stem cells and tumorigenesis be determined under a genetically intact *p53* background.

EMT-TFs orchestrate EMT, which plays an important role in intratumoral heterogeneity and breast basal-like tumor

progression (49). Recently, Kupperwasser's group reported that *Slug*, an EMT-TF, is aberrantly expressed in the breast of *Brca1*-mutant carriers and that it is necessary for the induction of the basal-like phenotypes of human breast cancers created in mice by transformation of *BRCA1*^{mut/+} patient-derived breast epithelial cells with four tumorigenic genes (8). Gene-expression profiling of mammary tumors from *p53^{+/−};Brca1^{fl/fl}*, K14-Cre and *p53^{+/−};Brca1^{fl/fl}*;Blg-Cre mice showed high mRNA levels of some of the basal and EMT-TFs, including *Foxc1* and *Twist* (9). Furthermore, *Brca1* was found to bind to the promoters of *FOXC1* and *FOXC2* and repress their transcription (27). These findings support the function of *Brca1* in suppressing EMT-TFs; however, all of these data were derived from either *BRCA1* mutation carriers with unknown patient genetic background, *Brca1*-mutant mice in *p53*-deficient background, or breast cancer cell lines (8, 9, 27). The present study shows, for the first time *in vivo*, that *Brca1* suppresses *Twist* and EMT in LSCs and breast cancer cells in *p53*-intact background.

Deficiency of *Brca1* in mammary stem or tumor cells results in the aberrant expression of almost all EMT-TFs tested (Figs. 1–5). However, only *TWIST* mRNA is significantly, and *FOXC2* mRNA is moderately, suppressed by *BRCA1* (Fig. 4). Further supporting these results, our data and previous findings show that *BRCA1* binds to putative GATA3 binding sites on the *TWIST* and *FOXC2* promoters, respectively (this report and ref. 27). It remains to be determined whether GATA3 is required for *BRCA1* binding and suppression of these genes in mammary stem cells and tumorigenesis *in vivo*. Given the critical roles of *TWIST* and *FOXC2* in regulating EMT and the complex positive regulatory network between these transcription factors (15, 39, 50–53), we believe that *Brca1* suppresses EMT, at least partially, by inhibiting *TWIST* and *FOXC2*, which, in turn, suppresses other EMT-TFs. Another line of evidence supporting this conclusion is that overexpressing *TWIST* along with an active form of RAS in mouse mammary luminal cells leads to claudin-low tumors with EMT features and stem cell–

like characteristics (54), which molecularly and histologically resembles breast cancers developed in *p18;Brca1* double-mutant mice.

Disclosure of Potential Conflicts of Interest

C.M. Perou is a board member for and has ownership interest (including patents) in Bioclassifier LLC and Genecentric Diagnostics. No potential conflicts of interest were disclosed by the other authors.

Authors' Contributions

Conception and design: F. Bai, A.S. Livingstone, X.-H. Pei
Development of methodology: F. Bai, H.L. Chan, A.J. Capobianco, X.-H. Pei
Acquisition of data (provided animals, acquired and managed patients, provided facilities, etc.): F. Bai, H.L. Chan, M.D. Smith, J.I. Herschkowitz, A.S. Livingstone
Analysis and interpretation of data (e.g., statistical analysis, biostatistics, computational analysis): H.L. Chan, A. Scott, M.D. Smith, C. Fan, J.I. Herschkowitz, C.M. Perou, D.J. Robbins, X.-H. Pei
Writing, review, and/or revision of the manuscript: H.L. Chan, A. Scott, M.D. Smith, J.I. Herschkowitz, C.M. Perou, A.S. Livingstone, D.J. Robbins, X.-H. Pei
Administrative, technical, or material support (i.e., reporting or organizing data, constructing databases): F. Bai, H.L. Chan, M.D. Smith
Study supervision: A.S. Livingstone, X.-H. Pei
Others (advice on design and interpretation of data, manuscript review and revision): A.J. Capobianco

Acknowledgments

The authors thank Dr. Yue Xiong for his invaluable support and discussion, Drs. Beverly Koller, Chuxia Deng, and Lothar Hennighausen for *Brca1*-mutant and MMTV-cre mice, Joyce Slingerland for discussion, the University of Miami FACS core facility for cell sorting, and the Division of Veterinary Resources (DVR) for animal husbandry.

Grant Support

This study was supported by DOD Idea Award (W81XWH-10-1-0302), DOD Idea Expansion Award (W81XWH-13-1-0282), Sylvester BFBCI Developmental Grant, IRG-98-277-13 from the American Cancer Society, and startup funds from the University of Miami (X.-H. Pei).

The costs of publication of this article were defrayed in part by the payment of page charges. This article must therefore be hereby marked *advertisement* in accordance with 18 U.S.C. Section 1734 solely to indicate this fact.

Received April 29, 2014; revised July 24, 2014; accepted August 24, 2014; published OnlineFirst September 19, 2014.

References

- Van Keymeulen A, Rocha AS, Ousset M, Beck B, Bouvencourt G, Rock J, et al. Distinct stem cells contribute to mammary gland development and maintenance. *Nature* 2011;479:189–93.
- Spike BT, Engle DD, Lin JC, Cheung SK, La J, Wahl GM. A mammary stem cell population identified and characterized in late embryogenesis reveals similarities to human breast cancer. *Cell Stem Cell* 2012;10:183–97.
- van Amerongen R, Bowman AN, Nusse R. Developmental stage and time dictate the fate of Wnt/beta-catenin-responsive stem cells in the mammary gland. *Cell Stem Cell* 2012;11:387–400.
- Lobo NA, Shimono Y, Qian D, Clarke MF. The biology of cancer stem cells. *Annu Rev Cell Dev Biol* 2007;23:675–99.
- Foulkes WD. BRCA1 functions as a breast stem cell regulator. *J Med Genet* 2004;41:1–5.
- Liu S, Ginestier C, Charafe-Jauffret E, Foco H, Kleer CG, Merajver SD, et al. BRCA1 regulates human mammary stem/progenitor cell fate. *Proc Natl Acad Sci U S A* 2008;105:1680–5.
- Lim E, Vaillant F, Wu D, Forrest NC, Pal B, Hart AH, et al. Aberrant luminal progenitors as the candidate target population for basal tumor development in BRCA1 mutation carriers. *Nat Med* 2009;15:907–13.
- Proia TA, Keller PJ, Gupta PB, Klebba I, Jones AD, Sedic M, et al. Genetic predisposition directs breast cancer phenotype by dictating progenitor cell fate. *Cell Stem Cell* 2011;8:149–63.
- Molyneux G, Geyer FC, Magnay FA, McCarthy A, Kendrick H, Natrajan R, et al. BRCA1 basal-like breast cancers originate from luminal epithelial progenitors and not from basal stem cells. *Cell Stem Cell* 2010;7:403–17.
- Bai F, Smith MD, Chan HL, Pei XH. Germline mutation of *Brca1* alters the fate of mammary luminal cells and causes luminal-to-basal mammary tumor transformation. *Oncogene* 2013;32:2715–25.
- Wright MH, Calcagno AM, Salcido CD, Carlson MD, Ambudkar SV, Varticovski L. *Brca1* breast tumors contain distinct CD44+/CD24– and CD133+ cells with cancer stem cell characteristics. *Breast Cancer Res* 2008;10:R10.
- Wicha MS. Cancer stem cell heterogeneity in hereditary breast cancer. *Breast Cancer Res* 2008;10:105.
- Wright MH, Robles AI, Herschkowitz JI, Hollingshead MG, Anver MR, Perou CM, et al. Molecular analysis reveals heterogeneity of mouse mammary tumors conditionally mutant for *Brca1*. *Mol Cancer* 2008;7:29.
- Kalluri R, Weinberg RA. The basics of epithelial-mesenchymal transition. *J Clin Invest* 2009;119:1420–8.

15. Yang J, Mani SA, Donaher JL, Ramaswamy S, Itzykson RA, Come C, et al. Twist, a master regulator of morphogenesis, plays an essential role in tumor metastasis. *Cell* 2004;117:927–39.
16. Pei XH, Bai F, Smith MD, Usary J, Fan C, Pai SY, et al. CDK inhibitor p18 (INK4c) is a downstream target of GATA3 and restrains mammary luminal progenitor cell proliferation and tumorigenesis. *Cancer Cell* 2009;15:389–401.
17. Koboldt DC, Fulton RS, McLellan MD, Schmidt H, Kalicki-Veizer J, McMichael JF, et al. Comprehensive molecular portraits of human breast tumours. *Nature* 2012;490:61–70.
18. Jonsson G, Staaf J, Vallon-Christersson J, Ringner M, Gruvberger-Saal SK, Saal LH, et al. The retinoblastoma gene undergoes rearrangements in BRCA1-deficient basal-like breast cancer. *Cancer Res* 2012;72:4028–36.
19. Jiang Z, Deng T, Jones R, Li H, Herschkowitz JI, Liu JC, et al. Rb deletion in mouse mammary progenitors induces luminal-B or basal-like/EMT tumor subtypes depending on p53 status. *J Clin Invest* 2010;120:3296–309.
20. Cheng L, Zhou Z, Flesken-Nikitin A, Toshkov IA, Wang W, Camps J, et al. Rb inactivation accelerates neoplastic growth and substitutes for recurrent amplification of cIAP1, cIAP2 and Yap1 in sporadic mammary carcinoma associated with p53 deficiency. *Oncogene* 2010;29: 5700–11.
21. Xu X, Wagner KU, Larson D, Weaver Z, Li C, Ried T, et al. Conditional mutation of Brca1 in mammary epithelial cells results in blunted ductal morphogenesis and tumour formation. *Nat Genet* 1999;22:37–43.
22. Wagner KU, Wall RJ, St-Onge L, Gruss P, Wynshaw-Boris A, Garrett L, et al. Cre-mediated gene deletion in the mammary gland. *Nucleic Acids Res* 1997;25:4323–30.
23. Shackleton M, Vaillant F, Simpson KJ, Stingl J, Smyth GK, Asselin-Labat ML, et al. Generation of a functional mammary gland from a single stem cell. *Nature* 2006;439:84–8.
24. Stingl J, Eirew P, Ricketson I, Shackleton M, Vaillant F, Choi D, et al. Purification and unique properties of mammary epithelial stem cells. *Nature* 2006;439:993–7.
25. Hollier BG, Tinnirello AA, Werden SJ, Evans KW, Taube JH, Sarkar TR, et al. FOXC2 expression links epithelial-mesenchymal transition and stem cell properties in breast cancer. *Cancer Res* 2013;73:1981–92.
26. Hill JW, Tansavatdi K, Lockett KL, Allen GO, Takita C, Pollack A, et al. Validation of the cell cycle G(2) delay assay in assessing ionizing radiation sensitivity and breast cancer risk. *Cancer Manag Res* 2009;1:39–48.
27. Tkocz D, Crawford NT, Buckley NE, Berry FB, Kennedy RD, Gorski JJ, et al. BRCA1 and GATA3 corepress FOXC1 to inhibit the pathogenesis of basal-like breast cancers. *Oncogene* 2011;31:3667–78.
28. Prat A, Parker JS, Karginova O, Fan C, Livasy C, Herschkowitz JI, et al. Phenotypic and molecular characterization of the claudin-low intrinsic subtype of breast cancer. *Breast Cancer Res* 2010;12:R68.
29. Curtis C, Shah SP, Chin SF, Turashvili G, Rueda OM, Dunning MJ, et al. The genomic and transcriptomic architecture of 2,000 breast tumours reveals novel subgroups. *Nature* 2012;486:346–52.
30. Shafee N, Smith CR, Wei S, Kim Y, Mills GB, Hortobagyi GN, et al. Cancer stem cells contribute to cisplatin resistance in Brca1/p53-mediated mouse mammary tumors. *Cancer Res* 2008;68:3243–50.
31. Buono KD, Robinson GW, Martin C, Shi S, Stanley P, Tanigaki K, et al. The canonical Notch/RBP-J signaling pathway controls the balance of cell lineages in mammary epithelium during pregnancy. *Dev Biol* 2006;293:565–80.
32. Lim E, Wu D, Pal B, Bouras T, Asselin-Labat ML, Vaillant F, et al. Transcriptome analyses of mouse and human mammary cell subpopulations reveal multiple conserved genes and pathways. *Breast Cancer Res* 2010;12:R21.
33. Wagner KU, McAllister K, Ward T, Davis B, Wiseman R, Hennighausen L. Spatial and temporal expression of the Cre gene under the control of the MMTV-LTR in different lines of transgenic mice. *Transgenic Res* 2001;10:545–53.
34. Weigelt B, Kreike B, Reis-Filho JS. Metaplastic breast carcinomas are basal-like breast cancers: a genomic profiling analysis. *Breast Cancer Res Treat* 2009;117:273–80.
35. Keller PJ, Lin AF, Arendt LM, Klebbä I, Jones AD, Rudnick JA, et al. Mapping the cellular and molecular heterogeneity of normal and malignant breast tissues and cultured cell lines. *Breast Cancer Res* 2010;12:R87.
36. Shakya R, Reid LJ, Reczek CR, Cole F, Egli D, Lin CS, et al. BRCA1 tumor suppression depends on BRCT phosphoprotein binding, but not its E3 ligase activity. *Science* 2011;334:525–8.
37. Buckley NE, Mullan PB. BRCA1 – conductor of the breast stem cell orchestra: the role of BRCA1 in mammary gland development and identification of cell of origin of BRCA1 mutant breast cancer. *Stem Cell Rev* 2012;8:982–93.
38. Herschkowitz JI, Zhao W, Zhang M, Usary J, Murrow G, Edwards D, et al. Comparative oncogenomics identifies breast tumors enriched in functional tumor-initiating cells. *Proc Natl Acad Sci U S A* 2012;109: 2778–83.
39. Taube JH, Herschkowitz JI, Komurov K, Zhou AY, Gupta S, Yang J, et al. Core epithelial-to-mesenchymal transition interactome gene-expression signature is associated with claudin-low and metaplastic breast cancer subtypes. *Proc Natl Acad Sci U S A* 2010;107: 15449–54.
40. Drost RM, Jonkers J. Preclinical mouse models for BRCA1-associated breast cancer. *Br J Cancer* 2009;101:1651–7.
41. Cao L, Kim S, Xiao C, Wang RH, Coumoul X, Wang X, et al. ATM-Chk2-p53 activation prevents tumorigenesis at an expense of organ homeostasis upon Brca1 deficiency. *EMBO J* 2006;25:2167–77.
42. Cao L, Li W, Kim S, Brodie SG, Deng CX. Senescence, aging, and malignant transformation mediated by p53 in mice lacking the Brca1 full-length isoform. *Genes Dev* 2003;17:201–13.
43. Kumar P, Mukherjee M, Johnson JP, Patel M, Huey B, Albertson DG, et al. Cooperativity of Rb, Brca1, and p53 in malignant breast cancer evolution. *PLoS Genet* 2012;8:e1003027.
44. Liu X, Holstege H, van der Gulden H, Treur-Mulder M, Zevenhoven J, Velds A, et al. Somatic loss of BRCA1 and p53 in mice induces mammary tumors with features of human BRCA1-mutant basal-like breast cancer. *Proc Natl Acad Sci U S A* 2007;104: 12111–6.
45. Chang CJ, Chao CH, Xia W, Yang JY, Xiong Y, Li CW, et al. p53 regulates epithelial-mesenchymal transition and stem cell properties through modulating miRNAs. *Nat Cell Biol* 2011;13:317–23.
46. Wang SP, Wang WL, Chang YL, Wu CT, Chao YC, Kao SH, et al. p53 controls cancer cell invasion by inducing the MDM2-mediated degradation of Slug. *Nat Cell Biol* 2009;11:694–704.
47. Wu WS, Heinrichs S, Xu D, Garrison SP, Zambetti GP, Adams JM, et al. Slug antagonizes p53-mediated apoptosis of hematopoietic progenitors by repressing puma. *Cell* 2005;123:641–53.
48. Herschkowitz JI, Zhao W, Zhang M, Usary J, Murrow G, Edwards D, et al. Breast Cancer Special Feature: comparative oncogenomics identifies breast tumors enriched in functional tumor-initiating cells. *Proc Natl Acad Sci U S A* 2011;108:2778–83.
49. Polyak K, Weinberg RA. Transitions between epithelial and mesenchymal states: acquisition of malignant and stem cell traits. *Nat Rev Cancer* 2009;9:265–73.
50. Mani SA, Guo W, Liao MJ, Eaton EN, Ayyanan A, Zhou AY, et al. The epithelial-mesenchymal transition generates cells with properties of stem cells. *Cell* 2008;133:704–15.
51. Mani SA, Yang J, Brooks M, Schwaninger G, Zhou A, Miura N, et al. Mesenchyme Forkhead 1 (FOXC2) plays a key role in metastasis and is associated with aggressive basal-like breast cancers. *Proc Natl Acad Sci U S A* 2007;104:10069–74.
52. Ansieau S, Morel AP, Hinkal G, Bastid J, Puisieux A. TWISTING an embryonic transcription factor into an oncoprotein. *Oncogene* 2010;29:3173–84.
53. Scheel C, Weinberg RA. Cancer stem cells and epithelial-mesenchymal transition: concepts and molecular links. *Semin Cancer Biol* 2012;22:396–403.
54. Morel AP, Hinkal GW, Thomas C, Fauvet F, Courtois-Cox S, Wierinckx A, et al. EMT inducers catalyze malignant transformation of mammary epithelial cells and drive tumorigenesis towards claudin-low tumors in transgenic mice. *PLoS Genet* 2012;8:e1002723.

p16^{INK4a} suppresses BRCA1-deficient mammary tumorigenesis

Alexandria Scott^{1,2}, Feng Bai¹, Ho Lam Chan¹, Shiqin Liu¹, Jinshan Ma¹, Joyce M Slingerland³, David J. Robbins^{1,4}, Anthony J. Capobianco^{1,4}, Xin-Hai Pei^{1,2,4}

¹Molecular Oncology Program, Department of Surgery, Miller School of Medicine, University of Miami, Miami, FL 33136

²The Sheila and David Fuente Graduate Program in Cancer Biology, Miller School of Medicine, University of Miami, Miami, FL 33136

³Braman Family Breast Cancer Institute, Sylvester Cancer Center, Miller School of Medicine, University of Miami, Miami, FL 33136

⁴Sylvester Cancer Center, Miller School of Medicine, University of Miami, Miami, FL 33136

Correspondence to: Xin-Hai Pei, **email:** xhpei@med.miami.edu

Keywords: *p16^{INK4a}, senescence, brca1, breast cancer*

Received: June 30, 2016

Accepted: October 25, 2016

Published:

ABSTRACT

Senescence prevents the proliferation of genetically damaged, but otherwise replication competent cells at risk of neoplastic transformation. *p16^{INK4A}* (*p16*), an inhibitor of CDK4 and CDK6, plays a critical role in controlling cellular senescence in multiple organs. Functional inactivation of *p16* by gene mutation and promoter methylation is frequently detected in human breast cancers. However, deleting *p16* in mice or targeting DNA methylation within the murine *p16* promoter does not result in mammary tumorigenesis. How loss of *p16* contributes to mammary tumorigenesis *in vivo* is not fully understood.

In this article, we reported that disruption of *Brca1* in the mammary epithelium resulted in premature senescence that was rescued by *p16* loss. We found that *p16* loss transformed *Brca1*-deficient mammary epithelial cells and induced mammary tumors, though *p16* loss alone was not sufficient to induce mammary tumorigenesis. We demonstrated that loss of both *p16* and *Brca1* led to metastatic, basal-like, mammary tumors with the induction of EMT and an enrichment of tumor initiating cells. We discovered that promoter methylation silenced *p16* expression in most of the tumors developed in mice heterozygous for *p16* and lacking *Brca1*. These data not only identified the function of *p16* in suppressing *BRCA1*-deficient mammary tumorigenesis, but also revealed a collaborative effect of genetic mutation of *p16* and epigenetic silencing of its transcription in promoting tumorigenesis. To the best of our knowledge, this is the first genetic evidence directly showing that *p16* which is frequently deleted and inactivated in human breast cancers, collaborates with *Brca1* controlling mammary tumorigenesis.

INTRODUCTION

Senescence is a well-established barrier to tumorigenesis that prevents the proliferation of genetically damaged, but otherwise replication competent cells at risk of neoplastic transformation. Control of the G1 phase of the cell cycle is intrinsically linked with the maintenance of quiescent and senescent states in stem and somatic cells, respectively, and is primarily controlled by the INK4-CDK4/6-Rb pathway. The INK4 family of cell cycle inhibitors comprising of *p16^{INK4A}*, *p15^{INK4B}*, *p18^{INK4C}* and

p19^{INK4D} (*p16*, *p15*, *p18* and *p19*) inhibit CDK4 and CDK6, leading to the functional inactivation of RB [1]. Functional inactivation of this pathway is a common event in the development of most types of cancers [2], and also causes the loss of quiescent and senescent states of cells [3].

Unlike other INK4 family proteins, *p16* is not expressed early, but is markedly increased with aging and senescence [4, 5]. Experiments in mice with a germline deletion of *p16* reveal that *p16* controls senescence in multiple organs during aging [6–9]. Importantly, *p16* is deleted in ~50% of breast cancer cell lines, and *p16*

inactivation by DNA methylation occurs in ~30% of human breast cancers [2, 10, 11]. However, deleting p16 in mice or targeting DNA methylation within the murine p16 promoter does not result in mammary tumorigenesis but rather, these mice develop lymphomas and sarcomas with long latency [12–14]. How loss of p16 contributes to mammary tumorigenesis *in vivo* is not fully understood.

Breast cancer is heterogeneous with tumors that are both pathologically distinct and diverse in their responsiveness to treatment. Breast cancer is comprised of three main subtypes: HER2-positive, luminal, and basal-like cancers (BLBCs). Basal-like breast cancers (BLBCs) are ER-negative and more metastatic with few therapeutic options [15–18]. BRCA1 is a tumor suppressor, and its function has been linked with multiple pathways including DNA damage repair and oxidative stress regulation [19]. Functional loss of *BRCA1* by germline or somatic mutation or by promoter methylation is associated with more than one third of basal-like breast cancers and cell lines [20–22]. Patients with a BRCA1 deficiency develop BLBCs that are enriched with tumor-initiating cells (TICs) and exhibit epithelial-mesenchymal transition (EMT) characteristics [15, 16]. EMT, a process in which epithelial cells lose many of their epithelial characteristics and acquire mesenchymal features, plays an important role in tumor heterogeneity and generation of TICs [23]. TICs are thought to drive clinical relapse and metastasis [17, 18].

BRCA1 deficiency in human and mouse mammary epithelial cells activates both the p16-RB and p53 pathways, inducing premature senescence [24–26]. Consistently, heterozygous germline deletion of *Brcal* or specific deletion of *Brcal* in mouse mammary epithelial cells rarely develop mammary tumors. About 10% of *Brcal^{+/−}* or *Brcal^{ff};MMTV-cre* mice develop mammary tumors by 18 months of age [24, 25, 27–29]. Loss of p53 or its downstream target, p21, *in vivo* as well as knockdown of p16 or its downstream target, Rb, *in vitro* partially rescues the premature senescence of *Brcal*-deficient cells [24–28, 30], suggesting that disruption of the p53 and p16-Rb pathway are required to overcome *Brcal*-deficiency induced senescence and induce breast cancers. Indeed, inactivation of the p53 pathway enhances mammary tumor incidence and shortens the time of tumor onset in *Brcal*-deficient mice [27, 28, 31, 32]. Notably, most human BLBCs with functional loss of BRCA1 have dysfunctional p16-RB and p53 pathways [33–36]. However, most genetic studies of *Brcal* in mice co-mutate *Brcal* with one of the genes in the p53 pathway [27, 28, 31, 32, 37]. It remains poorly understood whether p16 is involved in *Brcal*-deficient MEC senescence and tumorigenesis.

In this report, we generated *p16* and *Brcal* single and compound mutant mice to determine their function in controlling mammary epithelial cell (MEC) senescence and tumorigenesis.

RESULTS

p16 loss ameliorates *Brcal* deficiency-induced senescence in MECs

We and others previously demonstrated that heterozygous germline mutation of *Brcal* in human and mice leads to premature senescence in MECs [24, 26], though the molecular and cellular basis controlling *Brcal*-deficiency-induced senescence is not fully understood. To directly determine the role of *Brcal* loss in mammary epithelial cell senescence and tumorigenesis, we used *Brcal^{ff};MMTV-Cre* and *Brcal^{ff}*;MMTV-Cre mice (*Brcal^{MGKO}*) mice as we previously described [25]. We compared *Brcal^{MGKO}* mice to age-matched WT animals and found that mRNA levels of *p16* were increased in *Brcal^{MGKO}* mammary relative to WT counterparts (Figure 1A). Taking into consideration the growth defects and increased SA-β-gal positivity in *Brcal^{MGKO}* MECs relative to WT counterparts (see below), these data suggest that *Brcal*-deficiency induced senescence in the mammary epithelium correlates with increased expression of *p16*.

Considering that *Brcal* loss induces premature senescence with an increase of *p16* expression in MECs and that loss of p16 mitigates age-associated cellular senescence in compartments of the brain, pancreatic islets and blood [6–8], we were inspired to determine the role of p16 in controlling *Brcal* deficiency-induced MEC senescence and tumorigenesis. To this end, we generated *p16^{−/−};Brcal^{MGKO}* mice on a Balb/c-FVB-B6 mixed background. We found that the percentages of Ki67-positive MECs in *p16^{−/−}* and *p16^{−/−};Brcal^{MGKO}* mice (24.28 ± 2.1 and 24.06 ± 4.3) were significantly higher than those in WT mice (6.39 ± 1.3), which in turn were significantly higher than the percentage in *Brcal^{MGKO}* (2.20 ± 0.2) mice (Figure 1B). We then directly examined Rb phosphorylation in MECs of different genotypes by using an antibody specifically recognizing Rb proteins phosphorylated at Ser608 by CDK4 and CDK6 [38, 39], the functional targets of p16. A consistent increase of pRb-Ser608 phosphorylation was detected in *p16^{−/−}* mammary epithelia ($9.86 \pm 6.6\%$ in WT to $21.64 \pm 5.4\%$ in *p16^{−/−}*, Figure 1C), confirming the activation of CDK4 and/or CDK6. Consistent with our previous finding [24], $3.42 \pm 5.0\%$ pRb-Ser608 positive MECs were detected in *Brcal^{MGKO}* females, which is significantly less than those in WT counterparts. However, *p16^{−/−};Brcal^{MGKO}* mice had a significant higher percentage of positive MECs ($20.69 \pm 7.2\%$, Figure 1C) than *Brcal^{MGKO}* mice. Together with the data derived from Ki67 staining, these results indicate that loss of p16 stimulates CDK4 and/or CDK6 activity toward the Rb protein in MECs, increasing their proliferation and rescuing the proliferative decline observed in *Brcal*-deficient MECs.

To further consolidate the role of loss of p16 and Brca1 in the regulation of MEC proliferation, we isolated and cultured primary MECs from virgin mice. We observed that *Brca1^{MGKO}* MECs exhibited a large and flattened shape, a typical morphology of cellular senescence, while MECs from the other genotypes of mice were smaller and spindle-shaped (Figure 1D). Notably, most *Brca1^{MGKO}* MECs exhibited strong, peri-nuclear staining of SA- β -gal whereas only a small population of WT MECs and very few *p16^{-/-}* and *p16^{-/-};Brca1^{MGKO}* MECs showed positive staining (Figure 1E). We then pulse-labeled primary MECs with bromodeoxyuridine (BrdU) for 15 hours and performed FACS analysis. *Brca1^{MGKO}*-MECs had increased G1 and decreased S phase cells relative to their WT counterparts (G1 phase cells, 29% vs 15%; S phase cells, 60% vs 68% Supplementary Figure S1). Importantly, MECs from *p16^{-/-}* or *p16^{-/-};Brca1^{MGKO}* mice displayed similar BrdU incorporation rates, 81% for *p16^{-/-}* and 79% for *p16^{-/-};Brca1^{MGKO}*, which were significantly higher than their WT counterparts (Supplementary Figure S1). These data suggest that loss of *Brca1* induces senescence in MECs, which is rescued by p16 loss.

Loss of p16 transforms Brca1-deficient MECs and induces mammary tumors

45% ($n = 20$) of *p16^{-/-}* mice developed lymphoma and sarcoma in 24 months, which is consistent with previous reports [12, 13] (Table 1). Of the nine *p16^{-/-}* tumors, two were detected in the mammary gland and were highly composed of lymphoma cells, as evidenced by their lymphocyte-like morphology, positivity for CD45 and CD31 by FACS analysis and negativity for Cdh1, an epithelial cell marker, by IHC (Supplementary Figure S2A, S2C and S2E). Interestingly, FACS analysis revealed that 1.7%–3.5% of the total tumor cell population was negative for CD45 and/or CD31 respectively (Supplementary Figure S2C), and IHC showed that less than 4% of sporadic tumor cells were epithelial-like and positively stained with Cdh1 (Supplementary Figure S2E), indicating that this tumor was comprised predominantly of lymphoma cells and that a small portion of cells originated from the mammary epithelium. These results confirm the predominant role of p16 in suppressing the development of lymphoma and sarcoma, and suggest that mammary tumorigenesis in p16 null mice may be masked by lymphomas and sarcomas.

We then followed the mammary tumor development in older mice and found that 63% of the *p16^{-/-};Brca1^{MGKO}* mice ($n = 8$) and 44% of *p16^{+/-};Brca1^{MGKO}* mice ($n = 9$) developed mammary tumors at 11–20 months and 16–23 months, respectively (Table 1, and Supplementary Table S1), whereas no *p16^{-/-}*, *p16^{+/-}* or *Brca1^{MGKO}* mice did so at similar ages (Table 1). Median mammary tumor-free survival time in *p16^{-/-};Brca1^{MGKO}* mice (including *p16^{-/-};Brca1^{MGKO}* and *p16^{+/-};Brca1^{MGKO}* mice) was 18 months (Figure 2A).

These results indicate that haploid or complete loss of p16 transforms Brca1-deficient mammary epithelial cells and induces mammary tumors.

Depletion of both p16 and Brca1 leads to basal-like mammary tumors with EMT features

Mammary tumors developed in *p16^{-/-};Brca1^{MGKO}* mice were very aggressive and displayed typical morphological characteristics of highly malignant features (increased necrosis, spindle cells, nuclear-cytoplasm ratio, and mitotic indices) (Figure 2B, 2D, Supplementary Figure S2A, Supplementary Figure S3). 18% of the *p16^{-/-};Brca1^{MGKO}* mice ($n = 17$) developed two distinct mammary tumors in two separate mammary glands, demonstrating the ability of these mice to develop both intra- and inter-tumoral heterogeneity (Figure 2B, Supplementary Figure S3). Furthermore, 56% of the *p16^{-/-};Brca1^{MGKO}* mammary tumors ($n = 9$) metastasized to the lung in 17–20 months (Table 1, Figure 2D, Supplementary Table S1). All mammary tumors developed in *p16^{-/-};Brca1^{MGKO}* mice were positively stained with basal markers, Ck5 and Ck14 in 2–75% of total tumor cells (Figure 2C, 2D, Supplementary Figure S2B, Supplementary Figure S4, Supplementary Table S1). Further analysis revealed that most of these tumor cells expressed significantly reduced levels of Cdh1 protein when compared with levels in luminal cells of the mammary glands (Supplementary Figure S2E). Mammary tumors developed in *p16^{-/-};Brca1^{MGKO}* mice expressed 44% *Gata3*, and 54% *Eif5*, both of which are genes associated with luminal cell differentiation, relative to the tumor-free mammary tissues of the same mouse (Supplementary Figure S2D), confirming Brca1-deficiency impaired luminal differentiation during tumorigenesis, as we previously demonstrated [24, 25]. All mammary tumors derived from *p16^{-/-};Brca1^{MGKO}* mice were stained positively for vimentin (Vim), a mesenchymal marker, and Twist, an EMT transcription factor (Table 1, Supplementary Figure S2F). These data indicate that depletion of both p16 and Brca1 results in basal-like mammary tumors with activation of EMT, which is consistent with our previous finding that deletion of *Brca1* activates EMT in mammary tumorigenesis [25].

We screened 43 human invasive breast cancers and selected 10 ER-negative samples with the lowest *BRCA1* mRNA expression as previously described [25]. We compared tumor pathology and expression of CK5 and CK14 in these samples with mouse mammary tumors. We noticed that both the tumor cell morphology and expression pattern of CK5 and CK14 in *p16^{-/-};Brca1^{MGKO}* mice resembled human basal-like breast cancers that were ER-negative and expressed low *BRCA1* (Supplementary Figure S4).

Given the function of Brca1 in DNA damage repair, we also evaluated the role of Brca1 loss in inducing

Table 1: Spontaneous tumor development in WT and mutant female mice

Tumor	Wt	<i>p16</i> ^{+/-}	<i>p16</i> ^{-/-}	<i>Brcal</i> ^{MGKO} ^a	<i>p16</i> ^{+/-} ; <i>Brcal</i> ^{MGKO}	<i>p16</i> ^{-/-} ; <i>Brcal</i> ^{MGKO}
	11–24 m	11–24 m	11–24 m	11–24 m	11–24 m	11–24 m
Mammary Tumor	0/9 ^b	0/6 ^c	0/20 ^d	0/8 ^e	4/9 ^f (44%)	5/8 ^g (63%)
Metastasis					3/4 ^h	2/5 ⁱ
CK14 + tumor					4/4	5/5
EMT + tumor					4/4	5/5
Other tumors	1/9 ^j		9/20 ^k	1/8 ^l	3/9 ^m	5/8 ⁿ

^a*Brcal*^{MGKO}, *Brcal*^{fl/fl}; MMTV-Cre or *Brcal*^{fl/fl}; MMTV-Cre mice.^bone mouse was 24 months of age, and the remaining mice were 11–20 months of age.^cone mouse was 24 months of age, and the remaining mice were 11–20 months of age.^dtwo mice developed tumors in mammary glands composed of lymphoma cells and 1%–4.0% epithelial-like cells respectively.^eone mouse was 23 months of age, and the remaining mice were 11–19 months of age.^ffour mice developed mammary tumors at 18, 18, 19 and 20 months of age, respectively. One mouse developed two different mammary tumors at two separate mammary glands. One mouse was 23 months of age, and the remaining mice were 14–20 months of age. One mouse was a breeder. Mammary tumor incidence, *p16*^{+/-}; *Brcal*^{MGKO} vs *p16*^{+/-}, $P = 0.103$; *p16*^{+/-}; *Brcal*^{MGKO} vs *Brcal*^{MGKO}, $P = 0.082$.^gfive mice developed mammary tumors at 11, 12, 16, 17 and 20 months of age, respectively. Two mice developed two different mammary tumors at two separate mammary glands. One mouse was 20 months of age, and the remaining mice were 11–17 months of age. One mouse was a breeder. Mammary tumor incidence, *p16*^{-/-}; *Brcal*^{MGKO} vs *p16*^{-/-}, $P = 0.0006$; *p16*^{-/-}; *Brcal*^{MGKO} vs *Brcal*^{MGKO}, $P = 0.026$; *p16*^{+/-}; *Brcal*^{MGKO} (*p16*^{+/-} *Brcal*^{MGKO} and *p16*^{-/-}; *Brcal*^{MGKO}) vs *Brcal*^{MGKO}, $P = 0.022$.^hlung metastasis from primary mammary tumors was detected in 3 mice, whose ages were 18, 18 and 20 months of age, respectively.ⁱlung metastasis from primary mammary tumors was detected in 2 mice, whose ages were 17 and 20 months of age, respectively.^jone mouse developed an ovarian tumor at 24 months of age.^knine mice developed sarcoma or lymphoma.^lone mouse developed lymphoma at 15 months of age.^mthree mice with mammary tumors also developed lymphomas.ⁿone mouse developed pancreatic carcinoma at 16 months of age, and three mice with mammary tumors also developed lymphoma, sarcoma, lung adenoma, and hepatocellular carcinoma respectively.

DNA damage in tumor development. We determined the expression of γH2AX, a marker for DNA double-strand breaks, in spontaneous tumors from mutant mice. Since *p16* single-mutant mice only developed lymphoma and sarcoma, we compared γH2AX expression in these tumors with mammary tumors. We found that the number of γH2AX-positive cells in *p16*^{mt}; *Brcal*^{MGKO} tumors was significantly greater than in *p16* single-mutant tumors ($4.5\% \pm 2.5\%$ vs $0.84\% \pm 0.36\%$, $p < 0.05$, Supplementary Figure S2G, S2H), indicating a significant increase of cells with DNA damage in *Brcal*-deficient tumors.

Together, these results suggest that depletion of both *p16* and *Brcal* induces metastatic basal-like tumors that have an activated EMT program and enhanced DNA damage.

***p16* and *Brcal* double-mutant tumor cells are transplantable**

A small portion of epithelial-like cells observed in two primary *p16*^{-/-} lymphomas that developed in

mammary glands were sporadic and cuboid, luminal-like cells that were negative for Ck14 and positive for Cdh1 (Supplementary Figure S2B and S2E). We transplanted 1×10^6 cells from one of, and 4×10^6 cells from the other one of the two *p16*^{-/-} tumors that are mixed with lymphoma and epithelial-like cells into MFPs of NSG mice (three recipients per primary tumor). Tumors regenerated, like *p16*^{-/-} primary tumors, were predominantly composed of lymphoma cells mixed with Cdh1-positive and Ck14-negative tumor cells (Figure 3, Supplementary Figure S2B, S2I, and data not shown). The Cdh1-positive cells in the regenerated tumors accounted for < 5% of total tumor cells, however, they aggregated together and formed a larger mass of epithelial-like tissue than in primary tumors (Supplementary Figure S2I and S2E). This result suggests that *p16* loss stimulates luminal epithelial cell proliferation, possibly contributing to the development of premalignant lesions. These data are also consistent with our finding that loss of *p18*, another Ink4 family cell cycle inhibitor, promotes luminal epithelial cell proliferation and induces luminal tumorigenesis [40].

We transplanted 1×10^6 cells from a $p16^{-/-}$; $Brcal^{MGKO}$ mammary tumor, and 4×10^6 cells from a $p16^{+/-}$; $Brcal^{MGKO}$ mammary tumor, respectively, into MFPs of NSG mice (three recipients per primary tumor). We found that $p16^{mt};Brcal^{MGKO}$ tumor cells regenerated significantly larger tumors than $p16^{-/-}$ cells with the

same number of cells in the same time period (Figure 3A, and data not shown). Further analysis revealed that the generated $p16^{mt};Brcal^{MGKO}$ tumors resembled the pathology of the primary tumors and were positive for Ck14 recapitulating the phenotype observed in primary mammary tumors (Figure 3B). These data suggest that

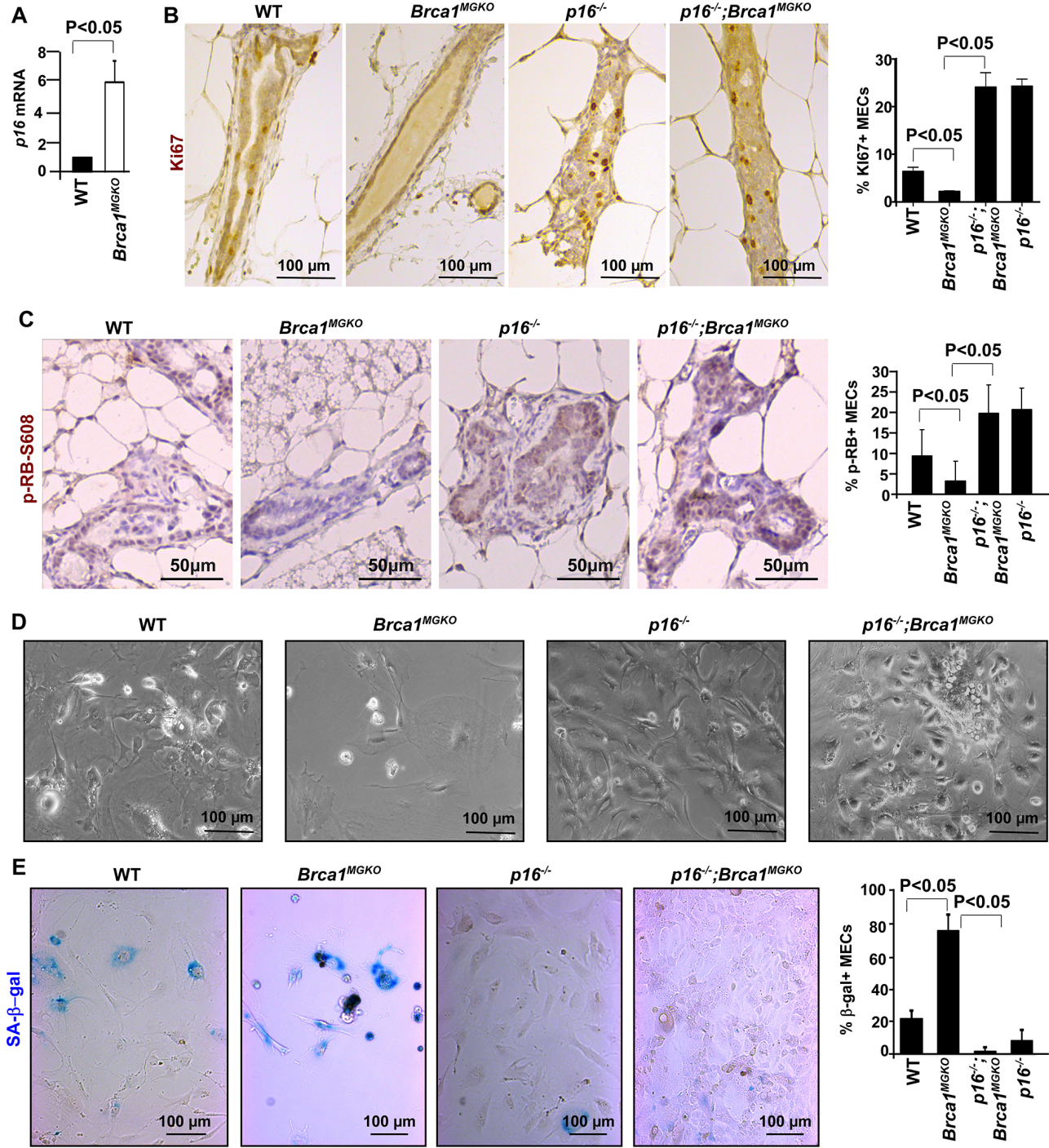


Figure 1: Loss of p16 rescues senescence caused by Brcal deficiency. (A) RT-QPCR of mammary tissue from age-matched WT and $Brcal^{MGKO}$ mice. Data represent the mean \pm SD from triplicates of three mice per genotype. (B, C) Immunohistochemical staining of Ki67 and pRB-s608 in mammary glands of the indicated genotypes. Results represent the mean \pm SD of three animals and two animals per group respectively. (D) MECs of the indicated genotypes were isolated and cultured to analyze cell morphology. (E) SA-β-gal assay of MECs of the indicated genotypes. Results represent the mean \pm SD of triplicates per genotype.

p16;Brca1 double-mutant mammary tumors are enriched with mammary tumor initiating cells.

Expression of *p16* is lost in *p16^{+/−};Brca1^{MGKO}* tumors due to promoter methylation

We determined the expression of *p16* in *p16^{+/−};Brca1^{MGKO}* mammary tumors. We found that *p16* mRNA expression was retained in one tumor (number 1255),

but clearly reduced in the other tumors when compared with tumor-free mammary tissues from the same mouse (Figure 4A). *p16* mRNA levels in tumor 1255 were 8.5-fold more than tumor-free mammary tissues, which could be caused by a reduction in the function of the Rb or p53 pathways [41, 42]. We performed loss of heterozygosity (LOH) analysis for DNA extracted from *p16^{+/−};Brca1^{MGKO}* mammary tumors and found that the remaining WT allele of *p16* was retained in all four tumors

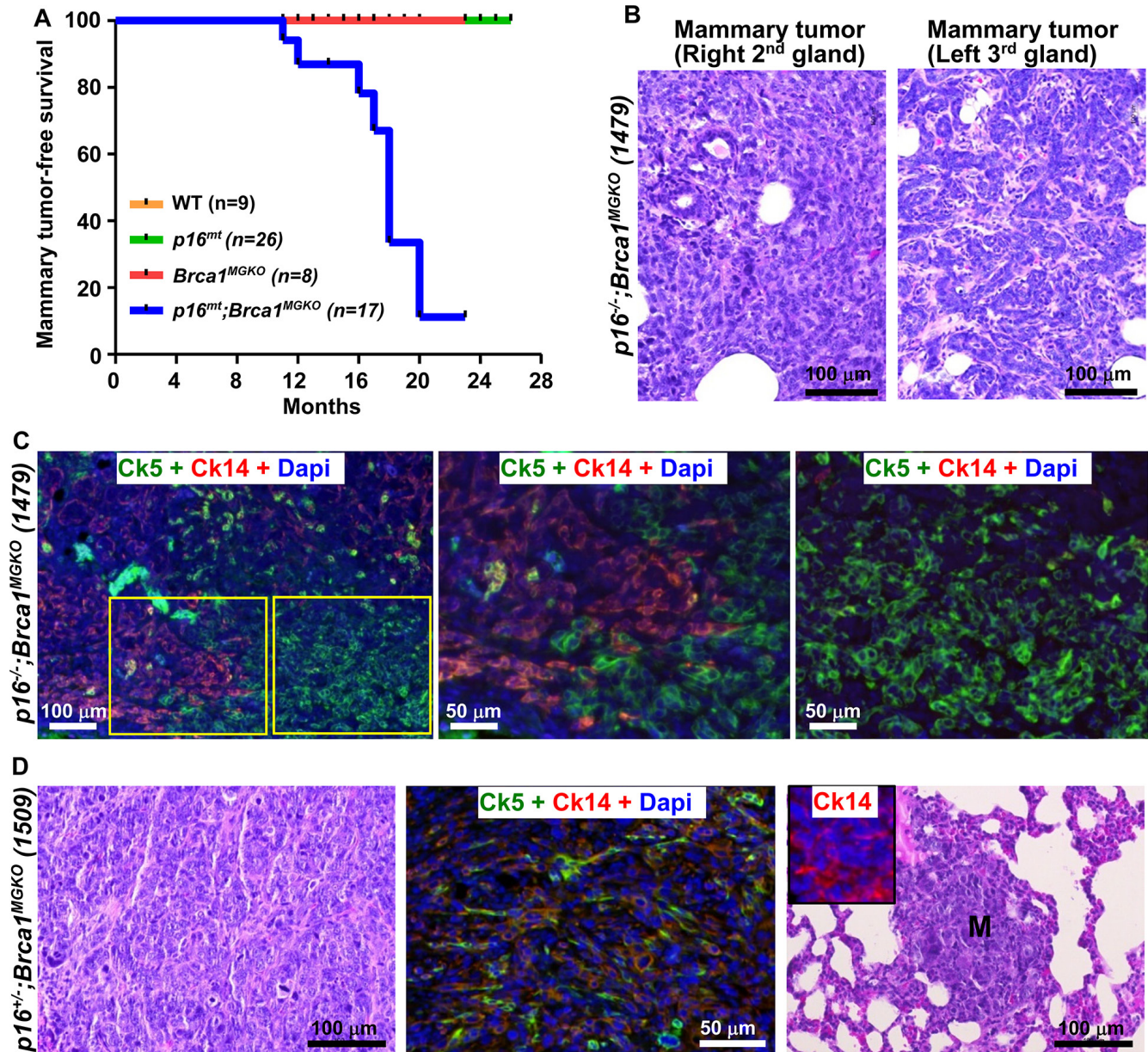


Figure 2: Characterization of primary tumors and distant metastases in mutant mice. (A) Mammary tumor-free survival curve. *p16^{mt};Brca1^{MGKO}* includes: *p16^{+/−};Brca1^{MGKO}* and *p16^{−/−};Brca1^{MGKO}* mice. *p16^{mt}* includes: *p16^{+/−}* and *p16^{−/−}* mice. Log-rank (Mantel-cox) test: $p < 0.0001$ (B) H.E. staining of tumors in a *p16^{−/−};Brca1^{MGKO}* mouse (1479) at 11 months of age. Note this mouse developed two different mammary tumors. (C) Immunofluorescence staining of mammary tumors in mouse 1479 with Ck14 and Ck5. The boxed areas in the left panel are enlarged in the middle and right panels. Note the majority of tumor cells are positive for either Ck5 or Ck14. (D) Immunofluorescence and H.E. staining of mammary tumor in a *p16^{−/−};Brca1^{MGKO}* mouse (1509) at 18 months of age. Note this tumor was comprised predominately of Ck5 and Ck14+ cells (middle panel) and developed a distant metastasis (M) to the lung (right panel), which also comprised of Ck14+ cells (inset in the right panel).

(Figure 4B). These results suggest that epigenetic silencing of *p16*, likely by promoter methylation as observed in DMBA-induced *p16^{+/−}* lymphomas and sarcomas [12], plays an important role in *p16^{+/−};Brca1^{MGKO}* mammary tumorigenesis. To determine the methylation status of the *p16^{+/−};Brca1^{MGKO}* mammary tumors, we performed methylation-specific PCR (MS-PCR) and detected methylation of the *p16* promoter in three tumors with

reduced expression of *p16*, but not in tumor 1255 in which *p16* expression was not decreased (Figure 4C). Notably, we also detected *p16* promoter methylation in a tumor-free, but premalignant lesion-containing mammary tissue in the mouse 1497 (Figure 4C), which explains why there was not a significant decrease in *p16* expression between tumor vs tumor-free tissues in mouse 1497 (Figure 4A). We isolated and cultured primary cells from *p16^{+/−};Brca1^{MGKO}*

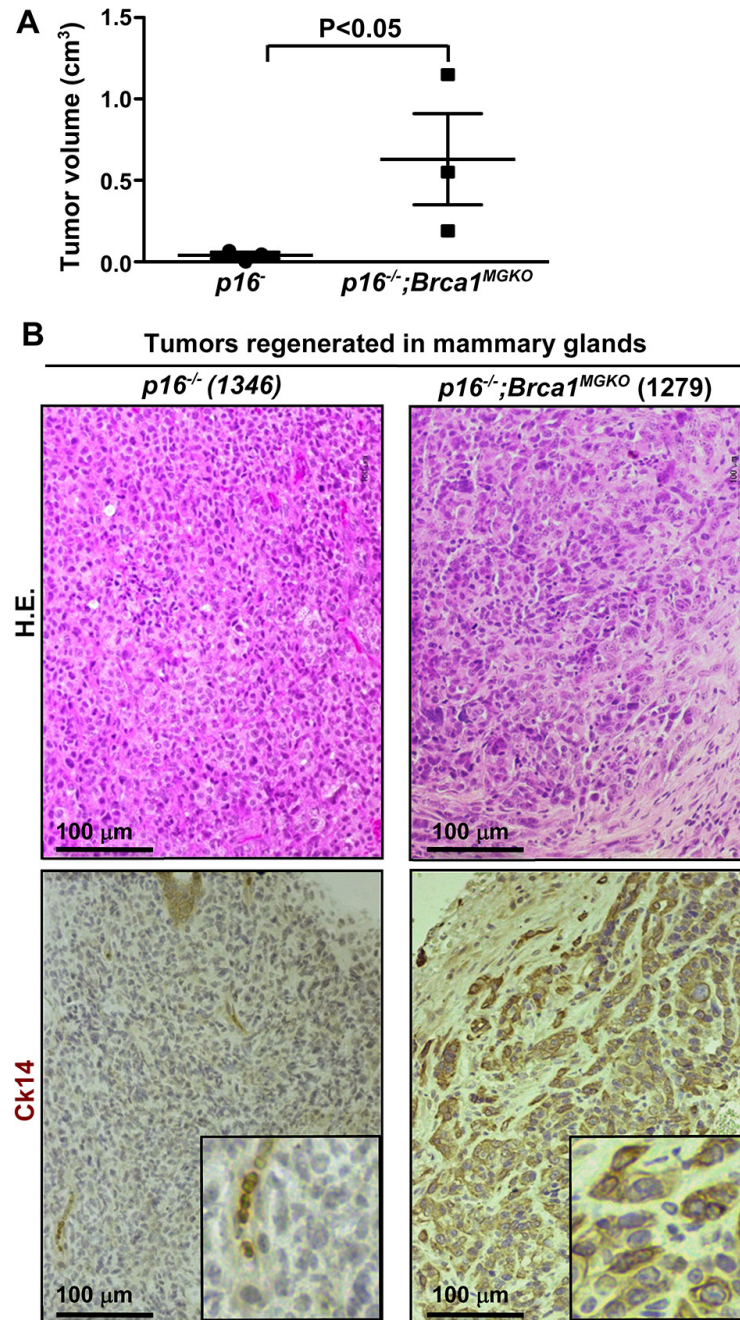


Figure 3: *p16;Brca1* compound mutant tumor cells are enriched with TICs and capable of generating basal-like mammary tumors. (A) 1×10^6 cells from the tumors developed in the mammary glands of *p16*^{-/-} and *p16*^{-/-};*Brca1*^{MGKO} mice were transplanted into the left and right inguinal MFPs of female NSG mice, respectively. Generated tumor volume was measured 4 weeks after transplant. Results are representative of the mean \pm SD of three tumors of each genotype. (B) Representative H.E. and immunostaining of Ck14 of regenerated mammary tumors.

mammary tumors and found that *p16* mRNA levels were significantly increased in the 1347 tumor cells treated with 5-aza-2'-deoxycytidine (DAC), a methylation inhibitor, but not in the 1255 tumor cells (Figure 4D), confirming the findings derived by MS-PCR in tumors. These results suggest that epigenetic silencing of *p16* by promoter methylation plays an important role in the development of, at least, some of the *p16^{+/−};Brca1^{MGKO}* mammary tumors.

DISCUSSION

In this article, we reported that disruption of *Brca1* in the mammary epithelium results in premature senescence with an increase of *p16* expression, which is rescued by *p16* loss. We found that loss of *p16* transforms *Brca1*-deficient mammary epithelial cells and induces mammary tumors, though *p16* loss alone is not sufficient to induce spontaneous mammary tumorigenesis. We showed that mammary tumors deficient for both *p16* and *Brca1* are highly aggressive, metastatic, and enriched for TICs. We demonstrated that loss of *p16* and *Brca1* collaboratively induce basal-like mammary tumor development with the induction of EMT. To the best of our knowledge, this is the first genetic evidence directly showing that *p16* which is frequently deleted and inactivated in human breast cancers, collaborates with *Brca1* controlling mammary tumorigenesis.

The functions of BRCA1 have been linked with multiple pathways. BRCA1 deficiency causes chromosomal abnormalities, leading to the activation of DNA-damage checkpoint pathways and premature senescence [26–28, 30]. It has also been reported that BRCA1 deficiency in MECs impairs stability and activation of Nrf2, a key transcription factor in regulating antioxidant response, and leads to the accumulation of reactive oxygen species (ROS), along with the increase of *p16* [43–45]. Interestingly, accumulation of ROS has been associated with cellular senescence [46], and Nrf2

activation restores ROS levels in *Brca1*-deficient MECs [43, 44]. These findings suggest that BRCA1 deficiency induced premature senescence in MECs, at least, partially resulted from accumulation of ROS. Our results that loss of *p16* rescues the MEC senescence caused by *Brca1* deficiency suggests that *p16* loss may allow Nrf2 levels to accumulate in *Brca1*-deficient cells and suppress ROS, which remains to be determined.

The finding that loss of *p16* rescues the MEC senescence caused by *Brca1* deficiency also suggests that *p16* blocks these cells from entering an active cell cycle. These results indicate that, in addition to the p53-p21 pathway that is activated by BRCA1 loss [27, 28, 30], *p16* is also a critical downstream target of BRCA1 in controlling mammary cell proliferation and senescence. In line with these data, it was recently reported *in vitro* that BRCA1 knockdown enhances the association of BRG1, a chromatin-remodeling factor that interacts with BRCA1, with the promoters of *p16* and *p21*, leading to activation of their transcription and senescence [30]. More recently, it was found that human mammary epithelial cells from BRCA1-mutation carriers exhibit senescence, which is triggered by pRb pathway activation [26]. Since deregulation of p53 alone induces DNA damage, *p16; Brca1* compound mutant mice and cells offer a unique opportunity to investigate the role of *Brca1* in DNA damage repair under a genetically p53 intact background.

The function of *p16* in breast cancer suppression has been extensively studied and confirmed in human breast cancer samples and cell lines [2, 47]. However, the role of *p16* in suppressing mammary tumorigenesis *in vivo* is elusive. Previous findings [12–14] that mice lacking *p16* or targeting DNA methylation within the *p16* promoter rarely develop mammary tumors suggests that *p16* loss alone is not sufficient for mammary tumorigenesis *in vivo*. Interestingly, loss of *p16* increases MEC proliferation, rescues *Brca1*-deficiency induced MEC senescence, and induces mammary tumors in a *Brca1*-deficient

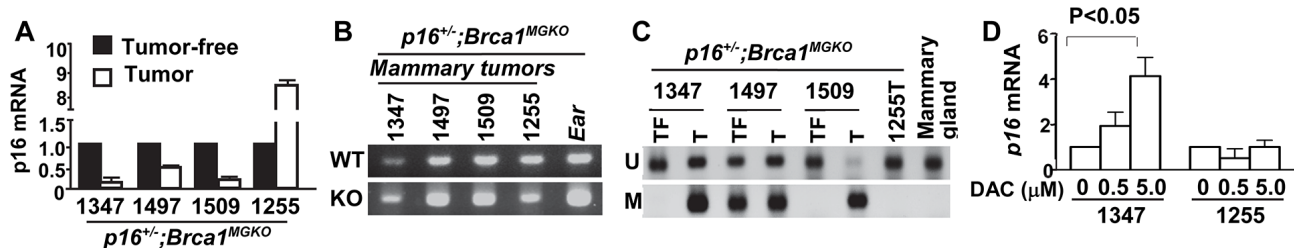


Figure 4: Promoter methylation silences *p16* expression in *p16^{+/−};Brca1^{MGKO}* tumors. (A) mRNA expression of *p16* in *p16^{+/−};Brca1^{MGKO}* mammary tumors was determined by q-RT-PCR. Corresponding tumor-free mammary tissues from the same mice were used as controls. Note the control mammary tissue for mouse 1497 tumor was from a premalignant lesion of the same mouse. Data are expressed as the mean of triplicate experiments. (B) LOH analysis of the *p16* gene in *p16^{+/−};Brca1^{MGKO}* mammary tumors. Ear DNA was used as a control. (C) Bisulphite-treated DNA from mammary tumors (T) or tumor-free mammary tissues (TF) from the same mice was analyzed for methylation of *p16*. U, unmethylated. M, methylated. A normal mammary gland from a WT mouse was used as a control. Note, no methylated *p16* was detected in the mammary tumor developed in mouse 1255 in which the *p16* mRNA level was not reduced relative to tumor-free mammary tissue of the same mouse. (D) *p16* mRNA analysis in primary mammary tumor cells after treatment with DAC at 0, 0.5, or 5 μM for 72 hours.

background, suggesting that p16 collaborates with Brca1 to suppress mammary tumorigenesis. Though the remaining WT allele of *p16* was retained in all *p16^{+/−};Brca1^{MGKO}* mammary tumors, the *p16* promoter was methylated and *p16* mRNA was significantly reduced in most of these tumors, indicating that silencing of p16 by promoter methylation plays a role in the development of, at least, some of the *p16^{+/−};Brca1^{MGKO}* mammary tumors. In line with these results are the clinical findings that methylation of BRCA1 and p16 is frequently detected in sporadic breast cancers and has a predictive value for tumor recurrence [48]. Together, our data not only support the function of p16 in suppression of Brca1-deficient mammary tumorigenesis, but also indicate that genetic mutation of p16 cooperates with epigenetic silencing of its transcription to promote tumorigenesis.

Of the four INK4 genes, p16 is frequently deleted and inactivated, and p18 expression is significantly downregulated in breast cancers ([1, 2, 10, 11, 34], and Pei XH, unpublished). The Rb family proteins consist of RB, p107, and p130, which are also frequently deleted and inactivated in breast cancers and are downstream targets of INK4 proteins [1, 2, 10, 11, 34]. RB is a major target for genomic disruption in *BRCA1* mutant human breast cancers and loss of both RB and BRCA1 is a feature of basal-like breast cancers [34, 36, 49]. Deletion of both Rb and p107 in mouse epithelia results in mammary luminal tumor development [49]. We demonstrated that deletion of *p18* in mice stimulates luminal progenitor cell proliferation, leading to mammary luminal tumorigenesis [40], and that depletion of Brca1 in *p18* null mice converts luminal tumors into basal like tumors and activates EMT [24, 25]. We observed that depletion of *p19* also stimulates mammary luminal cell proliferation [50]. In the present study, we report that loss of p16 increases MEC proliferation and induces mammary tumorigenesis in a Brca1- deficient background. More importantly, all *p16;Brca1* compound mutant mammary tumors are poorly differentiated basal-like tumors with enriched TICs and activated EMT features. These findings suggest that the INK4-Rb pathway suppresses mammary luminal cell proliferation and tumorigenesis, and collaborates with Brca1 to control basal-like tumorigenesis and EMT.

MATERIALS AND METHODS

Mice

The generation of *Brca1^{fl/fl}*;MMTV-Cre and *Brca1^{fl/fl}*;MMTV-Cre mice in a Balb/c-B6 mixed background has been described previously [25]. Virgin *Brca1^{fl/fl}*;MMTV-Cre and *Brca1^{fl/fl}*;MMTV-Cre (*Brca1^{MGKO}*) mammary express < 20% of Brca1 protein and mRNA relative to the levels in *Brca1^{fl/+}*;MMTV-Cre, indicating depletion of Brca1 in the mammary epithelia [25]. *p16* mutant mice in a FVB background were gifted by our collaborators,

Dr. Norman Sharpless [12]. Virgin female mice were used in the study unless otherwise specified. All animal procedures were approved by the Institutional Animal Care and Use Committee at the University of North Carolina and University of Miami.

Histopathology, IHC, and qRT-PCR

Histopathology and IHC were performed as previously described [24, 25]. Primary antibodies used are as follows: Ki67 (Novocastra Laboratories, Newcastle upon Tyne, UK), gH2AX, phosphor-RB (Cell Signaling), CK14 (Thermo Scientific), ERα, (Santa Cruz), Vim, Twist (Abcam), Cdh1 (BD Biosciences), CK5 (Covance prb-160p). Mammary tumors in which at least two EMT markers (decreased Cdh1, increased Vim or Twist) were detected in > 2% tumor cells are defined as EMT+ tumors, as we previously described [25]. The IACUC (Institutional Animal Care and Use Committee) at the University of Miami approved all procedures. QRT-PCR was carried out as previously described [24, 25].

Mammary cell preparation, cell cycle analysis, and mammary tumor cell transplantation

Mammary glands were dissected from virgin female mice at the indicated ages and genotypes. After mechanical dissociation, the tissue was processed as previously described [24, 25, 40]. MECs isolated from mice were cultured in DMEM, with 10% FBS, 10 µg/ml insulin, 10 ng/ml EGF, 10 µg/ml Hydrocortisone. For cell cycle analysis, MECs were pulse-labeled with bromodeoxyuridine (BrdU) for 15 hours. Cells were then stained with propidium iodide (PI) and an antibody against BrdU and analyzed via flow cytometry as described [50]. For mammary tumor cell transplantation, 1 × 10⁶ tumor cells were transplanted into MFPs of NSG mice as previously described [25]. Four weeks post-transplantation, newly generated tumors were dissected and analyzed.

LOH and methylation analysis

For LOH analysis, genomic DNA extracted from micro-dissected *p16^{+/−};Brca1^{MGKO}* mammary tumor cells was analyzed with primers amplifying wild-type (WT) and knock-out (KO) allele of *p16* as previously described [12, 24]. For methylation analysis, genomic DNA from *p16^{+/−};Brca1^{MGKO}* mammary tumors and tumor-free mammary tissues of the same mice were treated with bisulfide and analyzed for *p16* methylation with specific primers amplifying the unmethylated or methylated allele as described [12]. In addition, *p16* mRNA levels in primary *p16^{+/−};Brca1^{MGKO}* mammary tumor cells treated with DAC at the indicated concentrations for 72 hours were analyzed by q-RT-PCR.

Human breast cancer samples

Formalin fixed paraffin-embedded (FFPE) human breast cancer samples lacking patient-identifying information were obtained from the Tissue Bank Core Facility at the University of Miami. All samples obtained were non-treated invasive breast cancers with known ER status. The expression of *BRCA1* in tumors was determined by microdissection-based RNA extraction and Q-RT-PCR as we previously described [25].

Statistical analysis

All data are presented as the mean \pm SD for at least three repeated individual experiments for each group unless otherwise specified. Statistical analysis of mRNA expression, Ki67 positive cells, and tumor volume was performed using a two-tailed Student's *t*-test. Statistical analysis of tumor incidence was performed using a two-tailed Fisher's exact test. Statistical analysis of mammary tumor-free survival was performed using a Log-rank (Mantel-cox) test. $P < 0.05$ was considered statistically significant. Statistical analyses were conducted using Microsoft Excel and GraphPad Prism 5.

ACKNOWLEDGMENTS

We thank Drs. Norman Sharpless, Beverly Koller, Chuxia Deng, and Lothar Hennighausen for *p16*, *Brcal* mutant and MMTV-cre mice, Ergonul A. Bureu for discussion on tumor pathology, the FACS core facility at University of Miami for cell sorting, the DVR core facility for animal husbandry.

CONFLICTS OF INTEREST

The authors declare no conflicts of interest.

GRANT SUPPORT

This study was supported by DOD Idea Award (W81XWH-10-1-0302), DOD Idea Expansion Award (W81XWH-13-1-0282), Sylvester BFBCI Developmental Grant, IRG-98-277-13 from the American Cancer Society, and startup funds from the University of Miami Department of Surgery and Sylvester Cancer Center to Xin-Hai Pei.

REFERENCES

1. Pei XH, Xiong Y. Biochemical and cellular mechanisms of mammalian CDK inhibitors: a few unresolved issues. *Oncogene*. 2005; 24:2787–2795.
2. Sherr CJ, McCormick F. The RB and p53 pathways in cancer. *Cancer Cell*. 2002; 2:103–112.
3. Orford KW, Scadden DT. Deconstructing stem cell self-renewal: genetic insights into cell-cycle regulation. *Nat Rev Genet*. 2008; 9:115–128.
4. Zindy F, Quelle DE, Roussel MF, Sherr CJ. Expression of the p16INK4a tumor suppressor versus other INK4 family members during mouse development and aging. *Oncogene*. 1997; 15:203–211.
5. Krishnamurthy J, Torrice C, Ramsey MR, Kovalev GI, Al-Regaiey K, Su L, Sharpless NE. Ink4a/Arf expression is a biomarker of aging. *J Clin Invest*. 2004; 114:1299–1307.
6. Molofsky AV, Slutsky SG, Joseph NM, He S, Pardal R, Krishnamurthy J, Sharpless NE, Morrison SJ. Increasing p16INK4a expression decreases forebrain progenitors and neurogenesis during ageing. *Nature*. 2006; 443:448–452.
7. Janzen V, Forkert R, Fleming HE, Saito Y, Waring MT, Dombkowski DM, Cheng T, DePinho RA, Sharpless NE, Scadden DT. Stem-cell ageing modified by the cyclin-dependent kinase inhibitor p16INK4a. *Nature*. 2006; 443:421–426.
8. Krishnamurthy J, Ramsey MR, Ligon KL, Torrice C, Koh A, Bonner-Weir S, Sharpless NE. p16INK4a induces an age-dependent decline in islet regenerative potential. *Nature*. 2006; 443:453–457.
9. Sharpless NE, Sherr CJ. Forging a signature of *in vivo* senescence. *Nat Rev Cancer*. 2015; 15:397–408.
10. Kamb A, Gruis NA, Weaver-Feldhaus J, Liu Q, Harshman K, Tavtigian SV, Stockert E, Day RS, 3rd, Johnson BE, Skolnick MH. A cell cycle regulator potentially involved in genesis of many tumor types. *Science*. 1994; 264:436–440.
11. Herman JG, Merlo A, Mao L, Lapidus RG, Issa J PJ, Davidson NE, Sidransky D, Baylin SB. Inactivation of the *CDKN2/p16/MTS1* gene is frequently associated with aberrant DNA methylation in all common human cancers. *Cancer Res*. 1995; 55:4525–4530.
12. Sharpless NE, Bardeesy N, Lee KH, Carrasco D, Castrillon DH, Aguirre AJ, Wu EA, Horner JW, DePinho RA. Loss of p16^{Ink4a} with retention of p19^{Arf} predisposes mice to tumorigenesis. *Nature*. 2001; 413:86–91.
13. Sharpless NE, Alson S, Chan S, Silver DP, Castrillon DH, DePinho RA. p16(INK4a) and p53 deficiency cooperate in tumorigenesis. *Cancer Res*. 2002; 62:2761–2765.
14. Yu DH, Waterland RA, Zhang P, Schady D, Chen MH, Guan Y, Gadkari M, Shen L. Targeted p16(*Ink4a*) epimutation causes tumorigenesis and reduces survival in mice. *J Clin Invest*. 2014; 124:3708–3712.
15. Foulkes WD. BRCA1 functions as a breast stem cell regulator. *J Med Genet*. 2004; 41:1–5.
16. Althuis MD, Fergenbaum JH, Garcia-Closas M, Brinton LA, Madigan MP, Sherman ME. Etiology of hormone receptor-defined breast cancer: a systematic review of the literature. *Cancer Epidemiol Biomarkers Prev*. 2004; 13:1558–1568.
17. Wright MH, Calcagno AM, Salcido CD, Carlson MD, Ambudkar SV, Varticovski L. *Brcal* breast tumors contain

- distinct CD44+/CD24– and CD133+ cells with cancer stem cell characteristics. *Breast Cancer Res.* 2008; 10:R10.
18. Wicha MS. Cancer stem cell heterogeneity in hereditary breast cancer. *Breast Cancer Res.* 2008; 10:105.
 19. Marks JR. Refining the role of BRCA1 in combating oxidative stress. *Breast Cancer Res.* 2013; 15:320.
 20. Turner N, Tutt A, Ashworth A. Hallmarks of ‘BRCAness’ in sporadic cancers. *Nat Rev Cancer.* 2004; 4:814–819.
 21. De Summa S, Pinto R, Sambiasi D, Petriella D, Paradiso V, Paradiso A, Tommasi S. BRCAness: a deeper insight into basal-like breast tumors. *Ann Oncol.* 2013; 8:viii13-viii21.
 22. Elstrodt F, Hollestelle A, Nagel JH, Gorin M, Wasielewski M, van den Ouweland A, Merajver SD, Ethier SP, Schutte M. BRCA1 mutation analysis of 41 human breast cancer cell lines reveals three new deleterious mutants. *Cancer Res.* 2006; 66:41–45.
 23. Kalluri R, Weinberg RA. The basics of epithelial-mesenchymal transition. *J Clin Invest.* 2009; 119:1420–1428.
 24. Bai F, Smith MD, Chan HL, Pei XH. Germline mutation of Brcal alters the fate of mammary luminal cells and causes luminal-to-basal mammary tumor transformation. *Oncogene.* 2013; 32:2715–2725.
 25. Bai F, Chan HL, Scott A, Smith MD, Fan C, Herschkowitz JI, Perou CM, Livingstone AS, Robbins DJ, Capobianco AJ, Pei XH. BRCA1 Suppresses Epithelial-to-Mesenchymal Transition and Stem Cell Dedifferentiation during Mammary and Tumor Development. *Cancer Res.* 2014; 74:6161–6172.
 26. Sedic M, Skibinski A, Brown N, Gallardo M, Mulligan P, Martinez P, Keller PJ, Glover E, Richardson AL, Cowan J, Toland AE, Ravichandran K, Riethman H, et al. Haploinsufficiency for BRCA1 leads to cell-type-specific genomic instability and premature senescence. *Nature communications.* 2015; 6:7505.
 27. Cao L, Li W, Kim S, Brodie SG, Deng CX. Senescence, aging, and malignant transformation mediated by p53 in mice lacking the Brcal full-length isoform. *Genes Dev.* 2003; 17:201–213.
 28. Cao L, Kim S, Xiao C, Wang RH, Coumoul X, Wang X, Li WM, Xu XL, De Soto JA, Takai H, Mai S, Elledge SJ, Motoyama N, et al ATM-Chk2-p53 activation prevents tumorigenesis at an expense of organ homeostasis upon Brcal deficiency. *EMBO J.* 2006; 25:2167–2177.
 29. Xu X, Wagner KU, Larson D, Weaver Z, Li C, Ried T, Hennighausen L, Wynshaw-Boris A, Deng CX. Conditional mutation of Brcal in mammary epithelial cells results in blunted ductal morphogenesis and tumour formation. *Nat Genet.* 1999; 22:37–43.
 30. Tu Z, Zhuang X, Yao YG, Zhang R. BRG1 is required for formation of senescence-associated heterochromatin foci induced by oncogenic RAS or BRCA1 loss. *Mol Cell Biol.* 2013; 33:1819–1829.
 31. Deng CX, Scott F. Role of the tumor suppressor gene Brcal in genetic stability and mammary gland tumor formation. *Oncogene.* 2000; 19:1059–1064.
 32. Drost RM, Jonkers J. Preclinical mouse models for BRCA1-associated breast cancer. *Br J Cancer.* 2009; 101:1651–1657.
 33. Jonsson G, Staaf J, Vallon-Christersson J, Ringner M, Gruvberger-Saal SK, Saal LH, Holm K, Hegardt C, Arason A, Fagerholm R, Persson C, Grabau D, Johnsson E, et al. The retinoblastoma gene undergoes rearrangements in BRCA1-deficient basal-like breast cancer. *Cancer Res.* 2012; 72:4028–4036.
 34. Koboldt DC, Fulton RS, McLellan MD, Schmidt H, Kalicki-Veizer J, McMichael JF, Fulton LL, Dooling DJ, Ding L, Mardis ER, Wilson RK, Ally A, Balasundaram M, et al. Comprehensive molecular portraits of human breast tumours. *Nature.* 2012.
 35. Stefansson OA, Jonasson JG, Olafsdottir K, Hilmarsdottir H, Olafsdottir G, Esteller M, Johannsson OT, Eyjford JE. CpG island hypermethylation of BRCA1 and loss of pRb as co-occurring events in basal/triple-negative breast cancer. *Epigenetics.* 2011; 6:638–649.
 36. Herschkowitz JI, He X, Fan C, Perou CM. The functional loss of the retinoblastoma tumour suppressor is a common event in basal-like and luminal B breast carcinomas. *Breast Cancer Res.* 2008; 10:R75.
 37. Moynahan ME. The cancer connection: BRCA1 and BRCA2 tumor suppression in mice and humans. *Oncogene.* 2002; 21:8994–9007.
 38. Kitagawa M, Higashi H, Jung HK, Suzuki-Takahashi I, Ikeda M, Tamai K, Kato J, Segawa K, Yoshida E, Nishimura S, Taya Y. The consensus motif for phosphorylation by cyclin D1-Cdk4 is different from that for phosphorylation by cyclin A/E-Cdk2. *The EMBO journal.* 1996; 15:7060–7069.
 39. Zarkowska T, U S, Harlow E, Mittnacht S. Monoclonal antibodies specific for underphosphorylated retinoblastoma protein identify a cell cycle regulated phosphorylation site targeted by CDKs. *Oncogene.* 1997; 14:249–254.
 40. Pei XH, Bai F, Smith MD, Usary J, Fan C, Pai SY, Ho IC, Perou CM, Xiong Y. CDK inhibitor p18(INK4c) is a downstream target of GATA3 and restrains mammary luminal progenitor cell proliferation and tumorigenesis. *Cancer Cell.* 2009; 15:389–401.
 41. Zeng Y, Kotake Y, Pei XH, Smith MD, Xiong Y. p53 binds to and is required for the repression of Arf tumor suppressor by HDAC and polycomb. *Cancer Res.* 2011; 71:2781–2792.
 42. Kotake Y, Cao R, Viatour P, Sage J, Zhang Y, Xiong Y. pRB family proteins are required for H3K27 trimethylation and Polycomb repression complexes binding to and silencing p16INK4alpha tumor suppressor gene. *Genes Dev.* 2007; 21:49–54.
 43. Gorrini C, Baniasadi PS, Harris IS, Sylvester J, Inoue S, Snow B, Joshi PA, Wakeham A, Molyneux SD, Martin B, Bouwman P, Cescon DW, Elia AJ, et al. BRCA1 interacts with Nrf2 to regulate antioxidant signaling and cell survival. *J Exp Med.* 2013; 210:1529–1544.
 44. Gorrini C, Gang BP, Bassi C, Wakeham A, Baniasadi SP, Hao Z, Li WY, Cescon DW, Li YT, Molyneux S, Penrod N,

- Lupien M, Schmidt EE, et al. Estrogen controls the survival of BRCA1-deficient cells via a PI3K-NRF2-regulated pathway. *Proc Natl Acad Sci USA*. 2014; 111:4472–4477.
45. Cao L, Xu X, Cao LL, Wang RH, Coumoul X, Kim SS, Deng CX. Absence of full-length Brcal sensitizes mice to oxidative stress and carcinogen-induced tumorigenesis in the esophagus and forestomach. *Carcinogenesis*. 2007; 28:1401–1407.
46. Fridman AL, Tainsky MA. Critical pathways in cellular senescence and immortalization revealed by gene expression profiling. *Oncogene*. 2008; 27:5975–5987.
47. Tlsty TD, Crawford YG, Holst CR, Fordyce CA, Zhang J, McDermott K, Kozakiewicz K, Gauthier ML. Genetic and epigenetic changes in mammary epithelial cells may mimic early events in carcinogenesis. *J Mammary Gland Biol Neoplasia*. 2004; 9:263–274.
48. Feng J, Hu LH, Lu J, Li YR, Xie F. [Diagnostic value of BRCA1 and p16 gene methylation in sporadic breast cancer]. *Ai Zheng*. 2009; 28:436–440.
49. Jiang Z, Deng T, Jones R, Li H, Herschkowitz JI, Liu JC, Weigman VJ, Tsao MS, Lane TF, Perou CM, Zackenhaus E. Rb deletion in mouse mammary progenitors induces luminal-B or basal-like/EMT tumor subtypes depending on p53 status. *J Clin Invest*. 2010; 120:3296–3309.
50. Bai F, Chan HL, Smith MD, Kiyokawa H, Pei XH. p19Ink4d is a tumor suppressor and controls pituitary anterior lobe cell proliferation. *Mol Cell Biol*. 2014; 34:2121–2134.